ANALYSIS OF SOIL HEAT TRANSFER FOR THE EVAPOTRANSPIRATION SYSTEM

by

Wayne Clyma

A Dissertation Submitted to the Faculty of the

COMMITTEE ON HYDROLOGY AND WATER RESOURCES

In Partial Fulfillment of the Requirements
For the Degree of

DOCTOR OF PHILOSOPHY
WITH A MAJOR IN HYDROLOGY

In the Graduate College

THE UNIVERSITY OF ARIZONA

1 9 7 1

THE UNIVERSITY OF ARIZONA

GRADUATE COLLEGE

I hereby recommend that this dissertation prepared under my direction by Wayne Clyma

entitled Analysis of Soil Heat Transfer for the Evapotranspiration System

be accepted as fulfilling the dissertation requirement of the degree of Doctor of Philosophy

D D Evanylo — March 31, 1971

Dissertation Director — Date

After inspection of the final copy of the dissertation, the following members of the Final Examination Committee concur in its approval and recommend its acceptance:*

C. H. Wadleigh	April 2, 1971
W. D. Sellers	April 2, 1971
A. W. Warrick	April 2, 1971
[illegible]	April 2, 1971

*This approval and acceptance is contingent on the candidate's adequate performance and defense of this dissertation at the final oral examination. The inclusion of this sheet bound into the library copy of the dissertation is evidence of satisfactory performance at the final examination.

PLEASE NOTE:

Some pages have indistinct print. Filmed as received.

UNIVERSITY MICROFILMS.

STATEMENT BY AUTHOR

This dissertation has been submitted in partial fulfillment of requirements for an advanced degree at The University of Arizona and is deposited in the University Library to be made available to borrowers under rules of the Library.

Brief quotations from this dissertation are allowable without special permission, provided that accurate acknowledgment of source is made. Requests for permission for extended quotation from or reproduction of this manuscript in whole or in part may be granted by the head of the major department or the Dean of the Graduate College when in his judgment the proposed use of the material is in the interests of scholarship. In all other instances, however, permission must be obtained from the author.

SIGNED: Wayne Clyma

ACKNOWLEDGEMENTS

I wish to express my appreciation to Dr. D. D. Fangmeier, director of the dissertation, who provided encouragement and constructive criticism throughout the study.

I am indebted to Professor H. N. Stapleton for his suggestions and critique as leader of the project under which this study was conducted. Dr. A. W. Warrick provided mathematical assistance in the development of this work. Dr. W. D. Sellers, through his course and through informal consultations, taught me much of my understanding of the evapotranspiration process and many times aided me in this study. Dr. W. G. Matlock provided encouragement and persistent critique of the various stages of manuscript development.

Mr. R. P. Myers in System Engineering, Mr. F. L. Watson in Electrical Engineering, and Dr. D. F. Wanjura in Agronomy provided much assistance as fellow graduate students.

This study was conducted through the facilities of the Agricultural Engineering Department under Arizona Agricultural Experiment Station Project Number 653, which was also supported in part by grants from Cotton, Inc., and the the Cooperative State Research Service, USDA.

To my wife, Marjorie, and sons, Gary Wayne and Howard Earl, to whom I am indebted for much inspiration, this dissertation is dedicated.

TABLE OF CONTENTS

	Page
LIST OF ILLUSTRATIONS	vii
LIST OF TABLES	ix
ABSTRACT	x
PROBLEM DEFINITION AND OBJECTIVES	1
The Evapotranspiration System	1
Systems Theory	4
Objectives	5
DEFINITION OF THE EVAPOTRANSPIRATION SYSTEM	7
Subsystem Defining Equations	8
System Block Diagram Definition	14
LINEAR SYSTEMS THEORY	23
Systems Analysis	23
Time Series Analysis	28
Time Domain Analysis	30
Frequency Domain Analysis	36
LINEAR SYSTEMS ANALYSIS OF HEAT FLOW IN THE SOIL	50
Time Domain Analysis	52
Frequency Domain Analysis	55
System Constant Determination	59
ANALYTICAL VERIFICATION OF SYSTEM RESPONSE AND SYSTEM CONSTANT EVALUATION	63
System Response	63
System Constant Identification	65
Time Series Analysis	66
Numerical Convolution	78
Confidence Limits for System Constants	81
Summary	83

TABLE OF CONTENTS--Continued

Page

EXPERIMENTAL DETERMINATION OF SYSTEM CONSTANT AND SIMULATION OF SYSTEM RESPONSE 84

System Constant by Time Series Analysis. 85
System Constant by Numerical Convolution . . . 95
System Simulation 98
Confidence Limits for Diffusivity 102

SUMMARY AND CONCLUSIONS 104

RECOMMENDATIONS 107

APPENDIX A: RESULTS OF TIME SERIES ANALYSIS OF SIMULATED SURFACE AND 5-CM TEMPERATURES. 109

APPENDIX B: RESULTS OF TIME SERIES ANALYSIS OF 10- AND 15-CM TEMPERATURES, LOCATION I, DAVIS, CALIFORNIA, FROM WIERENGA (1968). 117

LIST OF SYMBOLS 128

REFERENCES 133

LIST OF ILLUSTRATIONS

Figure		Page
1.	Block diagram of the soil heat transfer system. .	17
2.	Block diagram of the radial flow of water to roots subsystem	17
3.	The evapotranspiration system as coupled subsystems	21
4.	A graph of sinusoidal temperature variation . . .	29
5.	Frequency domain graph of sinusoidal temperature variation	29
6.	Two sine waves and the sum of two sine waves. . .	31
7.	Frequency domain representation of one and two sine waves.	31
8.	Bode plots for the soil heat transfer subsystem for three different diffusivities and x = 5 cm. .	58
9.	Comparison of analytical and convolution computed soil temperature for the 4th cycle	64
10.	Autocorrelation of simulated sine wave of surface temperature, ΔT_S = 8°C, T_a = 28.0°C, P = 24 hr.	67
11.	Autocorrelation of simulated sine wave of soil temperature, x = 5 cm, K = 16.2 cm^2/hr.	67
12.	Cross correlation of simulated surface and soil temperatures	68
13.	Autospectrum of simulated surface temperature . .	70
14.	Autospectrum of simulated soil (5-cm) temperature	71
15.	Residual spectrum for simulated soil heat transfer subsystem	72
16.	Squared coherency spectrum for simulated soil heat transfer subsystem	74

LIST OF ILLUSTRATIONS--Continued

Figure		Page
17.	Gain spectrum for simulated soil heat transfer subsystem	76
18.	Phase spectrum for simulated soil heat transfer subsystem	76
19.	Optimum diffusivity based on minimum sum of squares between analytical and convolution computed temperatures	80
20.	Autocorrelation of 10-cm temperature as input for Davis, California, Location I	86
21.	Autocorrelation of 15-cm temperature as output for Davis, California, Location I	86
22.	Cross correlation of 10- and 15-cm temperatures for Davis, California, Location I	88
23.	Autospectrum of 10-cm temperature	89
24.	Autospectrum of 15-cm temperature	90
25.	Residual spectrum for 10- and 15-cm temperatures for soil heat transfer subsystem	92
26.	Standard deviation of computed from measured temperatures using numerical convolution and various values of diffusivity	96
27.	Comparison of measured and convolution computed 15-cm temperature for Davis, California, Location I.	99

LIST OF TABLES

Table		Page
1.	Summary of theoretical formulae as well as formulae for estimating properties of discrete data for time series analysis	45
2.	Comparison of values of diffusivity as computed by Wierenga (1968) and by time series analysis	95
3.	Autocovariances and cross covariances for simulated surface (X) and soil (Y) temperatures . .	110
4.	Time series analysis of simulated surface and soil temperatures	111
5.	Upper and lower confidence limits for gain and phase from time series analysis for simulated surface and soil temperatures.	114
6.	Autocovariances and cross covariances for 10-cm (X) and 15-cm (Y) soil temperatures, Location I, from Wierenga (1968).	118
7.	Time series analysis of 10- and 15-cm soil temperatures for Davis, California, Location I, from Wierenga (1968).	122
8.	Upper and lower confidence limits for gain and phase from time series analysis of 10- and 15-cm soil temperatures	125

ABSTRACT

An evapotranspiration system was defined as six coupled, parallel subsystems defined by five rectangular and one radial, one-dimensional diffusion equations. A block diagram and system transfer function were developed for each subsystem and the subsystems were coupled to obtain a block diagram of the evapotranspiration system.

The soil heat transfer subsystem was assumed to be defined by the diffusion equation for a homogeneous soil of infinite depth with constant diffusivity and heat transfer by conduction only. The solution of the diffusion equation was obtained in the frequency domain as the frequency response function and in the time domain as the convolution integral. The frequency response function was used as an analytical model in the form of a gain and a phase function in conjunction with time series analysis to determine the system constant. A numerical solution of the convolution integral was used to determine soil heat diffusivity from arbitrary time distributions of temperature at two depths. The system response as the temperature at a depth was computed from an arbitrary time distribution of input temperature given the diffusivity.

Results from time series analysis of analytically generated temperature data gave values for diffusivity from the gain and phase function of 16.24- and 16.21-cm^2/hr, respectively. The value used to generate the data was 16.2 cm^2/hr. The corresponding value of diffusivity obtained from a trial and error numerical convolution was 16.3 cm^2/hr. Values of numerical convolution computed temperature, obtained after 72 hours to remove a starting transient, differed from the analytically correct temperatures by less than 0.1° C for an 8° amplitude or a 16° range. For 50 days of 6-hour interval temperatures the 95 percent confidence interval on diffusivity was within two percent of the analytically correct value.

Soil temperature data for the 10- and 15-cm depth from an experiment where cold (4° C) irrigation water was applied, including the temperature data during the time of irrigation, was analyzed by time series analysis. The value of diffusivity obtained from time series analysis and the gain function was 14.7 cm^2/hr compared to a range of 15.1 to 16.9 for amplitude and phase plots and 16.6 for a finite difference solution of the diffusion equation. The value from phase was 21.61 cm^2/hr which is much higher due to the time-varying effects of diffusivity or improper alignment of the two time series. Confidence intervals for diffusivity were very wide because of the short period of record and because of heat transfer by moisture during the irrigation. Numerical

convolution determined values of diffusivity of 15.1- and 14.9-cm^2/hr for before and after irrigation indicated some change in soil heat diffusivity with time. Numerical convolution computed temperatures were within 0.17° C of the measured temperature except during and immediately after the application of the irrigation water. The maximum error between measured and computed temperature was 3.88° C.

Time series analysis can be used to determine the soil heat diffusivity from arbitrary time distributions of temperatures at two depths. Confidence limits for diffusivity can be established by certain assumptions as a measure of the adequacy with which the diffusivity has been determined. Numerical convolution can also be used to determine soil heat diffusivity by trial and error from arbitrary time distributions of temperatures measured at two depths. Simulation of soil temperatures from arbitrary time distributions of measured input can be achieved by numerical convolution.

PROBLEM DEFINITION AND OBJECTIVES

Evapotranspiration is an important factor in water resources management. For example, evapotranspiration has a primary role in plant growth and development and thus is a part of all aspects of irrigation from field application to project planning. The need to understand the dynamic variables of evapotranspiration to simulate the growth and development of a cotton plant provided the stimulus for this study (Stapleton and Meyers, 1969).

This study was to define a dynamic evapotranspiration system consisting of coupled diffusion processes for transporting heat and moisture through the soil, plant, and atmosphere. The conceptual role of systems theory will be presented to justify its use in defining the evapotranspiration system and for analyzing the soil heat transfer subsystem.

The Evapotranspiration System

Historically, evapotranspiration was considered as an empirical process. Evolution to the current concepts of a dynamic process has occurred as a greater understanding of the process was obtained. A brief review of the principal approaches to defining evapotranspiration is presented below.

Evapotranspiration has been predicted empirically by measuring pan evaporation (Pruitt, 1966), air temperature (Criddle, 1966), solar radiation and air temperature (Jensen, 1966) or combinations of various variables (Sellers, 1965, pp. 168-170). These methods of prediction generally provide estimates for time periods of a week to a year.

Evapotranspiration has also been treated as a dynamic phenomenon by variations of three basic methods. These are (Sellers, 1965, p. 146):

1. Eddy correlation method
2. Energy balance method
3. Aerodynamic method

The above methods treat evapotranspiration (ET) as a dynamic process and Van Bavel (1966) has shown that very good agreement between theory and experiment can be obtained when considering ET influenced principally by atmospheric variables.

Lemon (1966) has used the aerodynamic method for studying the relationships between evapotranspiration and plant growth. Plant response is affected by the variables describing dynamic evapotranspiration. Gardner and Ehlig (1963) and Cowan (1965) studied various aspects of water flow to roots and soil moisture transfer. They tested several forms of the diffusion equation as mathematical models for water flow to roots. The emphasis of their studies was on the soil-plant system.

Phillip (1966) expressed the idea of considering a soil-plant-atmosphere continuum. Dynamic studies of the continuum have been made. Ohmsteade (1966) used a finite difference, digital model to study a mulch-covered soil. An analog model was used by Halstead et al (1957) to study the dynamic continuum. Another analog model including stomatal control of transpiration was used by Woo, Boersma and Stone (1966). These studies have provided the basic concept for the formulation of the ET system.

The description of a dynamic ET system requires the definition of a soil-plant-atmosphere continuum (Phillip, 1966). Previous research has indicated the basis for describing the behavior of each subsystem. Van Bavel (1966) has shown that the effects of atmospheric variables can be defined by a diffusion equation. For some circumstances Woo, Boersma, and Stone (1966) concluded that the role of the plant can be restricted to transport. Ohmsteade (1966) described the diffusion equations for vertical moisture and heat transfer to the evaporating surface. Gardner and Ehlig (1963) and Cowan (1965) have shown the applicability of the radial form of the diffusion equation for describing the flow of water to roots. Thus, energy as heat and mass may be discussed as diffusion processes within the continuum.

Systems Theory

Systems theory has a major application in the analysis of dynamic systems. Systems for which defining differential equations can be developed from the physics of the system are especially adapted for systems analysis. The coupled diffusion processes of evapotranspiration can be described by coupled partial differential equations. Therefore, analysis of evapotranspiration by systems theory is appropriate.

System representation by using state variable theory and block diagram manipulation is useful for defining a system that is described by coupled multiple order differential equations (Melsa and Schultz, 1969, Ch. 2). Different block diagram representations are possible and different purposes may be served. Thus, better understanding of the system is achieved.

Systems theory permits the isolation of a component or subsystem in order to study its dynamic behavior independently of the remaining subsystems of the system (Schwarz and Friedland, 1965, p. 2). Complex systems may be investigated by studying carefully the dynamic behavior of simple components that can be reassembled to represent the total system.

Systems analysis deals largely with the solution of defining differential equations (time domain analysis) and

the Laplace or Fourier transforms of the differential equations (frequency domain analysis). Time domain analysis is important because real systems operate in time. Frequency domain analysis is important because the mathematics are simpler and it provides the most important bridge between theory and experimental evidence (Milsum, 1966, p. 142).

Time domain analysis will be used to compare the response of the mathematical model to the response of the real system, but frequency domain analysis will be used to obtain numerical values for the system parameters as well as to compare the performance of the mathematical model and the real system.

System identification from experimental data embodies a general procedure known as time series analysis (Jenkins and Watts, 1968). The procedures are equivalent to frequency domain analysis of differential equations. In the frequency domain, experimental data and mathematical models may be readily compared as algebraic equations and the mathematical model verified. These results provide the justification for the application of systems theory to the analysis of the evapotranspiration system.

Objectives

The objectives of this study are to:

1. Define an evapotranspiration system using linear systems theory.

2. Use systems analysis of the soil heat transfer subsystem to determine:
   a. system constant by time series analysis
   b. system response by convolution

DEFINITION OF THE EVAPOTRANSPIRATION SYSTEM

The evapotranspiration system receives incoming net solar radiation and achieves an energy balance at the soil surface by distributing energy to the soil and into the atmosphere. Energy is distributed by latent and sensible heat transfer into the atmosphere and by heat and moisture transfer into the soil.

The evapotranspiration system may be defined by six subsystems, three in the soil and three within the atmosphere. The three within the soil are:

1. heat transfer by conduction
2. heat transfer by vertical moisture movement
3. heat transfer by radial moisture movement.

The three within the atmosphere are:

4. sensible heat transfer
5. evaporation from the soil
6. transpiration from the plants.

The defining equations for each of the above subsystems are given below with the initial and boundary conditions and the assumptions necessary for the equations to be valid. All of the equations given are sometimes not valid for particular circumstances. Some of the equations assumed to define the particular subsystem are generally

not valid. The particular linear forms of the equations were assumed in order to use block diagram algebra to develop a block diagram of the relationships between subsystems.

Subsystem Defining Equations

The defining equation for heat transfer by conduction in the soil is:

$$\frac{\partial^2 T_{soil}}{\partial x^2} - \frac{1}{K_S} \frac{\partial T_{soil}}{\partial t} = 0 \qquad [1]$$

with initial and boundary conditions of:

$$T_{soil}(x,0) = T_o \qquad [1a]$$

$$T_{soil}(0,t) = T_S(t) \qquad [1b]$$

where:

T_{soil} = soil temperature
K_S = soil heat diffusivity
x = vertical distance
t = time
T_o = initial soil temperature
T_S = surface soil temperature

Equation [1] is valid for a homogeneous, isotropic soil with a constant soil heat diffusivity.

Moisture transfer in the soil transports some heat by convection, but more importantly moisture transferred to

the surface and converted to vapor results in large amounts of latent heat transfer. The defining equations for moisture transfer within soil provide a means for describing the processes that dynamically supply moisture for latent heat transfer. The result is a better description of the dynamic performance of the ET system.

Soil moisture transfer is a combination of vertical flow to the soil surface and radial flow to the roots of the plant. Phillip (1969) gives an equation for combined vertical and radial flow. The linearized form is:

$$\frac{\partial\theta}{\partial t} = \frac{K_\theta}{r}\frac{\partial}{\partial r}\left(r\frac{\partial\theta}{\partial r}\right) + K_\theta\frac{\partial^2\theta}{\partial x^2} - K_1\frac{\partial\theta}{\partial x} \qquad [2]$$

where:

θ = soil moisture content for combined flow

K_θ = soil moisture diffusivity (assumed constant)

r = radial distance from root

K_1 = derivative of the hydraulic conductivity with respect to moisture content (assumed constant)

Conceptually, Equation [2] has a radial flow component and a vertical flow component and these components may be considered individually.

The defining equation for vertical moisture movement alone is given from Equation [2] as:

$$K_\theta \frac{\partial^2 \theta_{soil}}{\partial x^2} - K_1 \frac{\partial \theta_{soil}}{\partial x} - \frac{\partial \theta_{soil}}{\partial t} = 0 \qquad [2a]$$

with initial and boundary conditions of:

$$\theta_{soil}\ (x,0) = \theta_o \qquad [2b]$$

$$\theta_{soil}\ (0,t) = \theta_S(t) \qquad [2c]$$

where:

θ_{soil} = volumetric soil moisture content for vertical flow

θ_o = initial soil moisture content

θ_S = surface soil moisture content

Phillip (1969) shows that Equation [2a] can be simplified further to give:

$$\frac{\partial^2 \theta^*}{\partial x^2} - \frac{1}{K_\theta} \frac{\partial \theta^*}{\partial t} = 0 \qquad [2d]$$

where:

$$\theta^*\ (x,t) = (\theta_{soil} - \theta_o)\ e^{-[(K_1\ x/2\ K_\theta) - (K_1^{\ 2}\ t/4K_\theta)]} \qquad [2e]$$

$$\theta^*\ (x,0) = 0 \qquad [2f]$$

$$\theta^*\ (0,t) = (\theta_S - \theta_o)\ e^{+(K_1^{\ 2}\ t/4K_\theta)} = \theta^*_S \qquad [2g]$$

Equation [2d] is of the form of Equation [1] and has the restricting assumption of a constant diffusivity. To permit the assumption of a constant diffusivity, moisture changes will be restricted to small increments about θ_o.

Phillip (1969) and Gardner (1959) have discussed the applicability of various forms of Equation [2d]. Approximate effects of gravity have been included.

The vertical component of Equation [2] was designated θ_{soil} and the radial component will be designated θ_{root}. The radial flow component of Equation [2] will now be written as a separate equation. The radial flow component which represents radial moisture movement to roots is described by the diffusion equation in cylindrical coordinates of the form:

$$\frac{\partial^2 \theta_{root}}{\partial r^2} + \frac{1}{r} \frac{\partial \theta_{root}}{\partial r} - \frac{1}{K_\theta} \frac{\partial \theta_{root}}{\partial t} = 0 \qquad [3]$$

with initial and boundary conditions of:

$$\theta_{root}\ (r,0) = \theta_o \qquad [3a]$$

$$\lim_{r \to r_o} \quad 2\pi r\ K_\theta \frac{\partial \theta}{\partial r} = -\ q_r \qquad [3b]$$

where:

r = radial distance from root

θ_{root} = soil moisture content for radial flow

r_o = outer radius of root

q_r = negative of volumetric flow per unit length of root. It is the transpiration rate per unit length of root.

Equation [3] is an equation for an infinite line sink with boundary condition [3b]. Thus, the equation is not appropriate at the surface at x = 0. At the surface radial flow is probably not as significant as vertical flow. At greater depths radial flow is significant and Equation [3] provides a means for dynamically removing water by transpiration. Gardner and Ehlig (1963) and Cowan (1965) have studied the applicability of various solutions of Equation [3].

For sensible heat transfer into the atmosphere the defining equation is:

$$\frac{\partial^2 T_{air}}{\partial x^2} - \frac{1}{K_A} \frac{\partial T_{air}}{\partial t} = 0 \qquad [4]$$

with initial and boundary conditions of:

$$T_{air}\ (x,0) = T_o \qquad [4a]$$

$$T_{air}\ (0,t) = T_S\ (t) \qquad [4b]$$

where:

T_{air} = air temperature

K_A = air heat diffusivity

To account for the effects of momentum transfer the effect of wind velocity must be considered. The assumption of a constant heat diffusivity, K_A, negates the effect of momentum transfer. The assumption was still necessary for the linear form of Equation [4]. For most conditions this is impractical. However, for some conditions the

assumption that K_A is constant over small increments of space may prove to be sufficient for practical purposes of analysis. Further, a constant K_A with height can perhaps be defined as a mean integrated diffusivity for x as defined by Gardner (1959) for K_θ for soil moisture.

Evaporation is dependent on vertical transfer of soil moisture to the soil surface. Transpiration depends upon radial flow of water to plant roots and then vertical transfer to the plant foliage. Radial flow into the roots of the plant is commonly assumed to be the process limiting water available for transpiration. Since two different dynamic equations are available, one to supply water for evaporation and one to supply water for transpiration, then latent heat transfer will be described by two equations, one for evaporation and one for transpiration.

The diffusion equation for evaporation from the soil surface is:

$$\frac{\partial^2 e_E}{\partial x^2} - \frac{1}{K_E} \frac{\partial e_E}{\partial t} = 0 \qquad [5]$$

with initial and boundary conditions of:

$$e_E\ (x,0) = e_o \qquad [5a]$$

$$e_E\ (0,\ t) = e_{ES}\ (t) \qquad [5b]$$

where:

e_E = specific humidity of air for evaporation

K_E = vapor diffusivity in air for evaporation

e_o = initial specific humidity

e_{ES} = specific humidity for evaporation at the soil surface

For transpiration from plants the defining equation is:

$$\frac{\partial^2 e_T}{\partial x^2} - \frac{1}{K_T} \frac{\partial e_T}{\partial t} = 0 \qquad [6]$$

with initial and boundary conditions of:

$$e_T\ (x,0) = e_o \qquad [6a]$$

$$e_T\ (0,t) = e_{TS}\ (t) \qquad [6b]$$

where: e_T = specific humidity of air for transpiration

K_T = vapor diffusivity of air for transpiration

e_{TS} = specific humidity for transpiration at the plant surface

The diffusivity of vapor into air is also influenced by momentum transfer. As in heat transfer, the diffusivity coefficient is assumed to be constant.

System Block Diagram Definition

The defining equations for evapotranspiration are second order, linear, partial differential equations of the diffusive type. A block diagram representation of the ET system will now be developed from the above equations.

Laplace transforms of the equations give the frequency domain representation of the system. In the frequency domain the system input and output can be related by algebraic equations, and the results can be shown in block diagram form (Melsa and Schultz, 1969, pp. 11-81).

Laplace transform of the time variable for the six equations for zero initial conditions gives:

$$\frac{d^2\overline{T}_{soil}}{dx^2} - \frac{p}{K_S}\overline{T}_{soil} = 0 \qquad [1c]$$

$$\frac{d^2\overline{\Theta}^*}{dx^2} - \frac{p}{K_\Theta}\overline{\Theta}^* = 0 \qquad [2d]$$

$$\frac{d^2\overline{\Theta}_{root}}{dr^2} + \frac{1}{r}\frac{d\overline{\Theta}_{root}}{dr} - \frac{p}{K_\Theta}\overline{\Theta}_{root} = 0 \qquad [3c]$$

$$\frac{d^2\overline{T}_{air}}{dx^2} - \frac{p}{K_A}\overline{T}_{air} = 0 \qquad [4c]$$

$$\frac{d^2\overline{e}_E}{dx^2} - \frac{p}{K_E}\overline{e}_E = 0 \qquad [5c]$$

$$\frac{d^2\overline{e}_T}{dx^2} - \frac{p}{K_T}\overline{e}_T = 0 \qquad [6c]$$

where p is called the Laplace transform parameter and the bar over the variable indicates the Laplace transform of the variable.

The roots of the characteristic equation of [1c] are:

$$(D^2 - \frac{p}{K_S})\ \overline{T} = 0 \qquad [7a]$$

$$D = \pm \sqrt{\frac{p}{K_S}} \qquad [7b]$$

D is the operator notation for d/dx and the Laplace transform of the boundary condition for Equation [1b] gives:

$$\mathcal{L}[T_S(0,t)] = \overline{T}_S(p) \qquad [8]$$

$\mathcal{L}$ indicates the Laplace transform

The solution of Equation [1c] in terms of the transform variables which requires that the temperature be finite as $x \to \infty$ and take on the value T_S as $x \to 0$ is:

$$\overline{T}(x,p) = \overline{T}_S(p)e^{-\sqrt{p/K_S}\ x} \qquad [1d]$$

where $\overline{T}_S$ is the surface temperature as the input and $\overline{T}(x,p)$ is the output.

The block diagram representation of this relationship is shown in Figure 1. The transfer function, H_1, is defined by:

$$H_1 = e^{-\sqrt{p/K_S}\ x} \qquad [1e]$$

and is explained as the operation of the system H_1 on $\overline{T}_S$ to produce $\overline{T}(x,p)$.

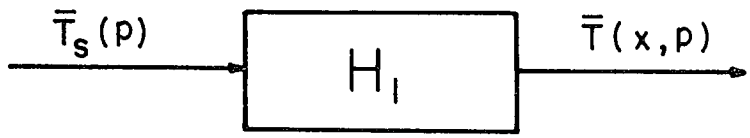

Figure 1. Block diagram of the soil heat transfer system

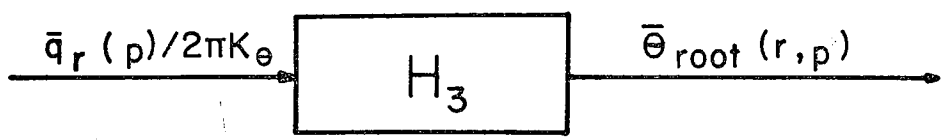

Figure 2. Block diagram of the radial flow of water to roots subsystem

The form of Equation [3c] for radial flow of water to roots is the modified Bessel equation and has a solution of the form (Hantush, 1964):

$$\bar{\theta}_{root}\ (r,p) = C_1\ K_o\ (r\sqrt{p/K_\theta}) + C_2\ I_o\ (r\sqrt{p/K_\theta}) \quad [9a]$$

and C_1 and C_2 are arbitrary constants to be evaluated from the boundary conditions. K_o is the modified Bessel function of zero order and second kind, and I_o is the modified Bessel function of zero order and first kind. The requirement that $\bar{\theta}_{root}\ (x,p)$ remain finite as $r \to \infty$ requires that $C_2 = 0$. The result is:

$$\bar{\theta}_{root}\ (r,p) = C_1\ K_o\ (r\sqrt{p/K_\theta}) \quad [9b]$$

From the boundary condition as $r \to r_o$ the evaluation of C_1 gives:

$$\bar{\theta}_{root}\ (r,p) = \frac{\bar{q}_r(p)}{2\pi K_\theta}\ K_o\ (r\sqrt{p/K_\theta}) \quad [9b]$$

where $\bar{q}_r(p)$ is the input or the rate of flow per unit length of the root and $\bar{\theta}\ (r,p)$ is the moisture content at any distance, r, taken radially from the root.

The block diagram representation of this relationship is shown in Figure 2. The transfer function, H_3, is given by:

$$H_3 = K_o\ (r\sqrt{p/K_\theta}) \qquad [4e]$$

Equations [1c] and [3c] were used to develop block diagrams for the subsystems for heat transfer in the soil and for water flow to roots. The defining equations for the other four subsystems may be used as was Equation [1c] to obtain the other four block diagrams.

The boundary conditions at the surface, $x = 0$, are defined in terms of the surface variables, θ^*_S, T_S, e_{ES}, e_{TS}. The energy balance equation is solved with T_S as the variable that achieves the energy balance. The specific humidities, e_{ES} and e_{TS}, are dependent variables that can be related to the surface temperature (Sellers, 1965, pp. 168-169). The moisture content, θ^*_S, is a dependent variable that can be related to the surface temperature and specific humidity (Ohmstede, 1966). The moisture content at the surface then defines the rate of moisture transfer to the surface by vertical moisture flow and by radial flow of water to roots. The flow rate, q_r, is thus related to the surface moisture content.

Since they are dependent, a new variable will be defined such that:

$$q_r \sim \theta^*_S \sim e_{ES} \sim e_{TS} = X_S \qquad [10]$$

where $\sim$ means is related to, and X_S uniquely specifies the values of the other variables.

The subsystems may be combined to describe the operation of an evapotranspiration system. The ET system is defined by the combined block diagram in Figure 3 with six subsystems acting in parallel. The input is net radiation, R_N.

Net radiation as an input to the ET system is a variable dependent upon total incoming and outgoing radiation. The outgoing radiation is a function of the surface temperature and other factors. It is possible to describe these relationships in Figure 3. However, the energy available for use by the ET system is the net radiation. Thus, the relationships between the various components of incoming and outgoing radiation have not been included.

The net radiation is a through variable and can be defined as the input of each subsystem or as an across variable that is a potential (Cannon, 1967, p. 32). Flow into each subsystem is from highest to lowest potential. Heat flow into each subsystem is positive and heat loss is negative.

The transfer functions H_2, H_4, H_5, and H_6 are defined by solutions of Equations [2d], [4c], [5c], and [6c] as:

$$H_2 = e^{-\sqrt{p/K_\Theta}\,x} \qquad [2e]$$

$$H_4 = e^{-\sqrt{p/K_A}\,x} \qquad [4e]$$

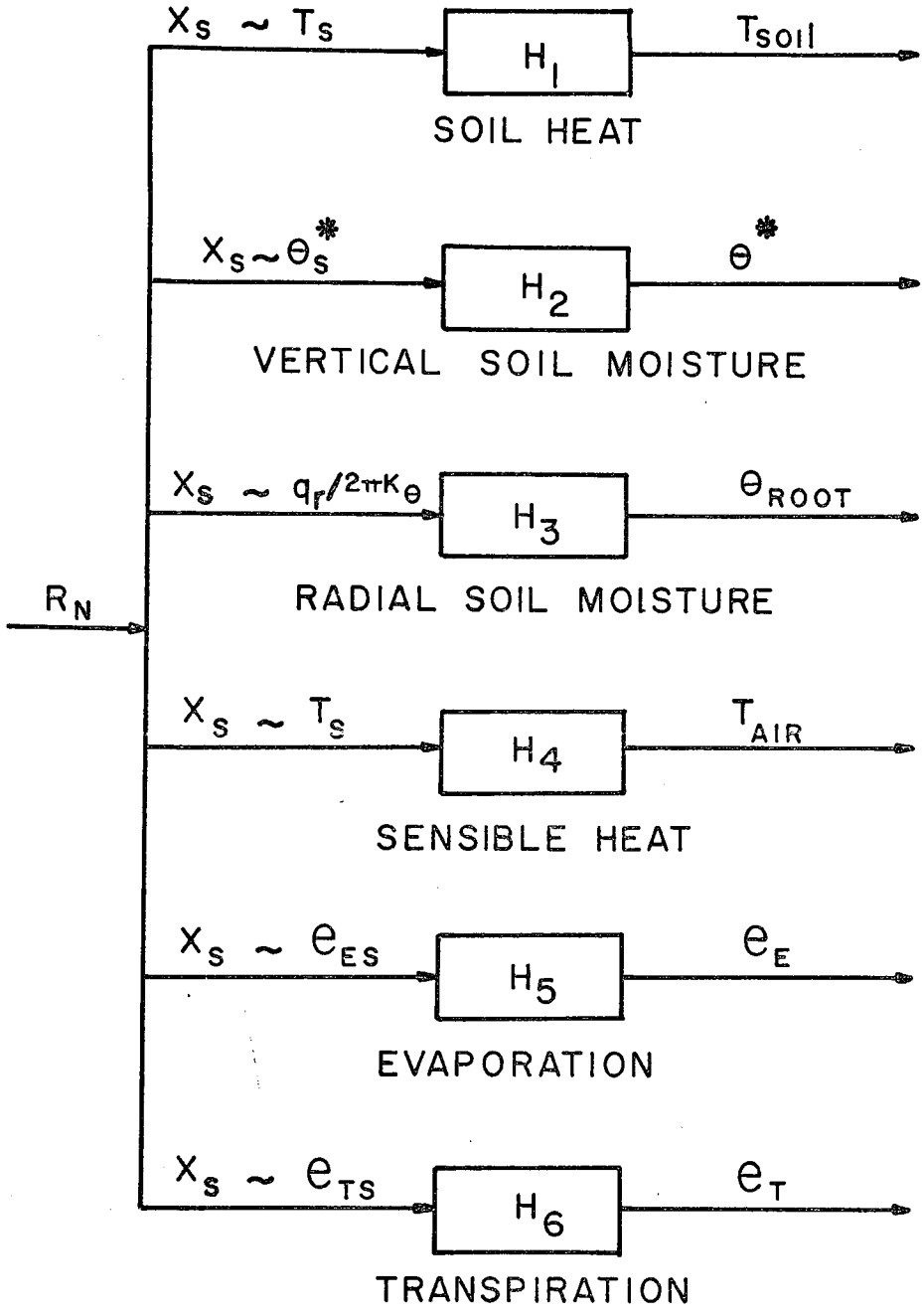

Figure 3. The evapotranspiration system as coupled subsystems

$$H_5 = e^{-\sqrt{p/K_E}\,x} \qquad [5e]$$

$$H_6 = e^{-\sqrt{p/K_T}\,x} \qquad [6e]$$

The block diagram of the ET system has been obtained.

The transfer functions defined by Equations [1e] through [6e] are in terms of the Laplace transform variable of time and the space variable, x. The inverse Laplace transforms of these functions define the time domain response of the subsystems. The frequency response is obtained by converting the Laplace transform to the Fourier transform.

The block diagram for the evapotranspiration system defined previously provides a conceptual definition of the relationships between the six subsystems of a relatively complex system. Segments of the system can be isolated for detailed study as, for example, isolating the subsystem that transfers heat within the soil. When a mathematical representation for a subsystem has been shown to adequately represent the real system, then the components may be placed together to represent the real subsystem. Thus, the block diagram for the system provides the basis for understanding the operation of the total system and for studying in detail each subsystem.

LINEAR SYSTEMS THEORY

The soil heat transfer subsystem was studied by the application of systems analysis and time series analysis. This section presents the basic theory of linear systems analysis necessary for the study.

Systems Analysis

Schwarz and Friedland (1965, pp. 1-2) defined a system as "... a collection of interconnected components in which there is specified a set of dynamic variables called inputs, or excitations, and another set called responses, or outputs." The objective of systems analysis is to determine the response of the system to a specified set of excitations or inputs.

A system is linear if it satisfies the principle of superposition (Schwarz and Friedland, 1965, p. 12). Mathematically,

$$H(A\ X_1 + B\ X_2) = A\ HX_1 + B\ HX_2 \qquad [12]$$

where

A, B are constants

H is the operator on X to produce a response or the system transfer function

X is the input to the system.

A system is linear if, and only if, it has the properties of additivity and homogeneity. If the response of the system to an input, X_1, is Y_1 and the response to an input, X_2, is Y_2, then the additive property of linear systems requires that the response of the system to the input, $X_1 + X_2$, be the sum of the responses, $Y_1 + Y_2$. It can be shown that the additive property implies the homogeneous property. A system is linear also if its behavior can be described by a linear differential equation.

Another important property of a system is time-invariance (stationarity) which is defined as a condition where the input and output relations do not change with time (Schwarz and Friedland, 1965, p. 7). The time-invariance property means that the response of the system to an input depends only on the shape of the input, and not on the time of application.

A causal system is one whose response to an input does not depend on future values of the input. A causal system is analogous to a physical system in that physical systems do not anticipate inputs.

A system may further be classified as dynamic or instantaneous (Schwarz and Friedland, 1965, pp. 10-11). An instantaneous system has an output at time, t_1, that depends only upon the input at time, t_1. Otherwise, the system is said to be dynamic. Thus, a dynamic system is a system that

has memory, and the output at any time, t_1, depends not only upon the input at time, t_1, but on past values of input also.

For a linear system the unit impulse response or any of the related elementary functions (i.e., unit step response, unit ramp response, etc.) completely characterize the system (Schwarz and Friedland, pp. 66-79). Thus, if the unit impulse response of a system is known, then the response of the system to any input can be determined, since any input function can be resolved into a continuum of impulse inputs.

The input and output relationship for a linear system is defined by the convolution integral (Jenkins and Watts, 1968, pp. 34-36). For a linear, time-invariant system the convolution relationship is written as:

$$Y(t) = \int_0^t h(t - \tau)\, X(\tau)\, d\tau \qquad [13]$$

$Y(t)$ is the system response at time, t.

$h(t - \tau)$ is the system impulse response at τ, $\tau \leq t$

$X(\tau)$ is the input to the system

Convolution involves the displacement of each $h(\tau)$ by t, folding of $h(t - \tau)$ about $t = 0$, and integration under the product curve of $[X(\tau)]\ [h(t - \tau)]$. Physically, convolution is the weighting of the input $X(\tau)$ from $\tau = 0$ to $\tau = t$ to produce the response $Y(t)$.

The convolution integral is of great importance in linear systems because if either of two characteristics are known, that is $Y(t)$, $h(t)$, or $X(t)$, then the other property

can be determined. Also, by using an input and output for the model identical to a physical system, then differences between h(t) for the model and h(t) for the system can be determined. Thus, the adequacy of the model in representing the physical system can be investigated. Techniques are also available to improve the adequacy of h(t) for the model in representing h(t) for the physical system.

The frequency response of a linear system is the steady-state response of the system to an oscillatory or sinusoidal input. Frequency response analysis has mathematical foundation, commonly by Fourier and Laplace transforms, and frequency response characteristics of a system can be determined experimentally. An extension of frequency response analysis is generalized harmonic analysis.

Harmonic analysis is the statistical analysis of time series of input and output for a linear system. Thus, not only does frequency response provide system characteristics, it also provides a means for conversion of experimental data to a form convenient for comparison with analytical results. It also permits the comparison of the results from statistical analysis of input and output functions for the system with the analytically assumed response developed from the mathematical model.

Schwarz and Friedland (1965, p. 184) show that the convolution relationship expressed by Equation [13] can be transformed by Laplace transform to obtain:

$$\bar{Y}(p) = \bar{H}(p)\ \bar{X}(p) \qquad [14]$$

where:

$\bar{Y}(p)$ = the steady state frequency response output

$\bar{H}(p)$ = the complex frequency response function

$\bar{X}(p)$ = the sinusoidal system input

The great utility of the Laplace transform is that $\bar{H}(p)$ is identically the Laplace transform of the impulse response function $h(t-\tau)$ given in Equation [13].

Substitution of the relation: $p = \sigma + i\omega$ with $\sigma = 0$ into Equation [14] obtains the frequency response defined by:

$$Y(i\omega) = H(i\omega)\ X(i\omega) \qquad [15]$$

Equation [15] is equivalent to the Fourier transform of Equation [13] and will be used later in time series analysis of data.

Frequency domain analysis provides two very useful advantages. One is that the difficult integration required in Equation [13] has been reduced to a simple multiplication, Equation [14], in order to obtain system response in the frequency domain. The other is that each segment of a true sinusoidal signal has been transformed to the frequency domain. The ratio of input to output can be used to define the system frequency response and the system constant determined using the experimental data. Convolution in the frequency domain is then used to obtain the response to all the sinusoidal signals that combine to make up the input. This advantage

or principle is the dominant justification for time series analysis of system data.

Time Series Analysis

The representation of time series by trigonometric functions is a part of Fourier analysis or harmonic analysis. With this method an aperiodic function can be represented by a finite number of sine or cosine functions. The aperiodic function is obtained by adding the finite number of harmonics necessary to reproduce the original signal.

It is difficult to describe how the transformation of a number of discrete data points that describe a time series can be transformed into a frequency domain. However, the time series, represented by the finite number of discrete data points, can be represented by the sum of a number of sine functions. Each of the sine functions is then multiplied by a complex exponential and integrated to transform each of the harmonics or sine functions into the frequency domain. In the frequency domain, the frequency representation of the original signal is obtained by summing the harmonics that were transformed into that domain.

The concepts discussed above can be illustrated by a simple example using harmonic analysis. Figure 4 is the graph of temperature versus time for a sinusoidal temperature variation. The amplitude is labelled ΔT and the period, P, is equal to the time for one full cycle of the sine wave.

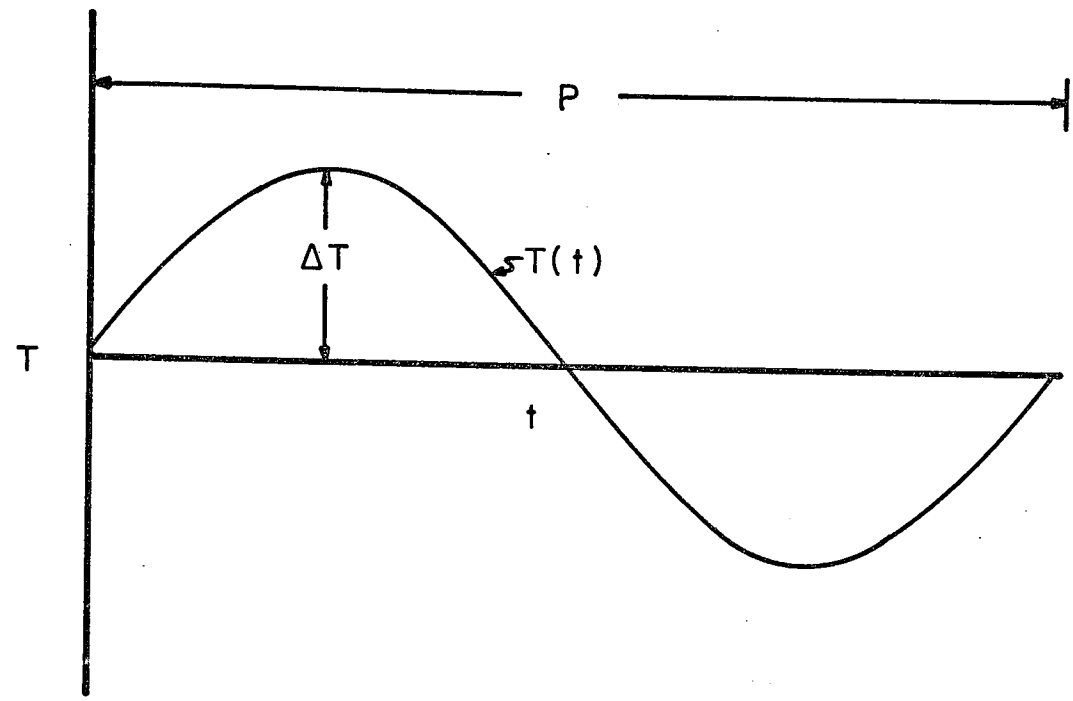

Figure 4. A graph of sinusoidal temperature variation

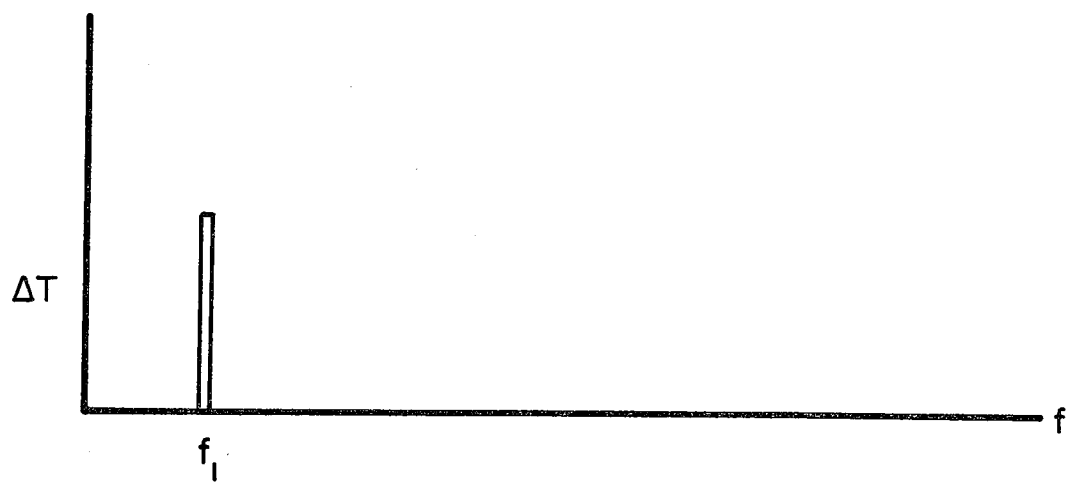

Figure 5. Frequency domain graph of sinusoidal temperature variation

The transformation of this time signal into the frequency domain results in the graph in Figure 5 where T is the amplitude as previously indicated in Figure 4 and f_1 is identically equal to $\frac{1}{p}$. Thus, a continuous time series that is a perfect sine wave in the time domain can be represented by a point in the frequency domain.

Figure 6 is the representation of a function, T(t), which is the sum of two sine waves. The first approximation is one sine wave, $T_1(t)$, which transformed into the frequency domain is shown in Figure 7a. A better representation of this signal is obtained by the sum of the two sine waves as shown in Figure 6. Transformation of those two sine waves results in the two points distributed at the two frequencies shown in Figure 7b. The total amplitude of the signal at any time would be the sum of the amplitudes of the two individual sine waves of different frequencies. Thus, the representation of any time signal by Fourier transform of each harmonic is the process of transformation into the frequency domain of a time series represented by discrete data points.

Time Domain Analysis

Time series analysis of discrete data from input and output of a system has been used for a number of different applications. Jenkins and Watts (1968) present the theory and some applications of time series analysis. A brief general description of the concepts of time series analysis

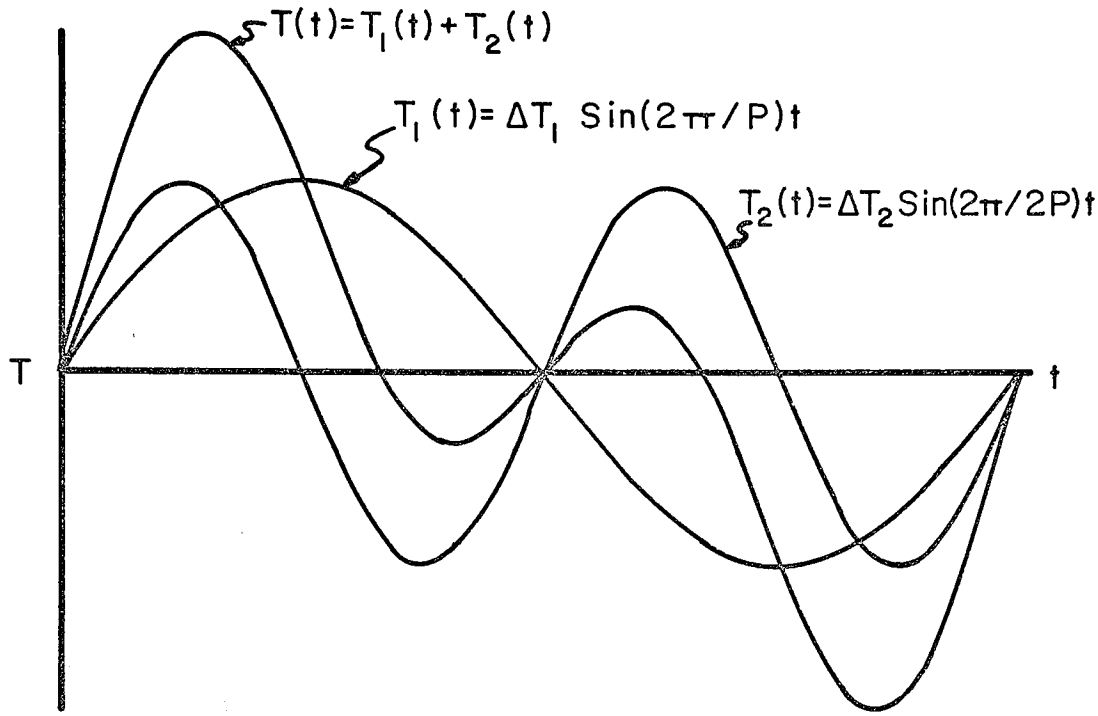

Figure 6. Two sine waves and the sum of two sine waves

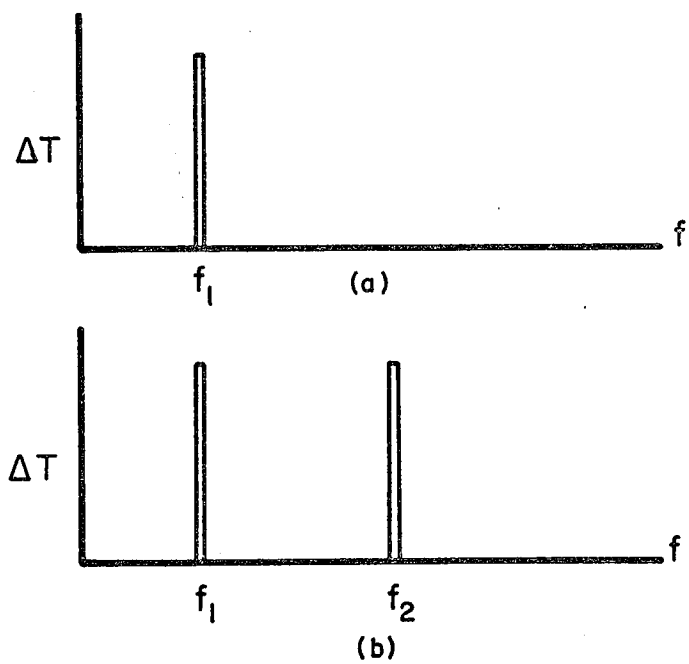

Figure 7. Frequency domain representation of one and two sine waves

will be presented here. The detailed theory and assumptions are given in Jenkins and Watts (1968).

A time series of discrete data points sampled at constant intervals can be represented by another relationship known as the autocorrelation function. The autocorrelation function is a function that presents the distribution of the mean and the distribution of variance as a function of lag between the initial data point and succeeding data points.

The autocovariance function is defined by (Jenkins and Watts, 1968, p. 149):

$$\gamma_{XX}(u) = E[(X(t) - \mu)(X(t+u) - \mu)] = \text{Cov}[X(t), X(t+u)] \quad [16]$$

where $\gamma_{XX}(u)$ is the autocovariance function as a function of lag, u; X(t) is the discrete values of the time series; μ is the mean of the array of discrete values of the time series; $E[(X(t) - \mu)]$ is the expected value of the time series; and Cov is the covariance of X(t) and X(t + u)

The autocorrelation function is defined by:

$$\rho_{XX}(u) = \frac{\gamma_{XX}(u)}{\gamma_{XX}(o)} \quad [17]$$

and is defined as the autocovariance function at lag, u, divided by the autocovariance function at zero lag or the variance of the time series.

The autocovariance function is estimated by:

$$\hat{c}_{xx}(u) = \frac{1}{N} \sum_{t=1}^{N-u} (X_t - \bar{X})\,(X_{t+u} - \bar{X}),\quad 0 \leq u \leq L - 1 \qquad [18]$$

and

$$\bar{X} = \frac{1}{N} \sum_{t=1}^{N} X_t$$

where N is the number of discrete data points; u is discrete time; L is the number of covariance lags; and $\bar{X}$ is the mean of the time series.

The autocorrelation function is estimated by:

$$\hat{r}_{xx}(u) = \frac{\hat{c}_{xx}(u)}{\hat{c}_{xx}(0)} \qquad [19]$$

When dealing with data of different scales of measurement, the autocorrelation function is used and it gives a visual picture of the manner in which the dependence between values of a series damps out as a function of time. However, its principal use is as an intermediate step in transferring the data into the frequency domain.

When two time series are involved, for example, the input and output of a linear system, then the cross covariance function is defined (Jenkins and Watts, 1968, p. 324):

$$\gamma_{xy}(u) = E\,[(X_x(t) - \mu_x)\,(X_y\,(t+u) - \mu_y)] \qquad [20a]$$

$$\gamma_{yx}(u) = E\,[(X_y(t) - \mu_y)\,(X_x(t+u) - \mu_y)] \qquad [20b]$$

where X_x is the input and X_y is the output of the linear system. The cross covariance function between the two time series can be described as above with two functions. The two functions are related by:

$$\gamma_{xy}(u) = \gamma_{yx}(-u) \qquad [20c]$$

The two functions may be replaced by one function, $\gamma_{xy}(u)$, which is defined over equal intervals on both sides of zero.

The cross covariance function, $\gamma_{xy}(u)$, defined over positive and negative intervals may be written as the sum of an even part $\lambda_{xy}(u)$ and an odd part $\psi_{xy}(u)$ as (Jenkins and Watts, 1968, p. 346):

$$\lambda_{xy}(u) = \frac{1}{2}\,[\gamma_{xy}(u) + \gamma_{xy}\,(-u)] \qquad [20d]$$

$$\psi_{xy}(u) = \frac{1}{2}[\gamma_{xy}(u) - \gamma_{xy}\,(-u)] \qquad [20e]$$

The cross correlation function is defined by:

$$\rho_{xy}(u) = \frac{\gamma_{xy}(u)}{\gamma_{xx}(0)\gamma_{yy}(0)} \qquad [21]$$

The cross covariance function is estimated by:

$$\hat{c}_{xy}(u) = \frac{1}{N} \sum_{t=1}^{N-u} (X_{xt}-\bar{X}_x)\,(X_{yt+u}-\bar{X}_y),\ 0 \le u \le L-1 \qquad [22a]$$

$$\hat{c}_{xy}(-u) = \frac{1}{N} \sum_{t=1}^{N-u} (X_{xt+u}-\bar{X}_x)\,(X_{yt}-\bar{X}_y),\ 0 \le u \le L-1 \qquad [22b]$$

$$\bar{X}_i = \frac{1}{N} \sum_{t=1}^{N} X_{it}, \quad i = x,y$$

The cross correlation function is estimated by:

$$\hat{r}_{xy}(u) = \frac{\hat{c}_{xy}(u)}{\sqrt{\hat{c}_{xx}(0)\hat{c}_{yy}(0)}} \qquad [23]$$

Equation [13] defined the relationships between the input and output for a linear system and states that the output can be calculated by taking a weighted average of the input with the weighting function $h(\tau)$. Jenkins and Watts (1968, p. 154-155) show that the linear system can be defined by:

$$\gamma_{xy}(u) = \int_{-\infty}^{\infty} h(v)\ \gamma_{xx}(u-v)\ dv, \quad u \geq 0 \qquad [24]$$

Of great importance is the fact that the linear system which best approximates the given process is completely defined by the covariance functions $\gamma_{xx}(u)$ and $\gamma_{xy}(u)$. Time series analysis and linear systems analysis are thus related. An alternate way of stating the relationship given in Equation [24] is, given time series of input, X, and output, Y, the weighting function, h (v), can be identified. Equation [24] has the form of the convolution relation given previously by Equation [13].

Frequency Domain Analysis

Since discrete data can be adequately represented by the covariance function, a basis is provided for transformation of time series into the frequency domain. Jenkins and Watts (1968) show that the Fourier transform of the autocovariance function is the spectrum for the time series being analyzed.

The power spectrum of a linear process is defined by Jenkins and Watts (1968, p. 217) as:

$$\Gamma_{xx}(f) = \int_{-\infty}^{\infty} \gamma_{xx}(u)\, e^{-i2\pi f u}\, du \qquad [25]$$

and $\Gamma_{xx}(f)$ is the theoretical power spectrum, and the other symbols have been previously defined.

Equation [25] shows that the power spectrum is the Fourier transform of the autocovariance function of the process. The spectrum shows how the variance of the X(t) process is distributed with frequency.

The spectral density function is defined by:

$$\frac{\Gamma_{xx}(f)}{\gamma_{xx}(0)} = \int_{-\infty}^{\infty} \rho_{xx}(u)\, e^{-i2\pi f u}\, du \qquad [26]$$

and is the Fourier transform of the autocorrelation function.

The smoothed spectral estimate of the power spectrum is given by Jenkins and Watts (1968, p. 259) as:

$$\hat{C}_{xx}(f) = \Delta \sum_{u=-(L-1)}^{L-1} W(u)\ \hat{c}_{xx}(u)\ e^{-i2\pi fu\Delta},\ \frac{-1}{2\Delta} \leq f < \frac{1}{2\Delta}$$

[27]

and W(u) is the lag window for smoothing; L is the number of lags and equals M/Δ; M is the truncation point for the lag window; and Δ is the sampling interval for the time series.

The smoothed spectral density function is defined by:

$$\hat{R}_{xx}(f) = \Delta \sum_{u=-(L-1)}^{L-1} W(u)\ \hat{r}_{xx}(u)\ e^{-i2\pi fu\Delta},\ \frac{-1}{2\Delta} \leq f < \frac{1}{2\Delta}$$

[28]

More simplified versions of these formulae are given by Jenkins and Watts (1968, pp. 259-261).

The cross spectrum is defined by Jenkins and Watts (1968, p. 347) as:

$$\Gamma_{xy}(f) = \int_{-\infty}^{\infty} \gamma_{xy}(u)\ e^{-i2\pi f\ u}\ du \qquad [29]$$

and shows that the cross spectrum is the Fourier transform of the cross covariance function. Two additional representations of the cross spectrum are available. The first is:

$$\Gamma_{xy}(f) = \alpha_{xy}\ (f)\ e^{+i\phi_{xy}(f)} \qquad [30]$$

where α_{xy} is the cross amplitude spectrum and ϕ_{xy} is the phase spectrum.

The second representation is:

$$\Gamma_{xy}(f) = \Lambda_{xy}(f) - i\ \Psi_{xy}(f) \qquad [31]$$

and Λ_{xy} is the co-spectrum and Ψ_{xy} is the quadrature spectrum.

The cross correlation function measures the correlation between two processes at different lags. The cross spectrum gives the distribution of covariance with frequency.

The cross spectrum is a complex quantity and may be defined as the product of a real function that is the cross amplitude spectrum and a complex function that is the phase function. This relationship is given by Equation [30]. The cross amplitude spectrum shows how the amplitudes at a particular frequency in one series are related to the amplitudes of another series at the same frequency. The phase spectrum shows whether a frequency component in one series leads or lags the component at the same frequency in the other series.

Since the cross spectrum is a complex quantity it may also be represented as the sum of a real part and an imaginary part. This definition is given in Equation [31].

The real part, $\Lambda_{xy}(f)$, measures the in-phase covariance between the two time series. Called the co-spectrum it is defined by:

$$\Lambda_{xy}(f) = \int_{-\infty}^{\infty} \lambda_{xy}(u)\ \cos\ 2\pi fu\ du \qquad [32a]$$

The complex part of Equation [31], $\Psi_{xy}(f)$, is called quadrature and measures the out of phase covariance between the two time series. The quadrature, Ψ, spectrum is defined by:

$$\Psi_{xy}(f) = \int_{-\infty}^{\infty} \psi_{xy}(u) \sin 2\pi fu \, du \qquad [32b]$$

The quadrature spectrum is an odd function of frequency.

The amplitude and phase spectrum and the co-spectrum and quadrature spectrum are related by the following equations:

$$\alpha_{xy}(f) = \sqrt{\Lambda^2_{xy}(f) + \Psi^2_{xy}(f)} \qquad [33a]$$

$$\phi_{xy}(f) = \arctan - \frac{\Psi_{xy}(f)}{\Lambda_{xy}(f)} \qquad [33b]$$

The previous relationships, Equations [29] through [33], that define the cross spectrum now can be combined with the spectrum to use the principles of time series analysis to define a linear system. The convolution equation as defined in terms of the input and output for a linear system was given previously in Equation [13]. The convolution relationship written in terms of the autocorrelation and cross correlation function was given also by Equation [24]. Transforming Equation [24] using the previously defined relationships for the transforms of the autocorrelation and cross correlation functions gives:

$$\Gamma_{xy}(f) = H(f)\ \Gamma_{xx}(f) \qquad [34]$$

Solving Equation [34] for the frequency response function gives:

$$H(f) = \frac{\Gamma_{xy}(f)}{\Gamma_{xx}(f)} \qquad [35]$$

The convolution of two time series in the frequency domain by use of Fourier techniques or time series analysis is given by Equation [34]. This convolution in the frequency domain is a multiplication operation instead of the difficult integration equation given by Equation [24].

The frequency response function defined by Equation [35] can be defined in terms of the cross amplitude spectrum (frequently called gain function) and phase spectrum of Equation [30]. The gain and phase function are related to the amplitude and phase function and thus can be related to the co-spectrum and quadrature spectrum as previously defined. This relationship is:

$$H(f) = G(f)\ e^{+i\phi(f)} = \frac{\Lambda_{xy}(f) - i\ \Psi_{xy}(f)}{\Gamma_{xx}(f)} \qquad [36]$$

The frequency response function, the gain function, and the phase function are now defined in terms of the co-spectrum and quadrature spectrum of the time series of input and output for the linear system. A procedure is provided for defining the gain and phase function for a linear system

by use of statistical analysis of time series of input and output. Thus, system identification can be achieved through statistical analysis of these time series.

The equations that relate the gain function and phase function to the spectra of the time series are:

$$G(f) = \frac{\sqrt{\Lambda^2_{xy}(f) + \Psi^2_{xy}(f)}}{\Gamma_{xx}(f)} = \frac{\alpha_{xy}(f)}{\Gamma_{xx}(f)} \qquad [37a]$$

$$\phi(f) = \arctan - \frac{\Psi_{xy}(f)}{\Lambda_{xy}(f)} \qquad [37b]$$

If the cross amplitude spectrum is a measure of the covariance between the time series of input and output at a particular frequency, and the power spectrum the variance in the input at a particular frequency, then the gain function is analogous to a regression coefficient but it is evaluated at each frequency.

Jenkins and Watts (1968, p. 352-353) define the squared coherency as:

$$K_{xy}^2(f) = \frac{\alpha^2_{xy}(f)}{\Gamma_{xx}(f)\,\Gamma_{yy}(f)} \qquad [38]$$

A plot of K_{xy}^2 is called the squared coherency spectrum which is a measure of the predictability of amplitude in the output when the amplitude of the input is known. For example, if the squared coherency is one, then the predictability of

the output when the input is known is perfect. The squared coherency is analogous to the squared correlation coefficient except that the squared coherency is evaluated at each frequency. When the squared coherency is zero, this implies that there is no relationship between the input and output functions. Intermediate values between zero and one imply that noise (i.e., errors in data measurements) exists in the time series of input or the time series of output or both.

The previously defined relationships for the various spectrums of the time series of input and output are defined theoretically. Jenkins and Watts (1968, pp. 382-383) define the smoothed spectral estimators for the previously defined theoretical spectrum. The smoothed covariance and cross variance functions have already been defined, Equations [18], [22a], and [22b].

The even and odd cross covariance estimates are defined by:

$$\hat{i}_{xy}(u) = 1/2\ [\hat{c}_{xy}(u) + \hat{c}_{xy}(-u)],\ 0 \leq u \leq L-1 \qquad [39a]$$

$$\hat{q}_{xy}(u) = 1/2\ [\hat{c}_{xy}(u) - \hat{c}_{xy}(-u)],\ 0 \leq u \leq L-1 \qquad [39b]$$

The smoothed co-spectrum and quadrature spectrum estimates are defined by:

$$\hat{L}_{xy}(f) = 2[\hat{l}_{xy}(0) + 2 \sum_{u=1}^{L-1} \hat{l}_{xy}(u)W(u) \cos \frac{\pi iu}{F}, \quad 0 \leq f \leq F \qquad [40a]$$

$$\hat{Q}_{xy}(f) = 4 \sum_{u=1}^{L-1} \hat{q}_{xy}(u)W(u) \sin \frac{\pi iu}{F}, \quad 1 \leq f \leq F - 1 \qquad [40b]$$

$$\hat{Q}_{xy}(0) = \hat{Q}_{xy}(F) = 0 \qquad [40c]$$

The smooth cross amplitude spectrum estimate is defined by:

$$\hat{A}_{xy}(f) = \sqrt{\hat{L}^2_{xy}(f) + \hat{Q}^2_{xy}(f)}, \quad 0 \leq f \leq F \qquad [41]$$

The gain and phase functions are defined by (Jenkins and Watts, 1968, p. 430):

$$\hat{G}(f) = \frac{\hat{A}_{xy}(f)}{\hat{C}_{xx}(f)} \qquad [42]$$

$$\hat{\phi}(f) = \arctan - \frac{\hat{Q}_{xy}(f)}{\hat{L}_{xy}(f)} \qquad [43]$$

The smoothed squared coherency spectrum estimate is defined by:

$$\hat{K}^2_{xy}(f) = \frac{\hat{A}^2_{xy}(f)}{\hat{C}_{xx}(f)\ \hat{C}_{yy}(f)}, \quad 0 \leq f \leq F \qquad [44]$$

When time series of different scales of measurement are to be compared then the equivalent spectral density functions may also be derived. These relationships are now

available for the definition of the spectrum for time series of input and output for a linear system. These time series will be used only for system identification, but the resulting relationships will be used for system simulation.

Linear systems theory as appropriate for analytical and experimental data analysis has been reviewed. These theories will now be applied to the analysis of the soil heat transfer subsystem.

Table 1 summarizes the theoretical and estimation formulae for time series analysis.

TABLE 1

Summary of theoretical formulae as well as formulae for estimating properties of discrete data for time series analysis.

Theoretical Autocovariance		Estimate	
$\gamma_{xx}(u) = E[X(t)-\mu)(X(t+u)-\mu)]$	[16]	$\hat{c}_{xx}(u) = \frac{1}{N}\sum_{t=1}^{N-u}(X_t-\bar{X})(X_{t+u}-\bar{X})$, $u=0,1,\ldots,N-1$	[18]
		$\bar{X} = \frac{1}{N}\sum_{t=1}^{N} X_t$	
Crosscovariance			
$\gamma_{xy}(u) = E[(X_x(t)-\mu_x)(X_y(t+u)-\mu_y)]$	[20]	$\hat{c}_{xy}(u) = \frac{1}{N}\sum_{t=1}^{N-u}(X_{xt}-\bar{X}_x)(X_{yt+u}-\bar{X}_y)$, $u\geq 0$	[22a]
		$\hat{c}_{xy}(-u) = \frac{1}{N}\sum_{t=1}^{N-u}(X_{xt+u}-\bar{X}_x)(X_{yt}-\bar{X}_y)$, $0\leq u\leq L-1$	[22b]
		$\bar{X}_i = \frac{1}{N}\sum_{t=1}^{N} X_{it}$, $i = x, y$	

TABLE 1--Continued

Summary of theoretical formulae as well as formulae for estimating properties of discrete data for time series analysis.

Power Spectrum

$$\Gamma_{xx}(f) = \int_{-\infty}^{\infty} \gamma_{xx}(u)\, e^{-i2\pi fu}\, du \qquad [25]$$

$$\hat{C}_{xx}(f) = \Delta \sum_{u=-(L-1)}^{L-1} W(u)\, \hat{c}_{xx}(u)\, e^{-i2\pi fu\Delta}, \qquad \frac{1}{2\Delta} \leq f \leq \frac{1}{2\Delta} \qquad [27]$$

Cross Spectrum

$$\Gamma_{xy}(f) = \int_{-\infty}^{\infty} \gamma_{xy}(u)\, e^{-i2\pi fu}\, du \qquad [29]$$

$$= \alpha_{xy}(f)\, e^{+i\phi_{xy}(f)} \qquad [30]$$

$$\hat{1}_{xy}(u) = \frac{1}{2}\,[c_{xy}(u) + c_{xy}(-u)], \qquad 0 \leq u \leq L-1 \qquad [39a]$$

TABLE 1--Continued

Summary of theoretical formulae as well as formulae for estimating properties of discrete data for time series analysis.

$$\Gamma_{xy}(f) = \Lambda_{xy}(f) - i\,\Psi_{xy}(f) \qquad [31]$$

Co-spectrum

$$\Lambda_{xy}(f) = \int_{-\infty}^{\infty} \lambda_{xy}(u) e^{-i2\pi fu}\, du$$

$$= \frac{1}{2} \int_{-\infty}^{\infty} [\gamma_{xy}(u) + \gamma_{xy}(-u)]$$

$$\cos\, 2\pi fu\, du \qquad [32a]$$

Quadrature Spectrum

$$\Psi_{xy}(f) = \int_{-\infty}^{\infty} \psi_{xy}(u)\, e^{-i2\pi fu}\, du$$

$$\hat{q}_{xy}(u) = \frac{1}{2}\,[c_{xy}(u) - c_{xy}(-u)],$$

$$0 \le u \le L-1 \qquad [39b]$$

$$\hat{L}_{xy}(f) = 2[\hat{l}_{xy}(0) + 2 \sum_{u=1}^{L-1} \hat{l}_{xy}(u) \cos\frac{\pi iu}{F}],$$

$$0 \le f \le F \qquad [40a]$$

$$\hat{Q}_{xy}(f) = 4 \sum_{u=1}^{L-1} q_{xy}(u)\, W(u)\, \sin\frac{\pi iu}{F},$$

$$1 \le f \le F-1 \qquad [40b]$$

TABLE 1--Continued

Summary of theoretical formulae as well as formulae for estimating properties of discrete data for time series analysis.

$$\Psi_{xy}(f) = \frac{1}{2}\int_{-\infty}^{\infty}[\gamma_{xy}(u) - \gamma_{xy}(-u)$$

$$\sin 2\pi f u\,du \qquad [32b]$$

Cross Amplitude Spectrum

$$\alpha_{xy}(f) = |\Gamma_{xy}(f)|$$

$$= \sqrt{\Lambda^2_{xy}(f) + \Psi^2_{xy}(f)} \qquad [33a]$$

$$\hat{A}_{xy}(f) = \sqrt{\hat{L}^2_{xy}(f) + \hat{Q}^2_{xy}(f)}, \qquad 0 \leq f \leq F \qquad [41]$$

Phase Spectrum

$$\phi_{xy}(f) = \arctan -\left[\frac{\Psi_{xy}(f)}{\Lambda_{xy}(f)}\right] \qquad [33b]$$

$$\hat{\phi}(f) = \arctan - \frac{\hat{Q}_{xy}(f)}{\hat{L}_{xy}(f)}, \quad 0 \leq f \leq F \qquad [42]$$

TABLE 1--Continued

Summary of theoretical formulae as well as formulae for estimating properties of discrete data for time series analysis.

Gain Spectrum

$$G(f) = \frac{\alpha_{xy}(f)}{\Gamma_{xx}(f)} \qquad [37a]$$

$$\hat{G}(f) = \frac{\hat{A}_{xy}(f)}{\hat{C}_{xx}(f)} \qquad [42]$$

Coherency Spectrum

$$K^2_{xy}(f) = \frac{\alpha^2_{xy}(f)}{\Gamma_{xx}(f)\Gamma_{yy}(f)} \qquad [38]$$

$$\hat{K}^2_{xy}(f) = \frac{\hat{A}^2_{xy}(f)}{\hat{C}_{xx}(f)\ \hat{C}^2_{yy}(f)} \qquad [44]$$

LINEAR SYSTEMS ANALYSIS OF HEAT FLOW IN THE SOIL

Calculations and measurement of heat flow within the soil are useful in a number of applications, including agriculture, meteorology, and engineering. Analytical approaches to heat flow problems have been divided into two methods. The first is an analytical model based on the mathematical law of heat conduction, and the second is based on analysis of temperature data by Fourier analysis.

The analytical model is limited by the assumptions implied in the method, i.e., the assumptions of homogeneity, constant diffusivity, and the particular form assumed for the input. The Fourier analysis method is limited by the same assumptions and is also only an approximate representation of temperature with time and depth in a soil. Temperatures do not vary exactly as a sinusoid as assumed in Fourier analysis.

Wierenga (1968) applied an iterative solution of the finite difference approximation of the diffusion equation to obtain a diffusivity that provides the best fit to measured temperature data. His method allows arbitrary time variations of temperature and permits non-constant diffusivity distributions with depth. The limitations for stability for the finite difference approximation of the

diffusion equation are imposed. The coupling of analytical and experimental results as in linear systems theory and time series analysis is not provided. Wierenga (1968) has also given an up-to-date review of the development and current state of soil temperature analysis.

Current methods of analysis assume that the process of heat flow in a soil is linear. This use of the word linear is in the context of systems analysis. Linear systems analysis can thus be applied directly to the analysis of the problem of heat flow in a soil by either of two methods. The first method is analytical and the results are useful because the restriction of sinusoidal inputs has been removed and the response of the system to any input can be calculated. The second method of time series analysis permits the analysis of discrete data for a linear system. The data are used for definition of the model, that is, system constant identification, and may also be used to predict system behavior, that is, system simulation. Again, no restrictions on the nature of the input are implied.

An additional advantage of linear systems analysis is that the heat flow process can be considered a subsystem of multiple transport processes and the total system analyzed. For example, extension of this analysis would be to consider changes of diffusivity as a time varying system constant and heat transport by moisture transport as an additional input to the heat flow system.

In the following section the analytical equations used to define the soil heat transfer subsystem are presented. The conceptual relationships, and the procedures for system identification and system simulation using the analytical equations from time series analysis are also described.

Time Domain Analysis

The equation for soil heat transfer for a homogeneous medium was given previously as:

$$\frac{\partial^2 T}{\partial x^2} - \frac{1}{K} \frac{\partial T}{\partial t} = 0 \qquad [1]$$

and the symbols are as previously defined. Since all diffusivities and temperatures refer to the soil, the subscripts referring to soil and air have been dropped.

If the surface temperature is assumed to be given by:

$$T(0,t) = T_a + \Delta T_S \sin \omega t \qquad [45]$$

where:

$T(0,t)$ is the temperature at $x = 0$ and time, t

T_a is the average daily or annual soil temperature

ΔT_S is the amplitude of the surface temperature wave

ω is the angular frequency of oscillation and equals $2\pi/P$

P is the period of the wave, 24 hours or 365 days

Then the solution given by Carslaw and Jaeger (1959, pp. 64-65) is:

$$T(x,t) = T_a + \Delta T_S \, e^{-x(\omega/2K)^{1/2}} \, [\sin[\omega t - (\omega/2K)^{1/2} x]] \qquad [46]$$

Equation [46] is an exact analytical solution of Equation [1] for the surface temperature input of Equation [45].

The solution of Equation [1] for the boundary condition given by Equation [1b] as given by Equation [1d] was:

$$\overline{T}\,(x,p) = \overline{T}_S\,(p) \, e^{-\sqrt{p/K}\, x} \qquad [1d]$$

If $\overline{T}_S\,(p)$ is specified as an arbitrary boundary condition, then the solution of Equation [1d] given by Carslaw and Jaeger (1959, p. 305) is:

$$T(x,t) = \frac{x}{\sqrt{4\pi K}} \int_o^t T_S(\tau) \, \frac{e^{-x^2/4\,K(t-\tau)}}{(t-\tau)^{3/2}} \, d\tau \qquad [47]$$

Equation [47] defines the relationships between temperature for any x and any t when $T_S(\tau)$ represents an arbitrary surface temperature as a function of time. This is the convolution relationship for heat flow or diffusion. It completely defines the response of the soil heat flow system for a homogeneous medium without moisture flow.

Equation [47] is of the form of the convolution integral of Equation [13]. The impulse response in Equation [47] is:

$$h\ (t-\tau)\ d\tau = \frac{x}{\sqrt{4\pi K}}\ \frac{e^{-x^2/4K\ (t-\tau)}}{(t-\tau)^{3/2}}\ d\tau \qquad [48]$$

Eagleson, Mejia and March (1965) defined a procedure for evaluation of system response by numerical convolution that involves using an arbitrary function, $T_S(\tau)$, as the input to convolute with the impulse response of the system. Numerical convolution is the method for numerically integrating Equation [47]. $T_S(\tau)$ is defined by the timewise variation of the surface temperature or input function. h(t) is now evaluated at particular values of time to obtain a time distribution for the impulse response function. Numerical convolution is then defined by:

$$T\ (k) = \sum_{j=1}^{k} T_S(j)\ \ h(k-j+1)\ \Delta j \qquad [49]$$

where:

$T\ (k)$ = the output at discrete time, k

$T_S(j)$ = the input at discrete time, j

$h\ (k-j+1)$ = the impulse response function

Δj = time interval

$T_S(j)$ is defined by the timewise distribution of input and h(k-j+1) is defined by Equation [48] with τ equal to zero. In other words, no lagging is necessary in evaluation of the impulse response. The numerical convolution computed by h(k-j+1) does the lagging.

Numerical convolution permits the evaluation of temperature distributions where the input temperature is an arbitrary function of time and the response is computed using the impulse response function for the system.

Frequency Domain Analysis

The frequency response characteristics of the diffusion equation are derived by use of the Laplace transform. Fourier transforms may also be used but substitution of the Laplace variable $p = \sigma + i\omega$ with $\sigma = 0$ results in identical frequency response functions.

A solution of Equation [1] given by Equation [1d] was:

$$\overline{T}\ (x,p) = \overline{T}_S\ (p)\ e^{-\sqrt{p/K}\ x} \qquad [1d]$$

for the initial and boundary conditions given. Substitution of the relation:

$$p = \sigma + i\omega \qquad [50]$$

for

$$\sigma = 0$$

to obtain the complex frequency response gives:

$$\frac{\overline{T}\ (x,i\omega)}{\overline{T}_S(i\omega)} = H\ (i\omega) = e^{-\sqrt{i\omega/K}\ x} \qquad [51]$$

When the roots of $\sqrt{i}$ are evaluated, a solution is:

$$H\ (i\omega) = e^{-(1+i)\ x\ \sqrt{\omega/2K}} \qquad [52]$$

Equation [52] is the frequency domain solution of the diffusion equation. It is called the system response function and completely characterizes the response of the system. By use of the convolution property of linear systems the response of the system was defined previously by Equation [15] as:

$$Y\ (i\omega) = H\ (i\omega)\ X\ (i\omega) \qquad [15]$$

where

$Y\ (i\omega)$ = system response or output

$X\ (i\omega)$ = arbitrary system input

The frequency response function may be represented in another form as was done in Equation [56]:

$$H\ (i\omega) = G\ (i\omega)\ e^{+i\phi\ (i\omega)} \qquad [36]$$

where:

$G\ (i\omega)$ = system gain function

$\phi\ (i\omega)$ = system phase function

From Equation [52]:

$$G\ (i\omega) = e^{-x\sqrt{\omega/2K}} \qquad [53]$$

$$e^{i\phi(i\omega)} = e^{-ix\sqrt{\omega/2K}} \qquad [54]$$

Taking the natural logarithms of each side of the gain function gives:

$$\ln\ [G\ (i\omega)] = -x\sqrt{\omega/2K} \qquad [55a]$$

or

$$K = \frac{x^2 \omega}{2[\ln^2 G(i\omega)]} \qquad [55b]$$

In a similar manner Equation [54] can be solved to give:

$$\phi(i\omega) = -x\sqrt{\omega/2K} \qquad [56a]$$

or

$$K = \frac{x^2 \omega}{2[\phi(i\omega)]^2} \qquad [56b]$$

The frequency response characteristics of a system are frequently represented as bode plots. Figures 8a and 8b give the bode plots of the diffusion equation for x = 5 cm and three values of diffusivity.

The gain function gives the ratio of output temperature to input temperature and indicates that the ratio of temperatures at two depths decreases as the frequency increases. As the diffusivity increases the attenuation at a given frequency decreases. Thc phase function is a measure of the time lag between input and output. The time lag between input and output is a linear function of frequency for the lower frequencies. The time lag at higher frequencies appears to asymptotically approach 90° out of phase. As the diffusivity increases the time lag between input and output decreases.

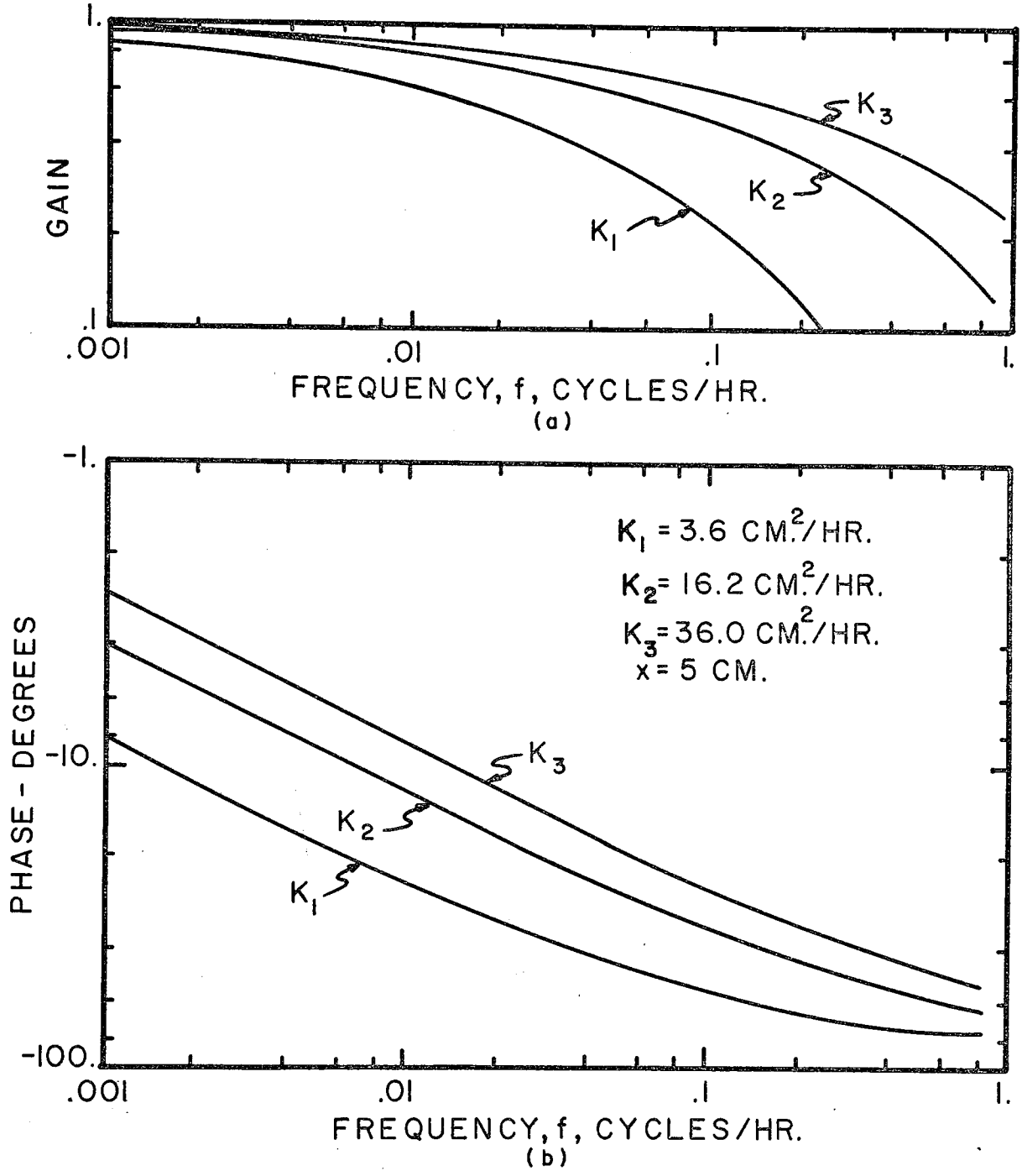

Figure 8. Bode plots for the soil heat transfer subsystem for three different diffusivities and x = 5 cm

This completes the analytical definition of the soil heat transfer subsystem. Both time domain and frequency domain analytical functions were given. Equivalent functions were given in the previous section that are evaluated from time series of input and output. The use of these equal but independent functions to determine the system constant will now be discussed.

System Constant Determination

The analytically derived gain and phase functions provide a parametric model for soil heat flow. The parametric model defines heat flow as a function of distance, x, frequency of the input, f, soil heat diffusivity, K, and the frequency distribution of input temperature. This parametric model is good for temperature inputs at all frequencies. Therefore, it is a general solution with unrestricted forms for the inputs.

Spectral analysis is a general procedure of system identification from experimental data with unrestricted forms for the input. Spectral analysis is restricted in that it provides system identification only for frequency ranges that are contained in the input. However, since spectral analysis defines the gain and phase functions for a linear system by statistical analysis of experimental data for the real system, then the two approaches to system definition can be compared. Equation [37a] and [37b] are the gain and phase functions defined from spectral analysis.

In the analytically derived relationships for input and output for a linear system no assumptions were made concerning the form of the time distribution of input. The time distribution of input was considered arbitrary. Likewise, in the developments for spectral analysis for system identification no assumptions were made concerning the time distribution of input and output. Therefore, these two methods place no restrictions on the form of the time distribution of input. Other assumptions that were made concerning the nature of the system were that the system was linear, and that the system was time-invariant. The assumption of linearity is, in a number of instances, not restrictive.

Time invariance is equivalent to assuming that the soil heat diffusivity is constant. This means that the manner in which the system operates on the input temperature to produce the output temperature does not change with time.

The next step is to define the information given from the analytically derived gain and phase functions and the information that may be obtained from the statistically derived gain and phase functions. The analytically derived gain and phase functions are parametric models that define the relationships between the parameters that identify the system. In a given application the gain function, for example, is dependent upon a number of parameters, all of which are known, except the system constant, soil heat diffusivity. The information obtained from a time distribution

of input and output temperatures is the value of the gain function as distributed with frequency. Thus, it is conceptually possible to equate the value of the gain function at a particular frequency derived from time series analysis to the analytically derived parameteric model for the heat flow system and solve for the unknown diffusivity that resulted in that particular value for the gain function. This is the approach that will be used in evaluating system constants and is applicable to any system where an analytically derived and a statistically derived gain and phase function are available.

When relatively short periods of input and output are available, then identification of system constants by time series analysis may not provide a value for the system constant with adequate confidence limits. Time domain analysis using the discrete form of Equation [47] as given in Equation [49] can be used to solve for the system constant by trial and error. If time distributions of T(k) and $T_S(j)$ for Equation [49] are available, then knowing the value of x and assuming a value of K permits the calculation of a temperature response. The sum of squares of the differences between measured and computed temperatures is a measure of the accuracy of the assumed value of K. The value of K is incremented and a new sum of squares computed. The procedure is repeated until a value of K is obtained that results in a minimum sum of squares of the difference between measured and

computed temperatures. This would require three or four days of temperature data at time intervals necessary to adequately define the input and output.

ANALYTICAL VERIFICATION OF SYSTEM RESPONSE AND SYSTEM CONSTANT EVALUATION

Model verification can be approached from a number of different viewpoints. The approach in this study was to use input and output data from an exact analytical model to compare with numerical convolution for system simulation. Analytical model input and output data were used for system identification by time series analysis and by numerical convolution. Any discrepancies can be related to deficiencies in the simulation procedure or in the system identification procedure since the input and output of the analytical model are exact.

System Response

The analytically computed temperature at 5 cm in the soil was obtained using Equation [46] for a sinusoidal surface temperature with a mean of 28°C and an amplitude of 8°. Numerical convolution was used to compute the temperature at 5 cm using Equation [49], the assumed initial temperature, and the same input as for the analytically computed temperature. The values of analytically computed temperature and numerical convolution for the fourth cycle are presented in Figure 9.

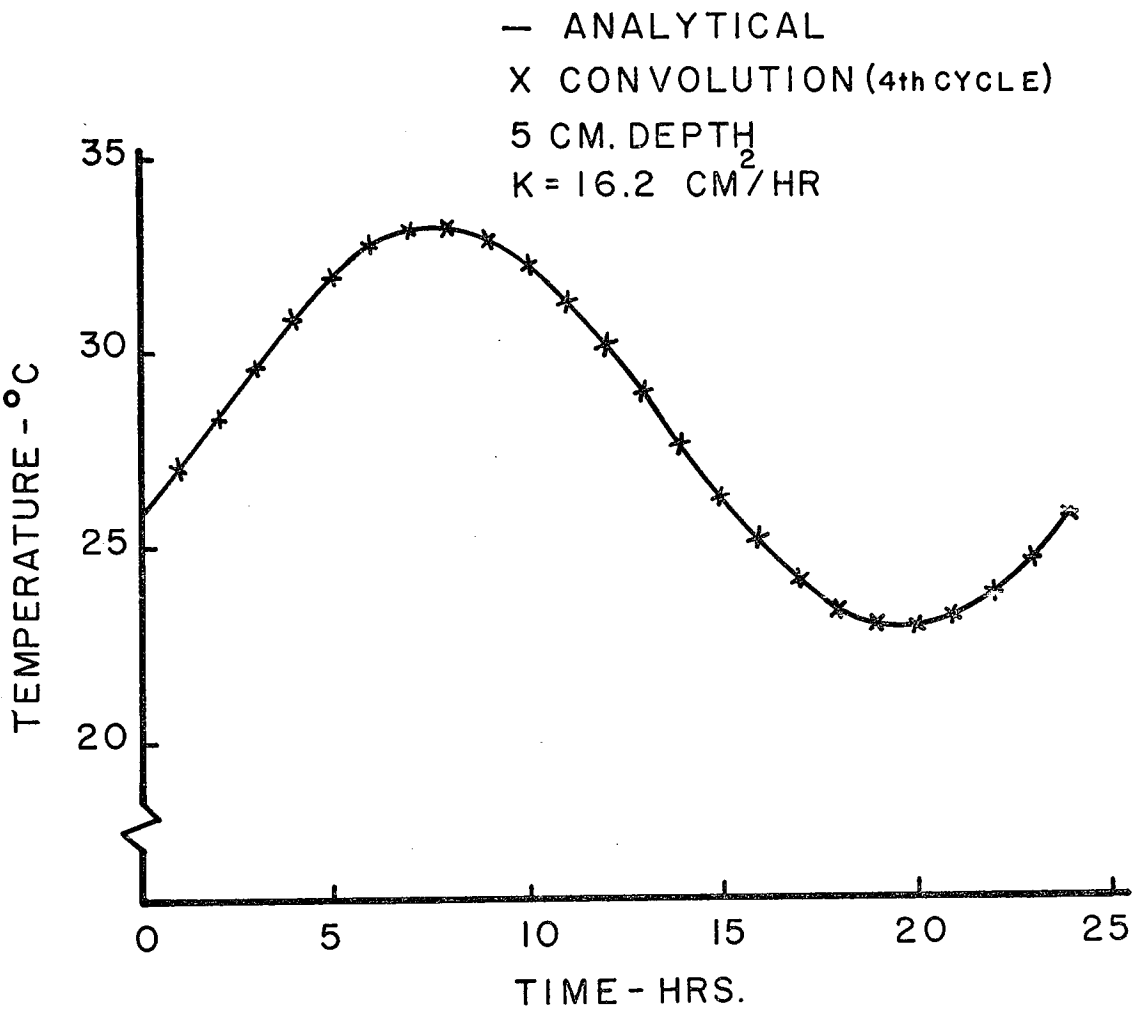

Figure 9. Comparison of analytical and convolution computed soil temperature for the 4th cycle

Computations for numerical convolution were made using hourly values of the input-temperature to the nearest 0.01 degree, and the impulse response function was evaluated through 96 hours. The first four hours of convolution used time increments of 0.001 hours; 0.1 hour was used from 4 to 96 hours in evaluating the impulse response function.

As seen in Figure 9, there is no difference between analytical and numerical convolution computed soil temperatures. In the fourth cycle of convolution computed temperatures, the maximum difference between numerical convolution and analytically computed temperatures was 0.05 degrees. The maximum difference between numerical convolution and analytically computed temperatures occurred in the first hour and was 2.22 degrees. This difference is associated with the starting transient for numerical convolution which begins with an assumed constant, vertical initial temperature and does not result in a steady-state sinusoidal response for the first few cycles.

Numerical convolutions thus provides an adequate means for computing soil temperature response for arbitrary time distributions of input temperature.

System Constant Identification

The exact analytical equation for heat flow in a soil, Equation [46], was used to obtain soil surface temperatures ($x = 0$) and 5-cm soil temperatures ($x = 5$) for a 50-day

interval. These two simulated time series were subjected to time series analysis for the purpose of system identification and system constant determination.

The values for surface and soil temperature at six-hour intervals were used for time series analysis. Analyses were also made for a sampling interval of one hour without significant improvement in the definition of the spectrums of the subsystem. The data were punched on cards and analyzed by time series analysis using computer programs described by Jenkins and Watts (1968).

Time Series Analysis

Figures 10 and 11 present the autocorrelation functions for simulated surface and soil temperatures computed from the relationships given by Equations [18] and [19]. The autocorrelation functions show the cyclic nature of the input temperatures and output temperatures for the simulated soil heat transfer subsystem.

The cross correlation function for the time series of input and output is given by Figure 12. The cross correlation function was defined by Equations [22] and [23]. The processes are related as evidenced by the high (near 1.0) cross correlation and the cyclic nature is again evident.

The cross correlation function is maximum at zero lag such that no alignment of the two times series is necessary. The spectrums were investigated at values of lag for

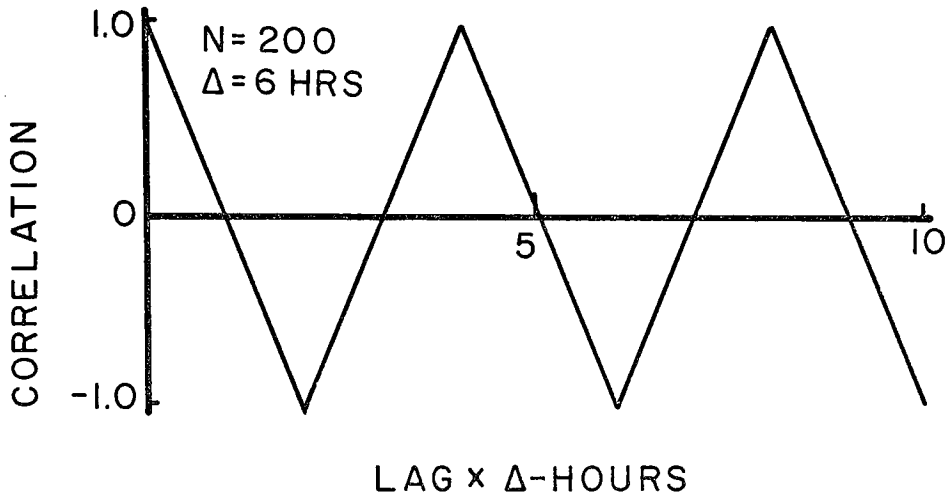

Figure 10. Autocorrelation of simulated sine wave of surface temperature, ΔT_S = 8° C, T_a = 28.0° C, P = 24 hr

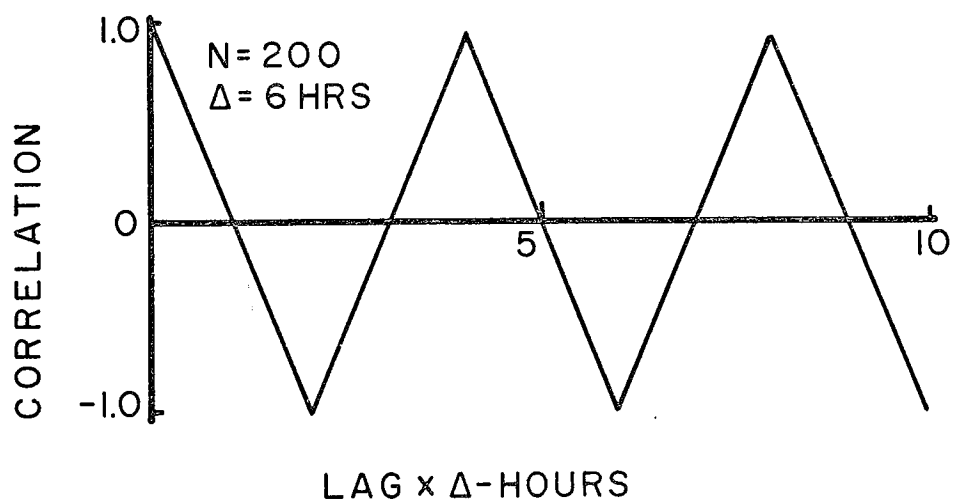

Figure 11. Autocorrelation of simulated sine wave of soil temperature, x = 5 cm, K = 16.2 cm^2/hr

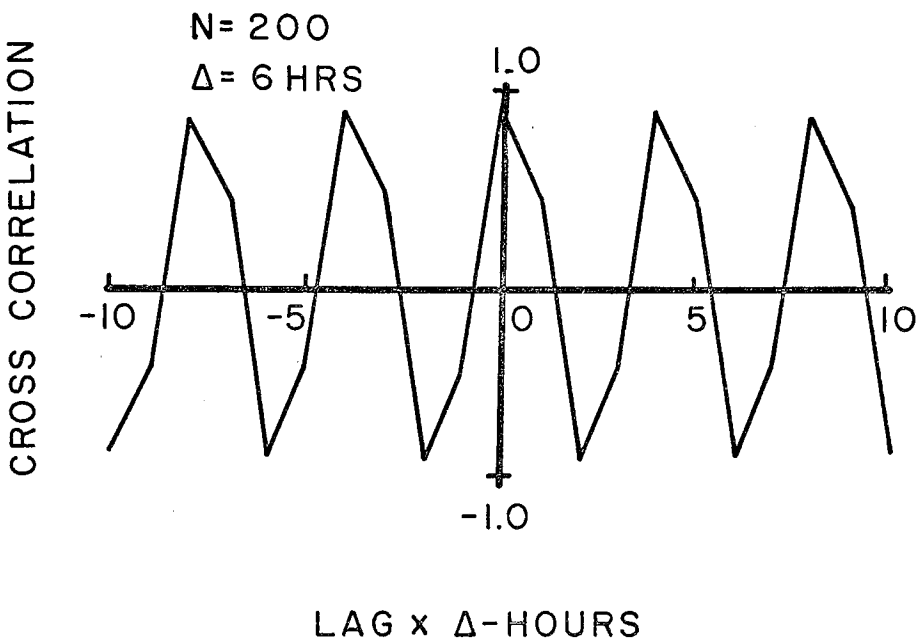

Figure 12. Cross correlation of simulated surface and soil temperatures

the correlation function of L = 4 and 6. A detailed discussion of the procedures of analysis and interpretation of the data is given by Jenkins and Watts (1968, pp. 437-448).

The autospectrums of input and output for the soil heat transfer subsystem are presented in Figures 13 and 14. The spectrums for two different values of lag are presented to illustrate the stability of the spectrum. Commonly three values of lag are presented. The spectrum could not be obtained for the next higher value of lag because of the relatively long sampling interval used for the time series (Δ = 6 hr.). However, a very stable spectrum with maximum power (autocorrelation) was obtained at 6 lags. This value of lag was used for further analyses.

The spectrum of input and output in Figures 13 and 14 for L = 4 has a wider bandwidth which averages the power over a wider range of frequencies and results in a reduction in peak power. A value of lag greater than the optimum will result in spurious peaks or oscillations in the spectrum and also a lower peak power.

The residual spectrum for the soil heat transfer subsystem is shown in Figure 15. The residual spectrum indicates that lag 6 is the optimum lag for analysis. Lag 6 resulted in the minimum residual spectrum, which indicates most of the output power is explained by the input power. The residual is not zero because the sampling window used in

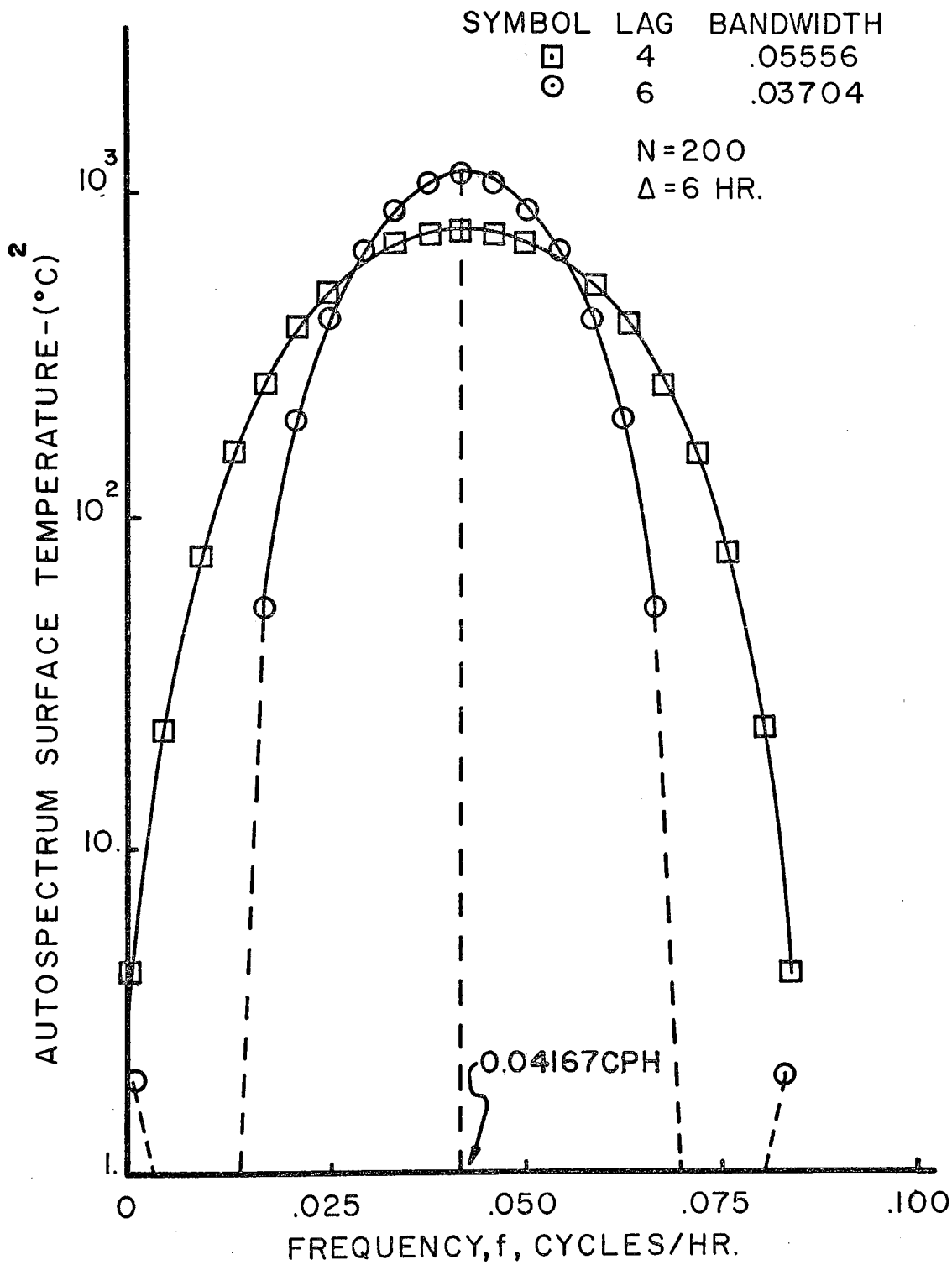

Figure 13. Autospectrum of simulated surface temperature

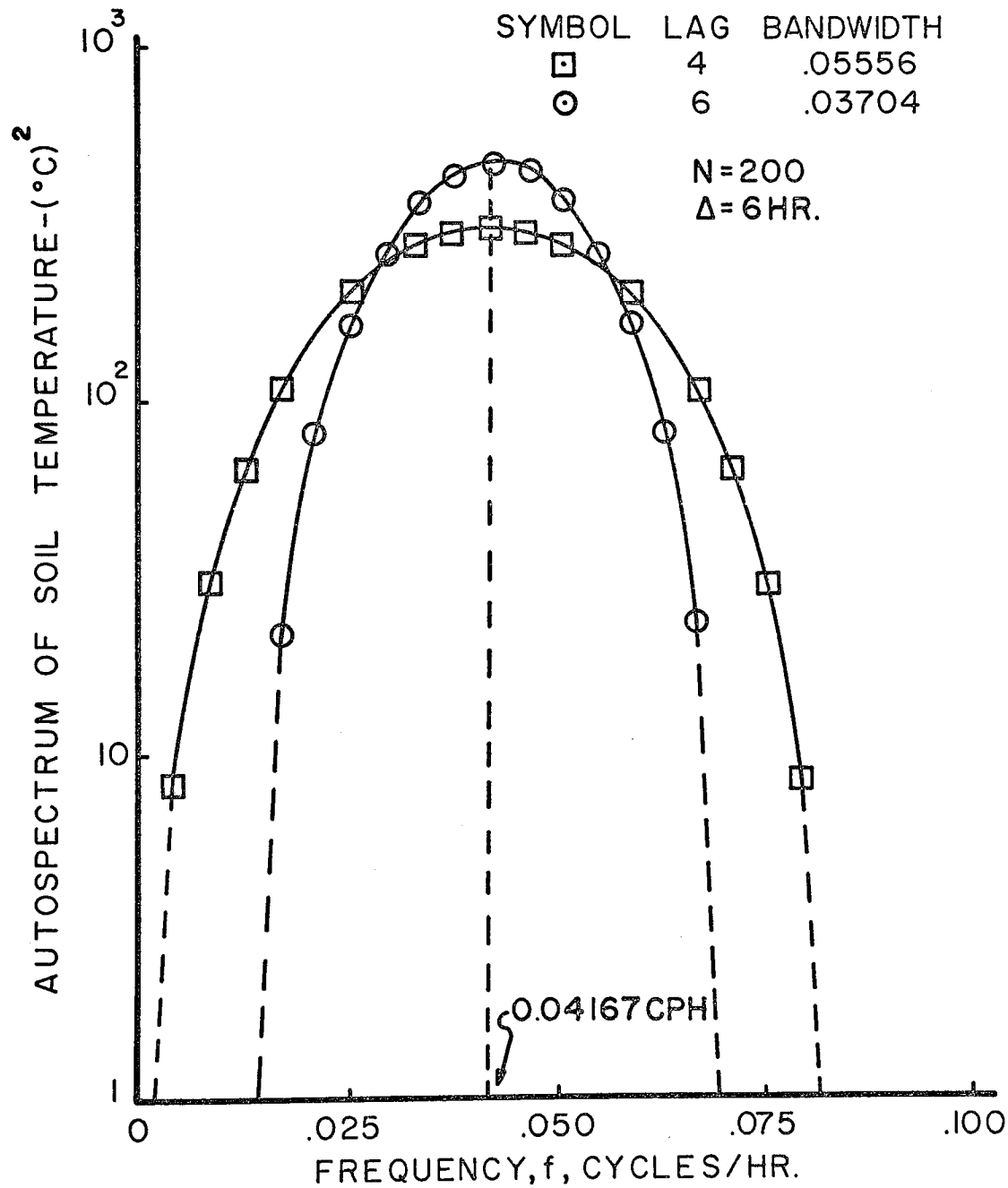

Figure 14. Autospectrum of simulated soil (5-cm) temperature

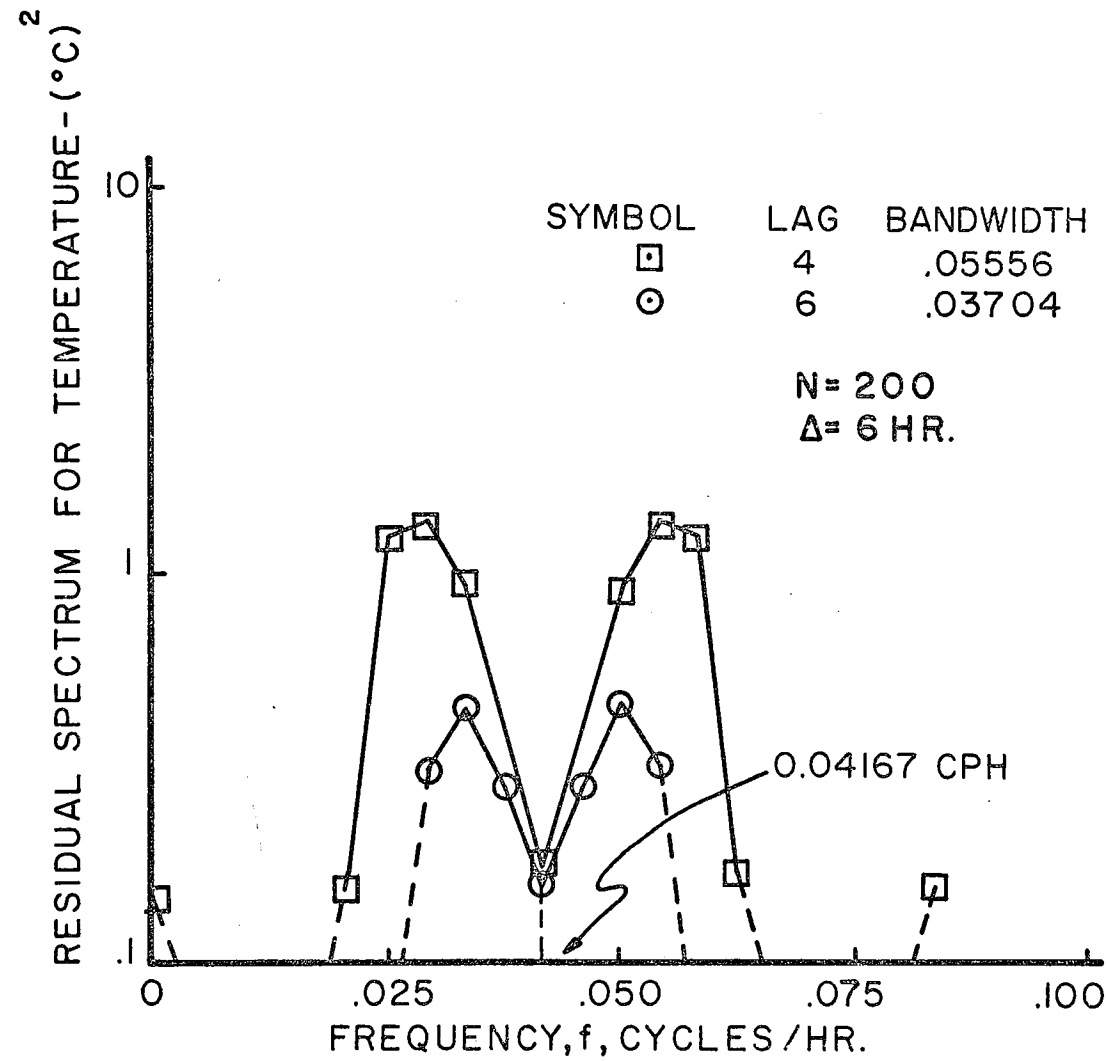

Figure 15. Residual spectrum for simulated soil heat transfer subsystem

spectral analysis averages the power over a range of frequencies.

Appendix A, Table 3, presents the covariance data for simulated time series of surface and soil temperatures. Tables 4 and 5 in Appendix A present the results of frequency response analysis for the same data. Values for computation of the system constant may be obtained from Tables 4 and 5, Appendix A, but the plots of the gain, phase, and coherency spectrums will be used to explain the procedure.

Figure 16 presents the squared coherency spectrum, as defined by Equations [38] and [44], for the simulated soil heat transfer subsystem for the sinusoidal input temperature. Since only one frequency was in the input, the frequency of importance in the squared coherency spectrum is the frequency of the input. This is the frequency at which the values of gain and phase as determined by time series analysis were used to compute the system constant. This frequency is also where the maximum value for coherency is obtained while substantial power is in the input and output. Thus, the minimum confidence interval for gain and phase also occurs at this frequency. The input frequency had a period of 24 hours resulting in an input frequency of 0.04167 cycles per hour (CPH). This is also the frequency at which coherency is maximum (Appendix A, Table 4).

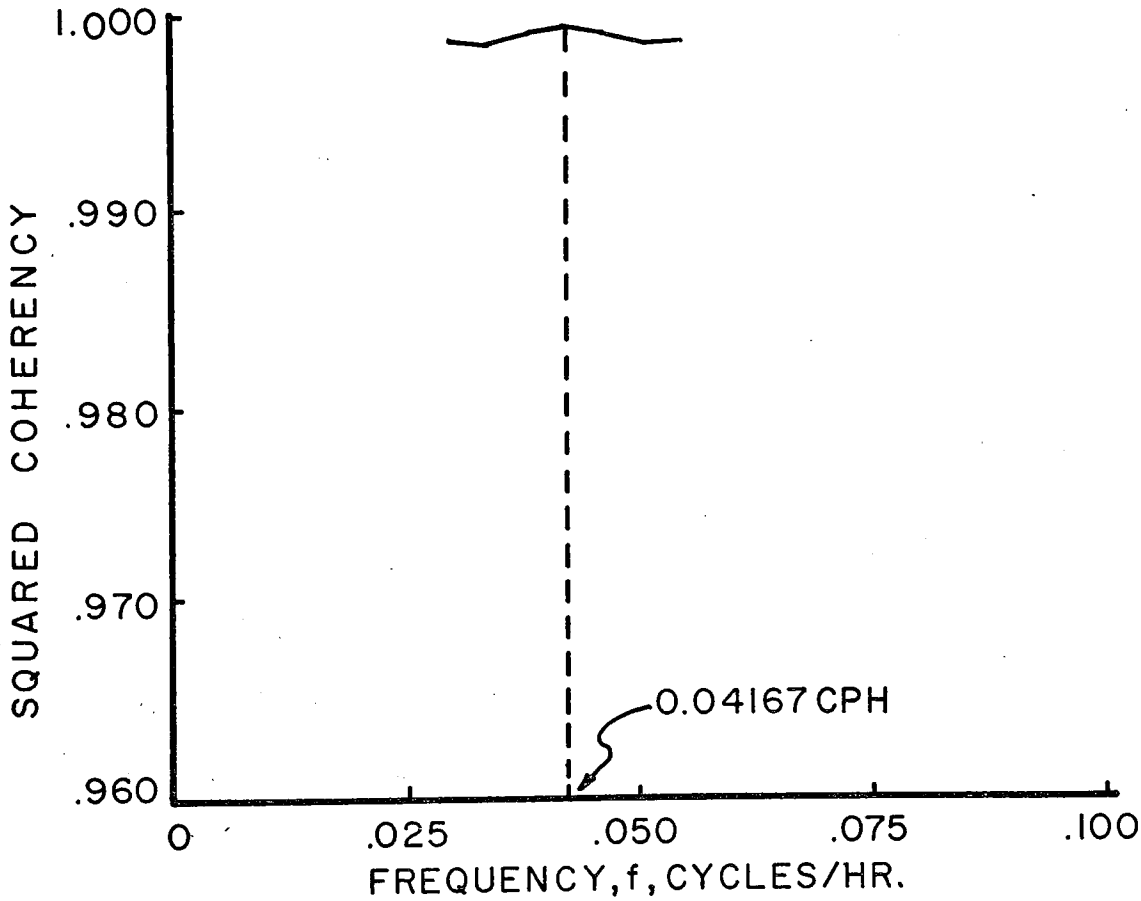

Figure 16. Squared coherency spectrum for simulated soil heat transfer subsystem

In Figure 16, the coherency is plotted over a range of frequencies above and below 0.04167 CPH. This was because very low power occurred in the input and output at the other frequencies. When low values of power in the input and output occur in the denominator of Equation [44], the resultant calculation can produce values for coherency greater than 1.0. This value (greater than 1.0) has no meaning so the computer program sets the coherency equal to 1.0. The spectrums are not defined for these arbitrarily set values of coherency and the data are not plotted.

The gain spectrum as identified by time series analysis is shown in Figure 17 and was defined by Equation [42]. This gain spectrum appears considerably different from the theoretical spectrum as given in Figure 8a. The difference is that the gain spectrum in Figure 17 is defined precisely only at .04167 CPH. At frequencies above and below this frequency the confidence interval for the gain is very wide, Appendix A, Table 5. Thus, the gain has not been accurately determined other than at the single frequency.

The characteristics of the phase spectrum, defined by Equation [43] and shown in Figure 18, are very similar to the gain spectrum in Figure 17. It does not resemble the theoretical phase spectrum of Figure 8b, and is defined accurately only at a point. The gain spectrum is not particularly sensitive to alignment of the time series for input and output, but the phase spectrum is (Jenkins and Watts, 1968,

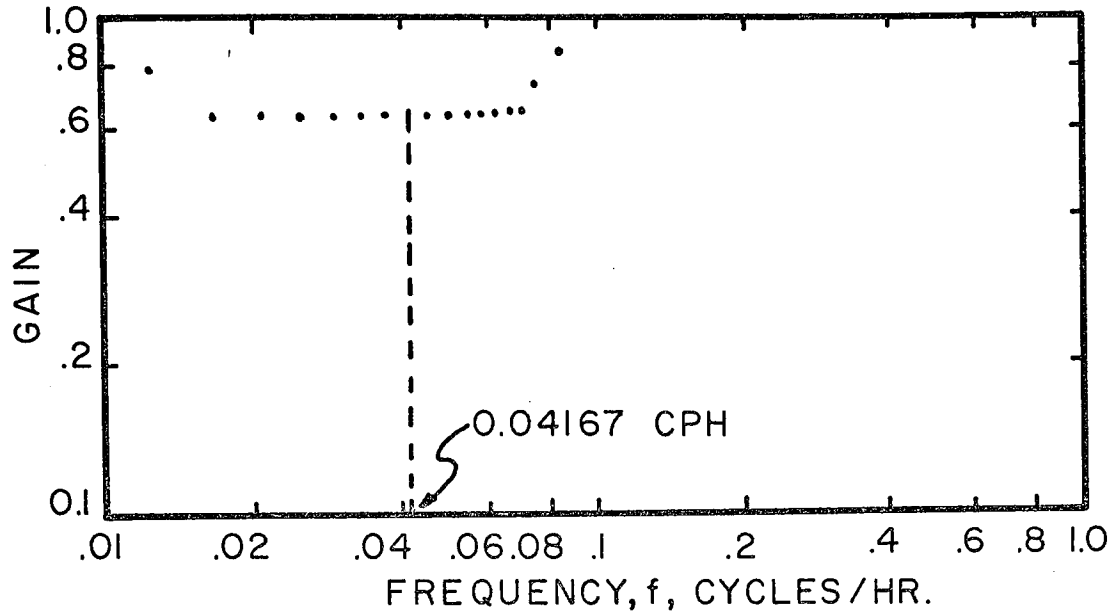

Figure 17. Gain spectrum for simulated soil heat transfer subsystem

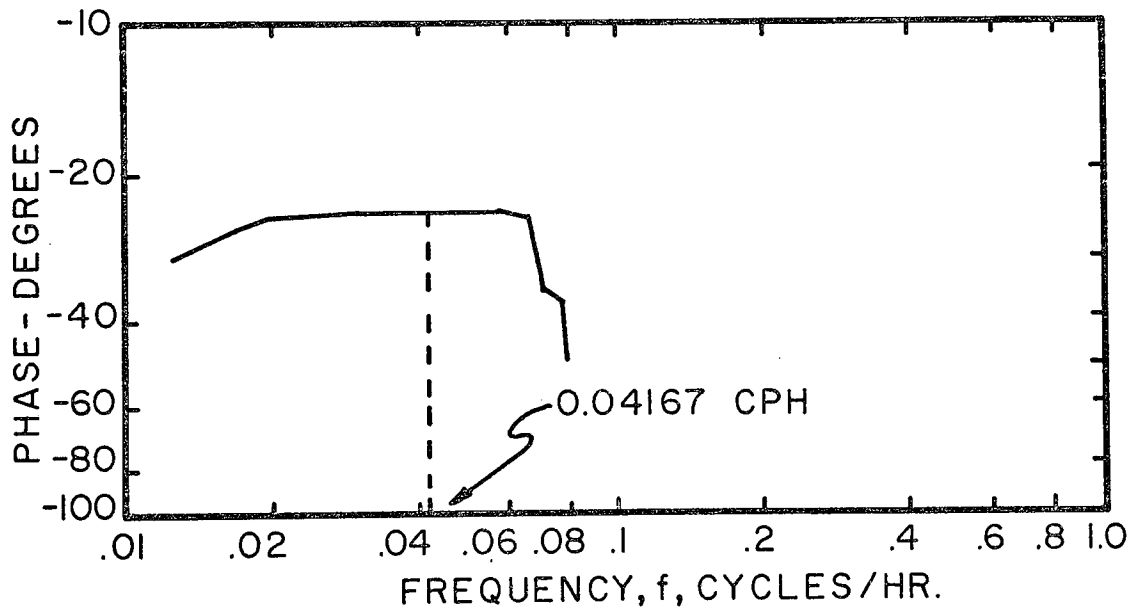

Figure 18. Phase spectrum for simulated soil heat transfer subsystem

p. 437). No alignment of the two series was necessary as the time difference between input and output was less than the time delay in one value of lag. The gain and phase spectrums will now be used to compute the system constant.

The gain function estimate of the system constant is computed from Equation [55b] and the value for gain at frequency 0.04167 given in Appendix A, Table 4. The system constant from gain is:

$$K = \frac{(5)^2(0.262)}{2[\ln(.63835)]^2} = 16.24 \text{ cm}^2/\text{sec} \qquad [65]$$

In a similar manner the system constant can be estimated from the phase function from the value of the phase at frequency 0.04167 given in Table 4, Appendix A. The system constant from phase is (Equation [56b]):

$$K = \frac{(5)^2(0.262)}{2(-0.44929)^2} = 16.21 \text{ cm}^2/\text{sec} \qquad [66]$$

The value of the system constant used in analytically generating the time series of input and output was 16.2 cm^2/sec. Thus, time series analysis very accurately defined the system constant from analysis of time series of input and output by using the analytically defined gain and phase functions for the system. System identification by time series analysis was achieved.

Fifty days of temperature data at six-hour intervals (N = 200 observations) were used to compute the system

constant from the time series analysis. A very accurate estimate (16.24 from gain) of the true (16.2 used in the simulation) system constant was obtained. The availability of fifty-day time series for actual systems is not common. Time series of ten to 20 days may be satisfactory and more readily obtainable. However, very short time series of three or four days length will not generally be adequate for system identification by time series analysis. Six to eight days with steps (sudden changes) in the input from clouds, for example, may be adequate. Time varying system constants may also restrict the length of the time series that can be analyzed as a time-invariant system. For lengths of record too short for time series analysis, time domain analysis can also be used to obtain the system constant.

Numerical Convolution

Time domain analysis by numerical convolution requires a length of record sufficient to eliminate the starting transient of convolution, if one occurs, plus additional measured values to compare with the computed values.

Four days of hourly values of simulated surface and soil temperatures were used for time domain, system constant identification. The four days were used because, as discussed earlier, the fourth daily cycle for convolution computed temperatures was essentially the same as the analytical values. A value of diffusivity was assumed and the response

was computed from the given input temperatures. The analytical response (measured) was compared to the convolution computed response using the temperatures from the 73rd to 96th hour. The criteria for the correct system constant was determined by:

$$SS = \sum_{k=73}^{96} [TM(k) - TD(k)]^2 \qquad [67]$$

where:

SS = the sum of squares of the differences between analytical (TM) and convolution computed (TD) temperatures.

The correct value of the system constant was assumed to be when SS is a minimum.

Figure 19 is a plot of sum of squares versus diffusivity for the previously described simulated data. The value of diffusivity for minimum SS is:

$$K = 16.3 \text{ cm}^2/\text{hr}$$

The actual values of the sum of squares were:

$$SS = .0138 \quad K = 16.2 \text{ cm}^2/\text{hr}.$$
$$SS = .0133 \quad K = 16.3 \text{ cm}^2/\text{hr}.$$

This minor discrepancy of 16.3 instead of 16.2 for the system constant is easily explained by the approximate nature of numerical convolution. The time intervals for numerical

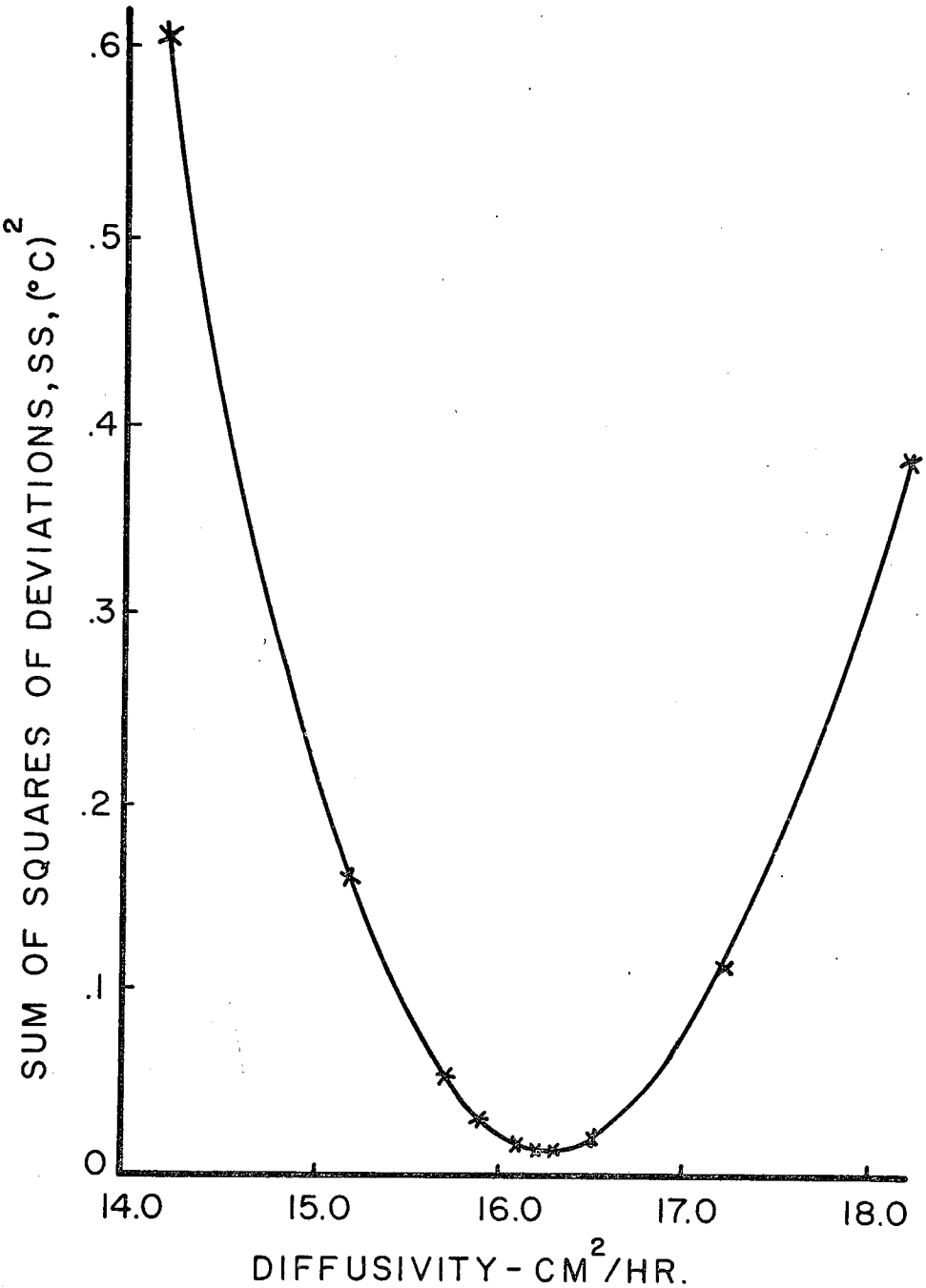

Figure 19. Optimum diffusivity based on minimum sum of squares between analytical and convolution computed temperatures

convolution can be modified to produce more accurate results if desired. The results from practical considerations are sufficiently accurate.

Confidence Limits for System Constants

When using input and output data for a real system, the measurements of input and output may include noise. In addition, the length of the time series of input and output will be a finite length and further data may be unobtainable. Thus, the accuracy of the determination of the system constant may be in question.

Jenkins and Watts (1968, pp. 434-436) presented methods for computing confidence intervals for the gain and phase spectrums. Thus, a 95 percent confidence that the value of gain is within a certain range can be hypothesized and the upper and lower limits on the interval computed. The confidence interval is a measure of the adequacy of the identification of the gain and phase functions.

Three variables appear in the equation for computation of the system constant from values of gain and phase. These are frequency, space parameter (x), and the value of gain. Frequency has no error associated with it as this is an arbitrary value used to select the value of gain for which to compute the system constant. The space parameter (x) in many instances can be measured very accurately or repeated

measurements can be used to improve the accuracy of the measurement of x.

If frequency and the space parameter are assumed to be known without error, then the confidence interval of the values of gain and phase can be used to compute a confidence interval for the system constant. This confidence interval can then be used as a relative measure of the adequacy of the determination of the system constant. When a wide interval results, more data or more accurate measurements may be warranted in order to determine the system constant with an accuracy that is necessary for use in computing system response.

Table 5, Appendix A presents the data on upper and lower confidence limits for the analysis of the simulated soil temperatures. Use of the upper and lower limits of gain and phase to compute upper and lower limits for the system constant gives:

For gain:

$$15.89 \leq K \leq 16.60 \text{ cm}^2/\text{hr}$$

For phase:

$$15.86 \leq K \leq 16.57 \text{ cm}^2/\text{hr}$$

Thus, the maximum range of the system constant is about two percent from both gain and phase.

Summary

Time series analysis permits a very accurate determination of the system constant and can also be used to establish a confidence interval for the system constant. Arbitrary time distributions of input and output can be used to evaluate the system constant. Numerical convolution can be used to evaluate the system constant from short duration, arbitrary time distributions of input and output.

EXPERIMENTAL DETERMINATION OF SYSTEM CONSTANT AND SIMULATION OF SYSTEM RESPONSE

The value of systems theory is in the understanding of real systems. The successful simulation of a dynamic, real system implies that the system is understood and that the system has been properly identified. This section applies the previous system identification techniques to actual soil temperature data and uses the previously defined mathematical models to simulate the soil heat transfer subsystem.

Data on soil temperatures were obtained from a report by Wierenga (1968) for an irrigated soil near Davis, California. The temperatures were published for time intervals of 30 minutes for the eight-day period from August 27 to September 3, 1968. The original data are available in the cited report. Details of the measurement procedure and operations during the data collection period were given by Wierenga (1968), and the results have also been published in more recent reports (Wierenga, Nielson, and Hagan, 1969; Wierenga, Hagan, and Nielson, 1970).

The analyses used in the previous section were for a linear, time-invariant system where heat transfer is due to conduction only (no heat transfer by moisture movement). Wierenga (1968) has concluded that between the surface and

the 10-cm depth the diffusivity changed significantly with time and space and was approximately constant below 10 cm. Thus, soil temperatures at 10 cm and below were used for this analysis.

System Constant by Time Series Analysis

The time distribution of temperature for 10- and 15-cm depths for Location I were used for time series analysis. This plot was irrigated with 4° C water approximately 42 hours after the data collection began. That some heat was transferred by moisture transfer is assured. That the heat transfer by moisture transfer was not appreciable was demonstrated by this analysis which assumes no heat was transferred by other than conduction.

The autocorrelation functions for the 10-cm (the input) and the 15-cm (the output) temperatures are presented in Figures 20 and 21. A periodicity exists in the input and output, but appears to damp out with lag. The periodicity is the normal 24-hour cyclic temperature, but the damped effect was caused by the application of a step input of temperature because of the application of very cold irrigation water.

In theory, data used for time series analysis are collected at a sampling interval (Δ) defined by $f_o = 1/2\Delta$ where f_o is the fundamental or highest frequency of interest in the time series. The best results were obtained with

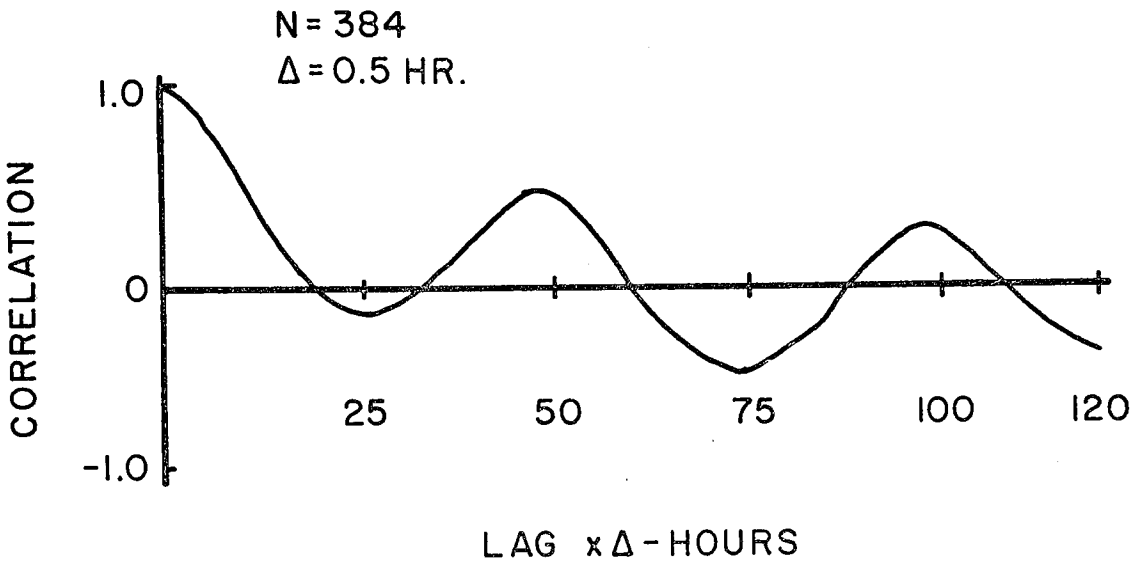

Figure 20. Autocorrelation of 10-cm temperature as input for Davis, California, Location I

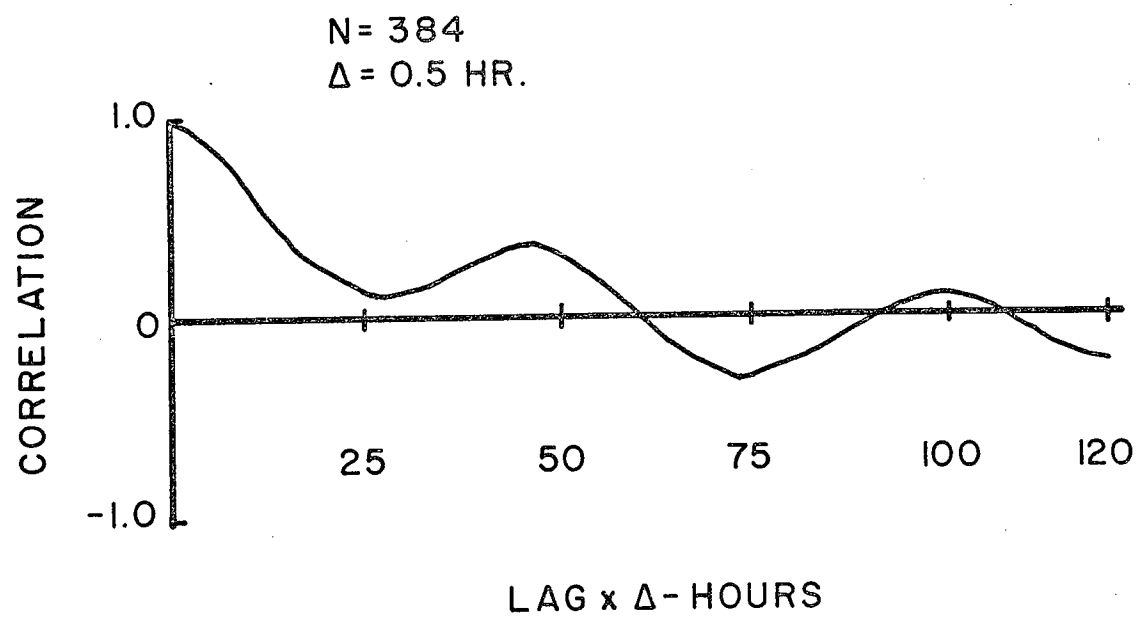

Figure 21. Autocorrelation of 15-cm temperature as output for Davis, California, Location I

the data from Wierenga (1968) using the 30-minute sampling interval. The addition of the cold water as a step input introduced high frequencies in the data and the shorter sampling interval provides additional information.

The cross correlation function (Figure 22) for the 10- and 15-cm temperatures is cyclic and is damped as the lag increases. The autocovariance and cross covariance data for these temperatures are presented in Table 6, Appendix B. The value of lag (L=2) where the cross correlation function peaks was used to align the series to obtain more stable and accurate gain and especially phase spectrums. The values of lag where the correlation function becomes zero were used in the frequency analysis to illustrate spectrum stability. Lags of 63, 91, and 111 were used.

The autospectrums of input and output for the soil temperatures are presented in Figures 23 and 24. The frequency scale has a maximum of $1/2\Delta$ and since $\Delta = 0.5$ hr the maximum is 1.0 CPH. The dominant frequency for power in the input is still 0.04167 CPH but some power is present over a wider range of frequencies. The scale of 0.0 to 1.0 for frequency results in fewer points in the frequency range of interest. Data points at additional frequencies do not alter the values of gain and phase for system identification.

The frequency at which peak power and maximum coherency occurred was used with the analytically defined gain

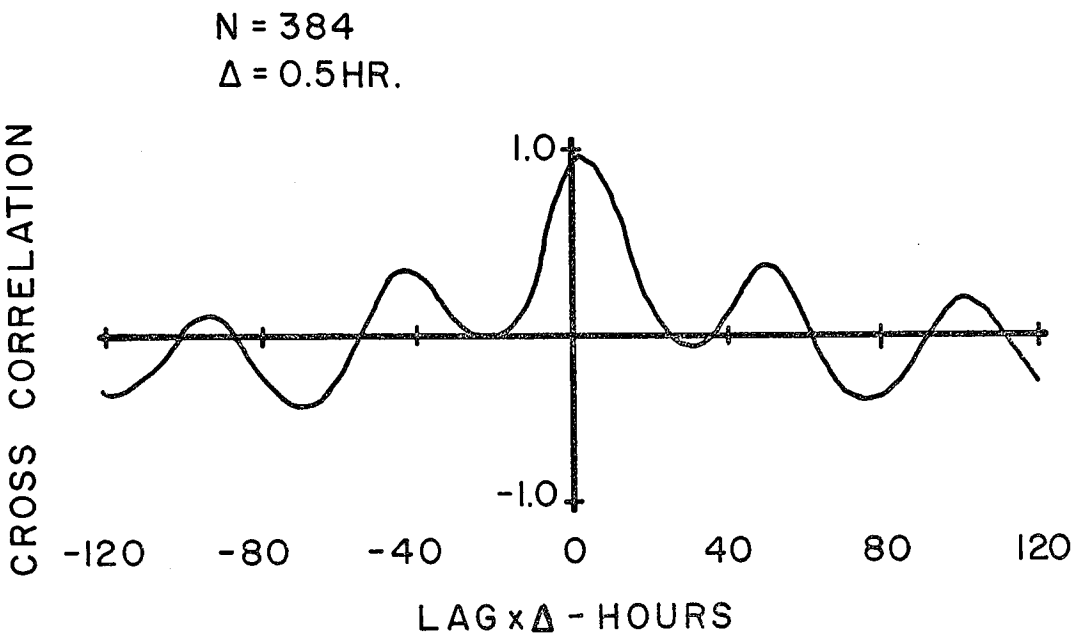

Figure 22. Cross correlation of 10- and 15-cm temperatures for Davis, California, Location I

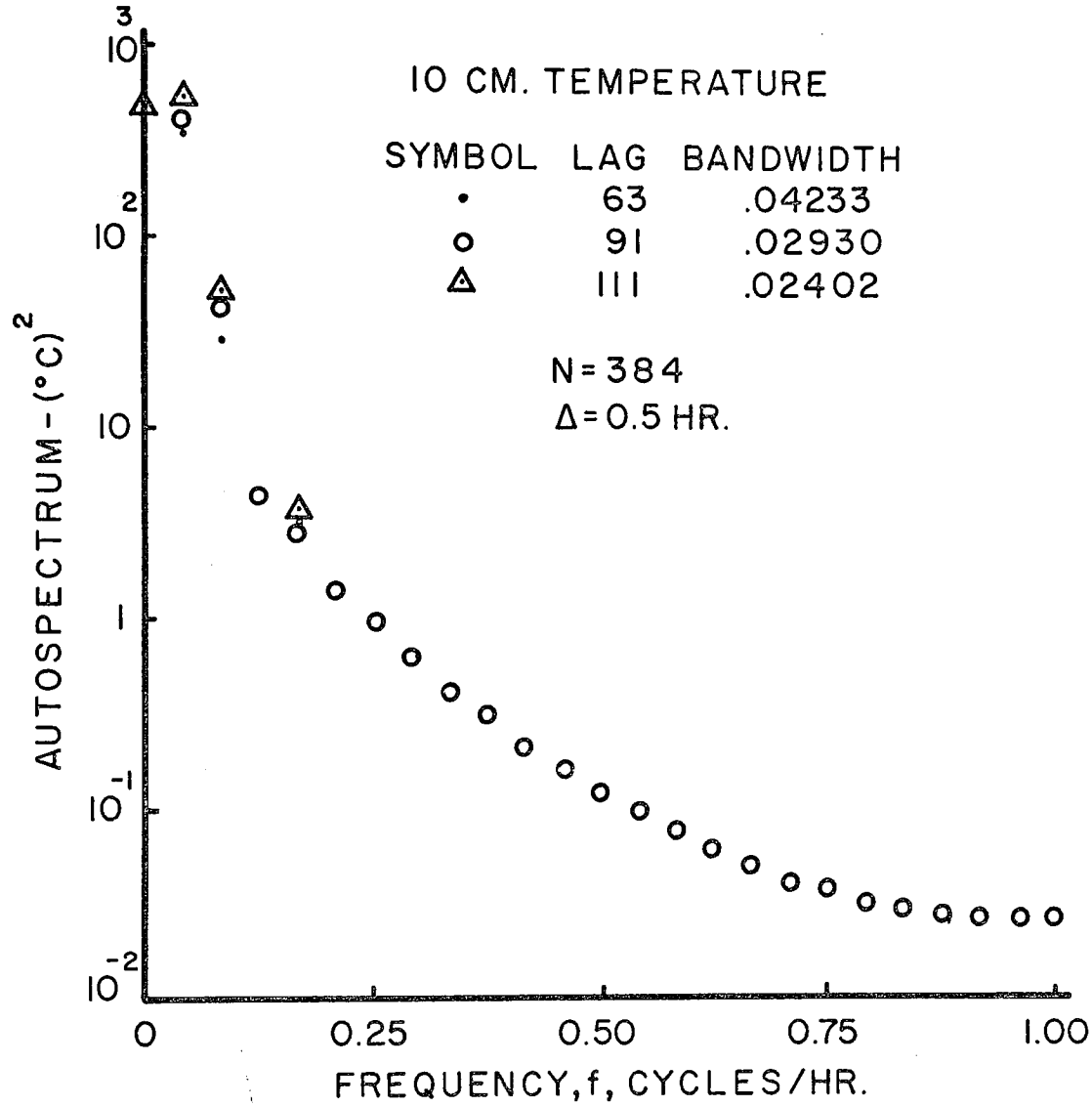

Figure 23. Autospectrum of 10-cm temperature

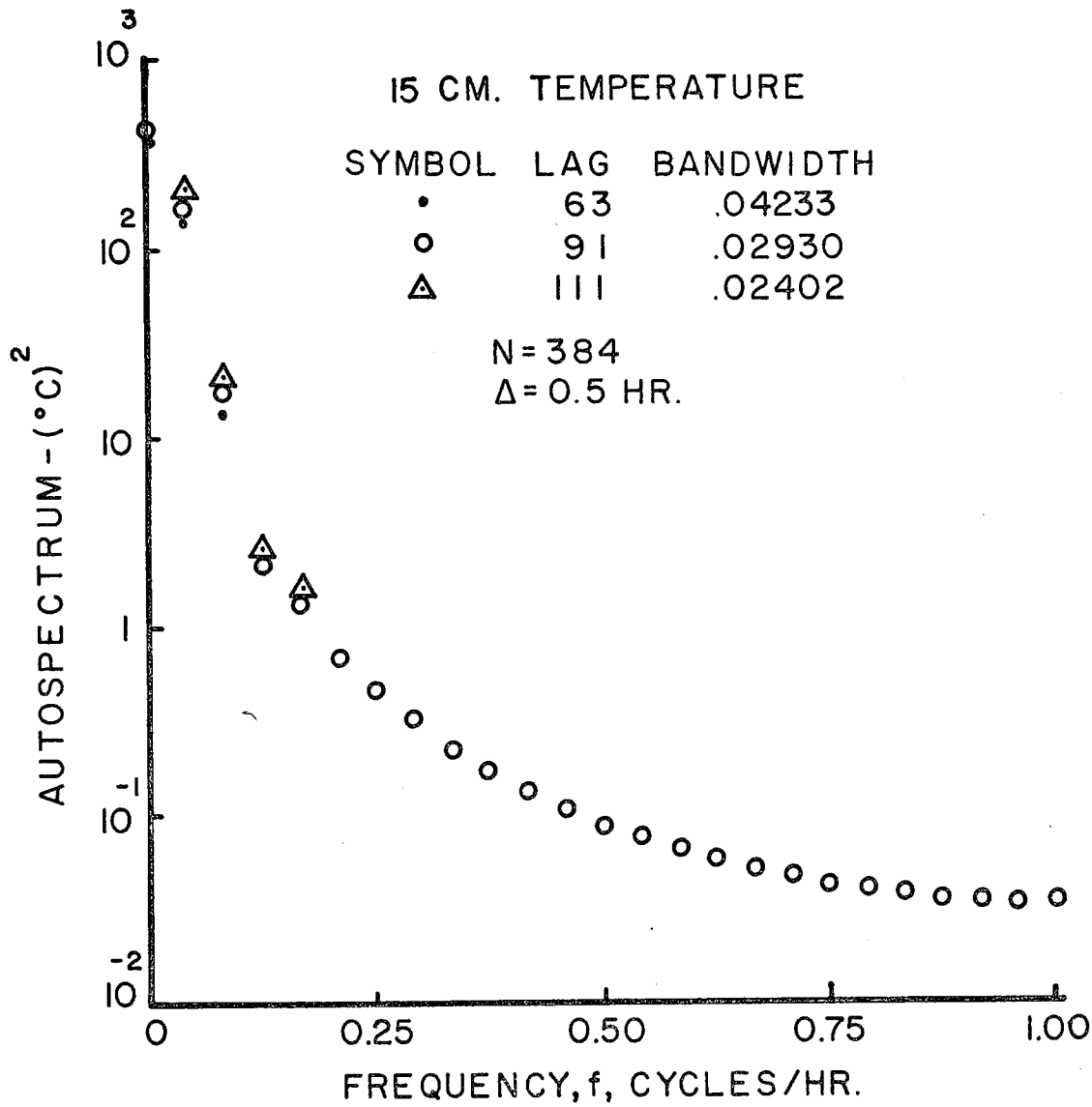

Figure 24. Autospectrum of 15-cm temperature

and phase functions to obtain values for the soil heat diffusivity as in the previous section using the analytical data. The maximum coherency occurs at a frequency of 1.0 CPH. (Table 7, Appendix B). The maximum power for the input occurred at 0.0 CPH on all except the L = 111 which was at 0.04167 CPH and for all three lags in the output at 0.0 CPH. The highest coherency occurred at very low power at 1.0 CPH such that the spectrum is not properly defined. The 0.0 CPH frequency has a lower coherency and cannot be used for defining the system transfer function. The frequency of 0.04167 still provides the best definition of the system transfer function.

The residual spectrum (Figure 25) shows power greater than 1.0 over a very small frequency range. The peak power in the input exceeds 500 and exceeds 200 in the output at lag 111. Thus, most of the power in the output is explained by the power in the input. Values for the autospectra and residual spectrum are usually plotted only when they exceed 1.0. These additional values were included for one lag to illustrate the low power at the higher frequencies for the spectra shown in Figures 23 through 25.

Very little difference between spectrums for different lags were observed indicating that stable spectrums for the input and output temperatures were achieved. The value of lag selected for the spectrum for system identification was 111. The values for system identification from

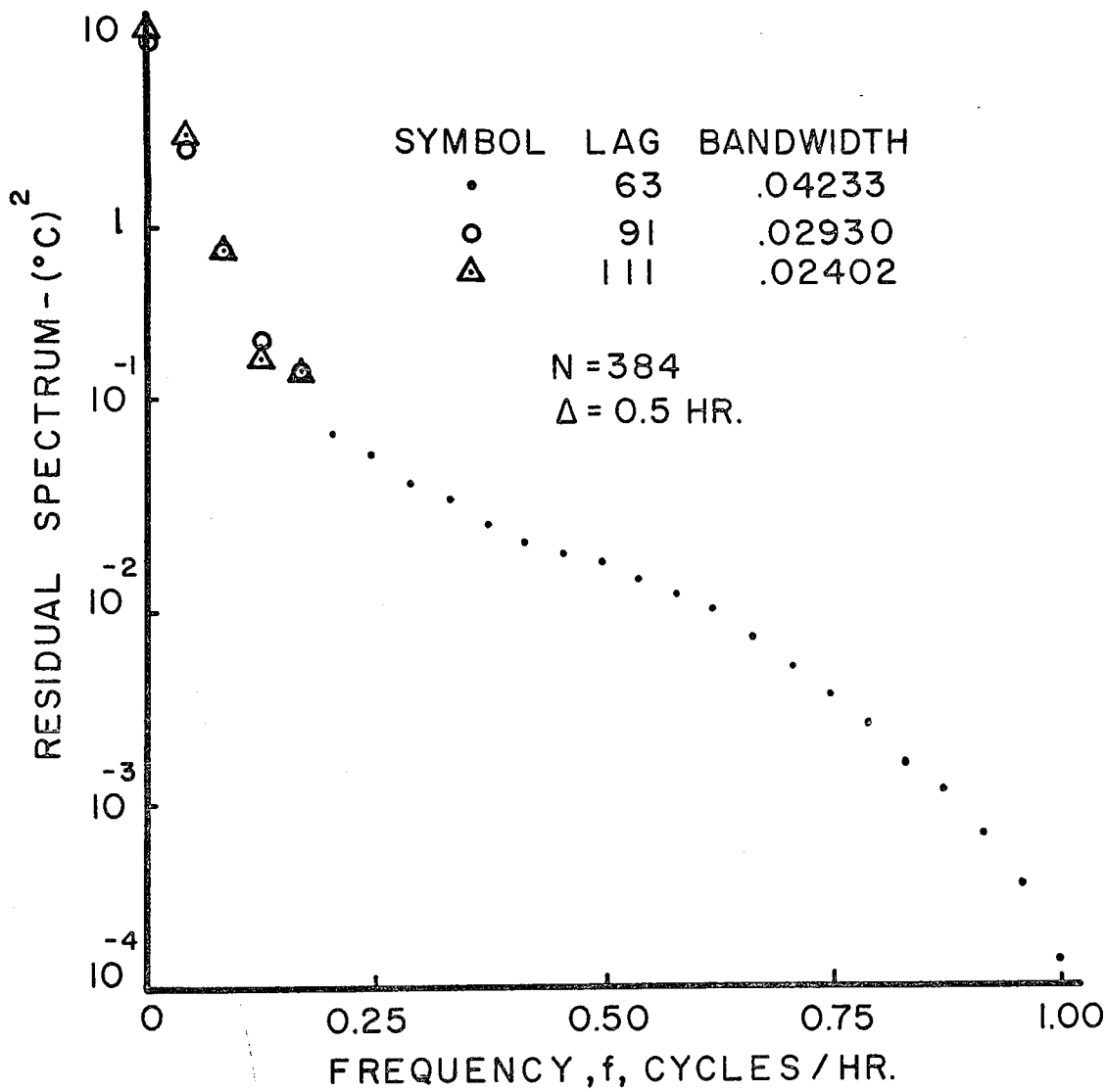

Figure 25. Residual spectrum for 10- and 15-cm temperatures for soil heat transfer subsystem

frequency analysis are presented in Table 7 and Table 8, Appendix B.

The squared coherency spectrum for the 10- and 15-cm temperatures shows values less than 1.0 over the range of frequencies, Table 7, Appendix B. This results from the small amount of power at all frequencies. The step input (irrigation with cold water) caused power at all frequencies, especially the higher frequencies.

The value for soil heat diffusivity for gain as defined by Equation [55b] and for phase as defined by Equation [56b] for a frequency of 0.04167 CPH and x = 5 cm is:

For gain:

$$K = \frac{(5)^2(2)(3.14)(0.04167)}{2[\ln^2(0.62413)]} = 14.73 \text{ cm}^2/\text{hr} \quad [68]$$

For phase:

$$K = \frac{(5)^2(2)(3.14)(0.04167)}{2(-0.38912)^2} = 21.61 \text{ cm}^2/\text{hr} \quad [69]$$

The phase angle of -0.38912 radians was obtained by adding the value for phase of -0.12732 radians in Table 7, Appendix B for a lag of 111 to the phase angle by which the time series were shifted (L=2) to provide alignment. The phase angle for alignment, ϕ_A, is computed by:

$$\phi_A = (-2\pi f \Delta L) \quad [70]$$

$$= (-2)(3.14)(0.5)(2)(0.04167)$$

$$= -0.26180$$

The value of the system constant as determined from phase was not as satisfactory as the value as determined from gain. The results from the analysis of the analytical data produced essentially the same value for diffusivity with the value from phase slightly better. The results above may be related to the inability to exactly align the two series as suggested by Jenkins and Watts (1968, p. 375). Results from the analysis of temperature data where the diffusivity varied with time gave higher values for diffusivity from the phase function than the gain function. There was a small decrease in diffusivity after the irrigation water was applied.

The value for diffusivity as computed by the amplitude and phase plots as well as the apparent diffusivity computed from the finite difference form of the one-dimensional diffusion equation as given by Wierenga (1968) are shown in Table 2 with the value as computed from time series analysis using the gain and phase functions. The values are similar. As discussed by Wierenga (1968) the data analyzed for the amplitude, phase, and numerical methods did not include the period of water application. It is not possible to include the data in the amplitude and phase plots because the input and output are assumed to be sinusoids. The numerical method did not use the data for reasons that will be discussed more fully later.

Table 2. Comparison of values of diffusivity as computed by Wierenga (1968) and by time series analysis.

	Wierenga			Time Series Analysis	
Date	Amplitude	Phase	Numerical	Gain	Phase
Aug. 27/28	15.12	16.92	16.56	14.73*	21.61*
Sept. 1/2	15.92	15.84	16.56		

*All data.

System Constant by Numerical Convolution

Time domain analysis by trial and error using numerical convolution was used to determine soil heat diffusivity. Since fewer days are needed for time domain analysis and numerical convolution iteratively determines the optimum diffusivity, only short periods of data were used at the beginning and end of record to solve for diffusivity. The two different values of diffusivity can be compared to the diffusivity from time series analysis. If the two values from convolution are not the same, diffusivity is not constant with time.

The results of using numerical convolution and incremented values of diffusivity to compute the sum of the squares of the differences between measured and computed soil temperature are presented in Figure 26. The optimum diffusivity was calculated on the basis of the standard deviation of the computed temperature from the measured

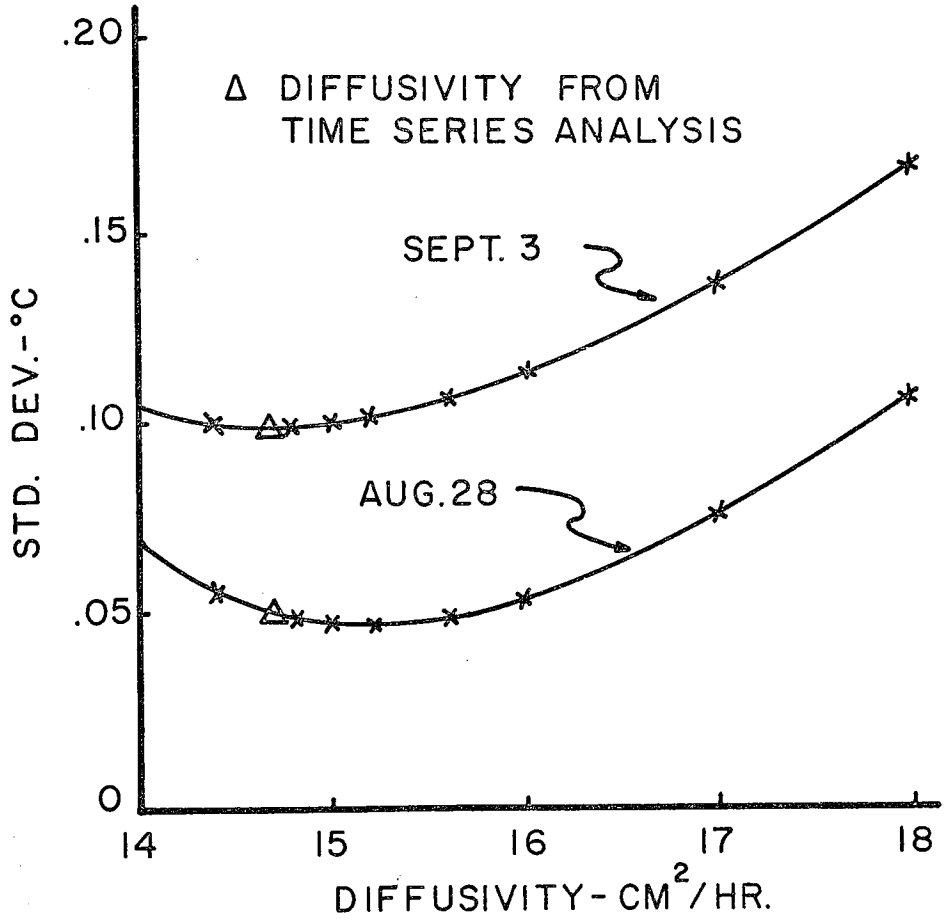

Figure 26. Standard deviation of computed from measured temperature using numerical convolution and various values of diffusivity

temperature. The standard deviation (SD) was computed by:

$$SD = \sqrt{\sum_{i=1}^{N} [TDM(k) - TD(k)]^2/N-1} \qquad [71]$$

where:

TDM = the measured temperature at 15 cm

TD = the convolution computed temperature

N = the number of observations

The number of observations used for August 28 was 15 and for September 3 was 49. The small number of observations for August 28 was used to eliminate as much of the starting transient as possible.

The optimum diffusivity from time domain analysis for the early period of data was 15.2 cm^2/hr and for the late period of data was 14.8 cm^2/hr. These values supported the thesis that there was a slight decrease in diffusivity after irrigation as concluded by Wierenga (1968). The values for diffusivity from time domain analysis are not substantially different from the value of diffusivity as determined by time series analysis. The value from time series analysis is marked on each line for standard deviations for both time periods for comparison.

Time series analysis resulted in a value for diffusivity very nearly the same as from time domain analysis. The results suggest that the two methods are equivalent when the

assumptions inherent in the model are sufficiently valid. As discussed earlier, time domain analysis may be more appropriate in many instances because the assumption of constant diffusivity is more nearly correct. Time series analysis can more efficiently evaluate long periods of record. Data during intermittent cloud cover where the input temperature has rapid fluctuations can also be more effectively used and define a frequency response function for multiple frequencies. This application was not possible with the available data.

System Simulation

The system constant identified from time series analysis was used to simulate the temperature at 15 cm given the time distribution of temperature at 10 cm. The results are shown in Figure 27. Except for the period between hour 42 and hour 65 the difference between measured and computed temperature is less than 0.2 degree. This is a maximum error and many of these computed temperatures differ from the measured temperatures by less than 0.1 degree.

While the cold irrigation water was being applied and was moving through the soil, some heat was being transferred by moisture transfer. The difference between measured and computed temperature is an indication of the heat transferred by moisture transfer. The maximum difference between measured and computed temperature assuming heat transfer by

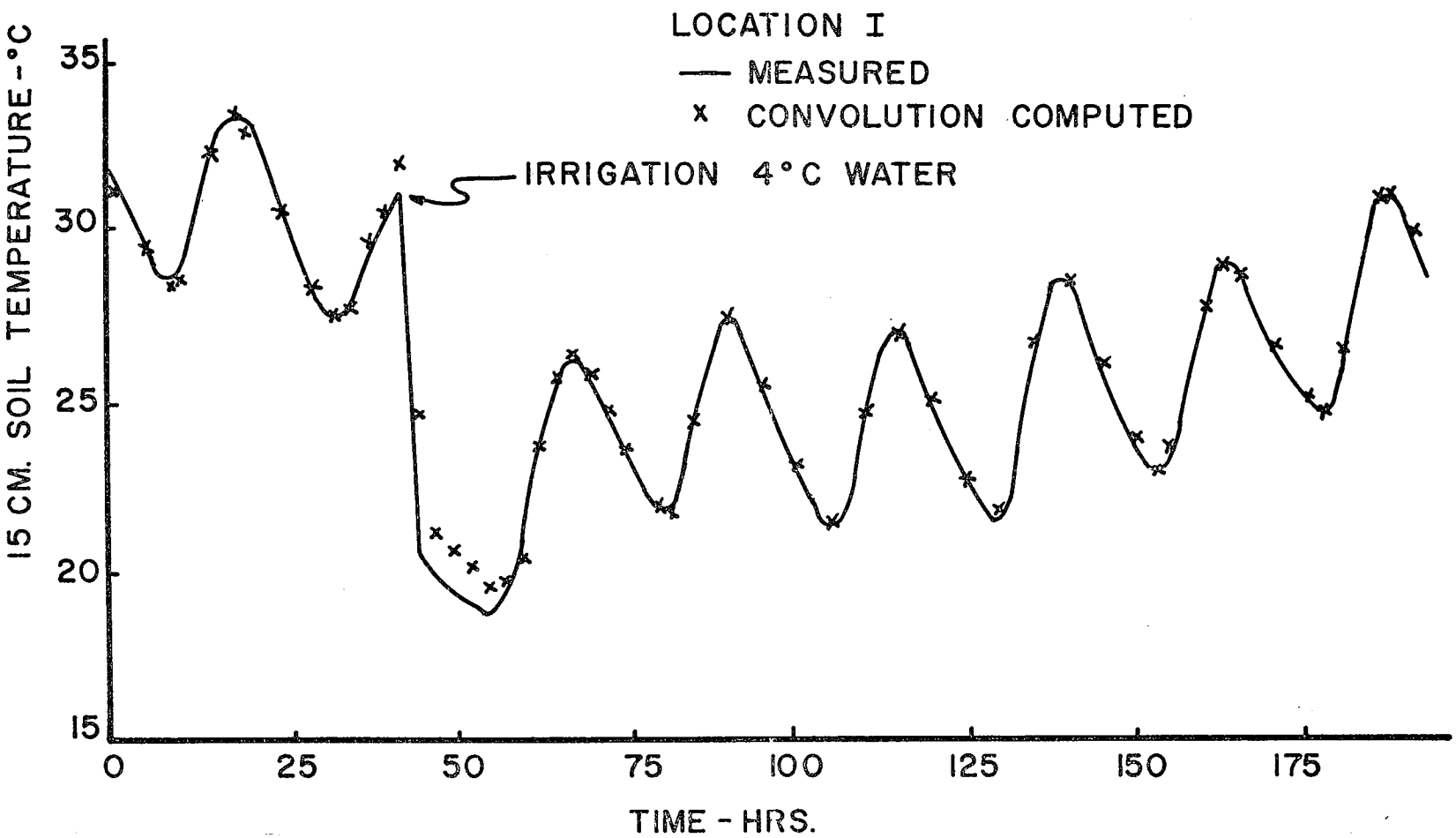

Figure 27. Comparison of measured and convolution computed 15-cm temperature for Davis, California, Location I

conduction only was 3.88° C and occurred about one hour after the water reached the 10-cm depth. The actual temperature change in this interval was approximately 12° C. Thus, about 70 percent of the temperature change can be related to heat transfer by conduction and 30 percent was caused by moisture transfer. The amount of heat transferred by moisture transfer was accentuated by the large difference between soil temperature and the water temperature. Water at nearly the same temperature as the soil would transmit only small quantities of heat and cause very little change in temperature due to moisture transfer.

Wierenga (1968) concluded that significant heat was transferred by moisture transfer during the infiltration of the cold irrigation water. This conclusion was reached because the 20-cm temperature was approximately 15° C less than the numerically computed temperature when using the input temperature as the 10-cm temperature. This large temperature difference would seem to be explained by heat transfer by moisture transfer.

Time series analysis of the 10- and 15-cm temperatures resulted in a value for the system constant that was acceptable and which was used to compute 15-cm temperatures that were very close to the measured temperature. The conclusion was that heat transfer by conduction was the dominant transfer process. Application of the same procedure

to the 15- and 20-cm, and 10- and 20-cm temperatures did not produce acceptable results. The coherency between input and ouptut in each of the instances was very poor. This indicated that some other mechanism explained the temprature changes at 20 cm.

Wierenga (1968, p. 76) commented on the erratic behavior of the 20-cm temperature probe. Inspection of the data suggest that for several hours after the application of irrigation water the 20-cm temperature was colder than the 15-cm temperature and that initially this difference exceeded 5^{o} C. Both the data and the results of time series analysis suggest that the temperature response is explained as rapid travel of the water down cracks near the 20-cm probe. This rapid travel of water down cracks would explain the large temperature change at 20-cm. Thus, heat transfer by water transfer through cracks caused the temperature change. The conclusion of Wierenga (1968) that most of the heat transfer occurs from normal moisture transfer does not seem justified if the anomalous water movement occurred. Even less heat would be transferred by moisture from 15- to 20-cm than was transferred from 10- to 15-cm because the water became closer to the initial soil temperature as it traveled deeper into the soil. The percentage of the total heat transferred by moisture may have been greater.

Time series analysis can be used to determine soil heat diffusivity. The short period of record and heat transfer by soil moisture transfer did not permit accurate determination of the diffusivity. The diffusivity determined by time series analysis did produce temperatures with a maximum error of .17 except when significant soil moisture transfer occurred. This is approximately the same magnitude of error Wierenga (1968) obtained from the finite difference solution of the diffusion equation.

Confidence Limits for Diffusivity

The confidence limits for the soil heat diffusivity for the 10- and 15-cm temperatures were obtained using the upper and lower confidence intervals for the gain and phase spectrums as given in Table 8, Appendix B. The 95 percent confidence limits for soil heat diffusivity were:

For gain:

$$8.8 \leq K \leq 26.9 \text{ cm}^2/\text{hr}$$

For phase:

$$12.1 \leq K \leq 49.1 \text{ cm}^2/\text{hr}$$

The confidence intervals for the system constant from gain and phase are much wider than for the analytical data. The dominant effects are the lower value for coherency caused by some heat transfer by moisture transfer and the reduced number of degrees of freedom caused by the eight-day

record versus the 50-day record for the analytical data. The results suggest that better system identification is necessary by collecting data from a system that more nearly satisfies the assumptions of heat transfer by conduction and of constant diffusivity with depth and time.

SUMMARY AND CONCLUSIONS

Analyses of time distributions of temperature generated by an analytical model and measured for a soil were made by frequency domain analysis using time series analysis and by time domain analysis using numerical convolution. The objective was to use time series analysis and numerical convolution for system identification and numerical convolution for system simulation. System identification and system simulation were achieved from arbitrary time distributions of input. Previous methods of analysis involved the assumption that the time distribution of the input and output were sinusoids. An alternate method using the finite difference form of one-dimensional, partial differential equation for heat flow gave approximately the same results as numerical convolution. Finite difference solutions require careful control of the space and time measurements of temperature to insure solution stability.

Procedures for time series analysis established a confidence interval for the system frequency response function which, by certain assumptions, can be transferred to a confidence interval for the system constant. The confidence interval is a measure of the accuracy by which the system constant has been determined or the system identified.

Soil heat diffusivities of 14.7 cm^2/hr from time series analysis and 14.8 to 15.2 cm^2/hr from numerical convolution are similar to values of 15.1 to 16.6 obtained from analysis of segments of the record before and after irrigation and using amplitude and phase plots, which assume sinusoids, and by the finite difference method. The confidence interval for the diffusivity for gain was several hundred percent reflecting the reduced coherency between input and output caused by the heat transfer by moisture transfer which was not considered in the model. The results from the analytical data resulted in excellent identification of the soil heat diffusivity and a two percent range in diffusivity defined by the confidence interval.

The conclusions are:

1. Time series analysis can be used for system identification for arbitrary time distributions of input and output. When one dominant frequency is in the input then the analytically defined frequency response function is used.
2. Confidence intervals from the system transfer function from time series analysis can be used to measure the adequacy of system constant determination.
3. Numerical convolution can be used to determine the system constant and for simulation of the

soil heat transfer subsystem using arbitrary time distributions of input.

4. Soil moisture status and soil heat transfer by moisture transfer must be defined to adequately describe the soil heat transfer subsystem.

RECOMMENDATIONS

This analysis was based on a linear, time-invariant soil heat transfer subsystem with zero or constant initial condition. Much greater flexibility in the use of numerical convolution would be achieved by starting numerical convolution with an arbitrary initial condition. Carslaw and Jaeger (1959, p. 357) give the solution for the equation of heat conduction for an arbitrary initial condition plus the convolution integral for an arbitrary surface temperature. The effect of an arbitrary initial temperature can be obtained by numerically solving the integral for the arbitrary initial condition. The arbitrary initial condition would permit evaluation of a constant diffusivity, with only a few hours of temperature data. Discrete changes in diffusivity could be used to simulate a time-varying system by numerical convolution.

Time series analysis may be used to investigate the transfer function for surface layers of soil where the diffusivity varies with depth and the heat transfer is non-linear. The approximation of the non-linear heat transfer process by an equivalent lumped, linear process may be possible. This is important as it would permit the simulation of the total soil system by a two-layer equivalent system.

The coupling of heat transfer by conduction and heat transfer by moisture transfer by simultaneous defining equations would permit greater flexibility and provide more information on the status of the soil subsystem. This approach was used in defining the ET system and seems to provide means for simulating the transfer of energy in the soil-plant-air continuum.

The application of the procedures with some modifications to each subsystem of the previously defined ET system seems to offer the opportunity for a better understanding of the system and the means for developing a general simulation model for evapotranspiration.

APPENDIX A

RESULTS OF TIME SERIES ANALYSIS OF SIMULATED SURFACE AND 5-CM TEMPERATURES

TABLE 3

Autocovariances and cross covariances for simulated surface (X) and soil (Y) temperatures.

	Autocovariances		Cross Covariances	
Lag	Input-X	Output-Y	XY	YX
0	3.20000E+01	1.30442E+01	1.84000E+01	1.84000E+01
1	0.	-5.10600E-02	8.79120E+00	-8.88000E+00
2	-3.16800E+01	-1.29138E+01	-1.82160E+01	-1.82160E+01
3	0.	5.10600E-02	-8.70240E+00	8.79120E+00
4	3.13600E+01	1.27833E+01	1.80320E+01	1.80320E+01
5	0.	-5.10600E-02	8.61360E+00	-8.70240E+00
6	-3.10400E+01	-1.26529E+01	-1.78480E+01	-1.78480E+01
7	0.	5.10600E-02	-8.52480E+00	8.61360E+00
8	3.07200E+01	1.25224E+01	1.76640E+01	1.76640E+01
9	0.	-5.10600E-02	8.43600E+00	-8.52480E+00
10	-3.04000E+01	-1.23920E+01	-1.74800E+01	-1.74800E+01

TABLE 4

Time series analysis of simulated surface and soil temperatures

Freq. (CPH)	Autospec X $(Deg.\ C)^2$	Autospec Y $(Deg.\ C)^2$	Residual $(Deg.\ C)^2$	Coherency Sq	Gain	Phase Radians
0.00000	1.9200E+00	1.6908E-01	0.	1.0000E+00	2.9750E-01	-0.
.00417	-6.1058E+00	-3.1311E+00	0.	1.0000E+00	1.3061E+00	-1.0354E+00
.00833	-1.9189E+01	-8.5500E+00	0.	1.0000E+00	7.9592E-01	-7.0156E-01
.01250	-9.3233E+00	-4.6657E+00	0.	1.0000E+00	7.8385E-01	-5.8001E-01
.01667	5.5562E+01	2.1616E+01	0.	1.0000E+00	6.3258E-01	-4.8766E-01
.02083	1.9584E+02	7.8647E+01	0.	1.0000E+00	6.3711E-01	-4.6400E-01
.02500	4.0799E+02	1.6505E+02	0.	1.0000E+00	6.3658E-01	-4.5317E-01
.02917	6.6103E+02	2.6828E+02	3.1733E-01	9.9882E-01	6.3668E-01	-4.4947E-01
.03333	9.0348E+02	3.6736E+02	4.7324E-01	9.9871E-01	6.3724E-01	-4.4891E-01
.03750	1.0786E+03	4.3914E+02	2.8961E-01	9.9934E-01	6.3788E-01	-4.4924E-01
.04167	1.1424E+03	4.6568E+02	1.5906E-01	9.9966E-01	6.3835E-01	-4.4929E-01
.04583	1.0786E+03	4.4017E+02	2.8961E-01	9.9934E-01	6.3862E-01	-4.4867E-01
.05000	9.0348E+02	3.6922E+02	4.7324E-01	9.9872E-01	6.3886E-01	-4.4770E-01
.05417	6.6103E+02	2.7064E+02	3.1733E-01	9.9883E-01	6.3948E-01	-4.4736E-01
.05833	4.0799E+02	1.6756E+02	0.	1.0000E+00	6.4139E-01	-4.4952E-01
.06250	1.9584E+02	8.1014E+01	0.	1.0000E+00	6.4652E-01	-4.5673E-01
.06667	5.5562E+01	2.3681E+01	0.	1.0000E+00	6.6130E-01	-4.6476E-01
.07083	-9.3233E+00	-2.9360E+00	0.	1.0000E+00	6.5491E-01	-7.1542E-01
.07500	-1.9189E+01	-7.0955E+00	0.	1.0000E+00	7.4679E-01	-7.5855E-01
.07917	-6.1058E+00	-1.8483E+00	0.	1.0000E+00	1.2230E+00	-1.1642E+00
.08333	1.9200E+00	1.3945E+00	0.	1.0000E+00	8.5250E-01	3.1245E-13

Lag = 6; Degrees of Freedom = 88; Number of data pts = 200; Bandwidth (CPH) = .03704

TABLE 4--Continued

Freq. (CPH)	Autospec X $(\text{Deg. C})^2$	Autospec Y $(\text{Deg. C})^2$	Residual $(\text{Deg. C})^2$	Coherency Sq	Gain	Phase Radians
0.00000	3.8400E+00	6.9828E-01	1.4735E-01	7.8899E-01	3.7878E-01	-0.
.00417	2.2446E+01	8.2762E+00	0.	1.0000E+00	8.3787E-01	-8.6860E-01
.00833	7.6444E+01	3.0271E+01	0.	1.0000E+00	6.9584E-01	-6.2356E-01
.01250	1.6055E+02	6.4540E+01	0.	1.0000E+00	6.5510E-01	-5.1507E-01
.01667	2.6652E+02	1.0774E+02	0.	1.0000E+00	6.4113E-01	-4.6845E-01
.02083	3.8400E+02	1.5566E+02	1.7149E-01	9.9890E-01	6.3634E-01	-4.4983E-01
.02500	5.0148E+02	2.0363E+02	1.2257E+00	9.9398E-01	6.3531E-01	-4.4427E-01
.02917	6.0745E+02	2.4696E+02	1.3698E+00	9.9445E-01	6.3585E-01	-4.4448E-01
.03333	6.9156E+02	2.8143E+02	9.3715E-01	9.9667E-01	6.3687E-01	-4.4657E-01
.03750	7.4555E+02	3.0367E+02	4.0374E-01	9.9867E-01	6.3778E-01	-4.4845E-01
.04167	7.6416E+02	3.1150E+02	1.7360E-01	9.9944E-01	6.3828E-01	-4.4906E-01
.04583	7.4555E+02	3.0416E+02	4.0374E-01	9.9867E-01	6.3829E-01	-4.4807E-01
.05000	6.9156E+02	2.8237E+02	9.3715E-01	9.9668E-01	6.3793E-01	-4.4577E-01
.05417	6.0745E+02	2.4827E+02	1.3698E+00	9.9448E-01	6.3753E-01	-4.4322E-01
.05833	5.0148E+02	2.0520E+02	1.2257E+00	9.9403E-01	6.3777E-01	-4.4244E-01
.06250	3.8400E+02	1.5740E+02	1.7149E-01	9.9891E-01	6.3988E-01	-4.4716E-01
.06667	2.6652E+02	1.0955E+02	0.	1.0000E+00	6.4638E-01	-4.6434E-01
.07083	1.6055E+02	6.6348E+01	0.	1.0000E+00	6.6364E-01	-5.0780E-01
.07500	7.6444E+01	3.2050E+01	0.	1.0000E+00	7.1236E-01	-6.0698E-01
.07917	2.2446E+01	1.0023E+01	0.	1.0000E+00	8.8307E-01	-8.1008E-01
.08333	3.8400E+00	2.4313E+00	1.4735E-01	9.3940E-01	7.7122E-01	-3.2315E-13

Lag = 4; Degrees of Freedom = 11; Number of data pts = 384; Bandwidth (CPH) = .02930

TABLE 4--Continued

Freq. (CPH)	Autospec X $(\text{Deg. C})^2$	Autospec Y $(\text{Deg. C})^2$	Residual $(\text{Deg. C})^2$	Coherency Sq	Gain	Phase Radians
0.00000	3.8400E+02	1.5592E+02	2.9570E+01	8.1035E-01	5.7361E-01	-0.
.00417	3.8400E+02	1.5593E+02	2.8853E+01	8.1495E-01	5.7525E-01	-7.5157E-02
.00833	3.8400E+02	1.5595E+02	2.6774E+01	8.2831E-01	5.7999E-01	-1.4765E-01
.01250	3.8400E+02	1.5598E+02	2.3536E+01	8.4911E-01	5.8730E-01	-2.1509E-01
.01667	3.8400E+02	1.5603E+02	1.9456E+01	8.7531E-01	5.9638E-01	-2.7561E-01
.02083	3.8400E+02	1.5610E+02	1.4932E+01	9.0434E-01	6.0631E-01	-3.2785E-01
.02500	3.8400E+02	1.5617E+02	1.0409E+01	9.3335E-01	6.1611E-01	-3.7102E-01
.02917	3.8400E+02	1.5625E+02	6.3287E+00	9.5950E-01	6.2484E-01	-4.0469E-01
.03333	3.8400E+02	1.5634E+02	3.0904E+00	9.8023E-01	6.3174E-01	-4.2869E-01
.03750	3.8400E+02	1.5643E+02	1.0114E+00	9.9353E-01	6.3620E-01	-4.4301E-01
.04167	3.8400E+02	1.5653E+02	2.9496E-01	9.9812E-01	6.3786E-01	-4.4768E-01
.04583	3.8400E+02	1.5663E+02	1.0114E+00	9.9354E-01	6.3659E-01	-4.4272E-01
.05000	3.8400E+02	1.5672E+02	3.0904E+00	9.8028E-01	6.3252E-01	-4.2812E-01
.05417	3.8400E+02	1.5681E+02	6.3287E+00	9.5964E-01	6.2600E-01	-4.0389E-01
.05833	3.8400E+02	1.5689E+02	1.0409E+01	9.3365E-01	6.1763E-01	-3.7006E-01
.06250	3.8400E+02	1.5696E+02	1.4932E+01	9.0487E-01	6.0817E-01	-3.2682E-01
.06667	3.8400E+02	1.5703E+02	1.9456E+01	8.7610E-01	5.9855E-01	-2.7459E-01
.07083	3.8400E+02	1.5708E+02	2.3536E+01	8.5016E-01	5.8971E-01	-2.1420E-01
.07500	3.8400E+02	1.5711E+02	2.6774E+01	8.2959E-01	5.8260E-01	-1.4698E-01
.07917	3.8400E+02	1.5714E+02	2.8853E+01	8.1638E-01	5.7799E-01	-7.4801E-02
.08333	3.8400E+02	1.5714E+02	2.9570E+01	8.1183E-01	5.7639E-01	-5.1643E-15

Lag = 2; Degrees of Freedom = 266; Number of data pts = 200; Bandwidths (CPH) = .11111

TABLE 5

Upper and lower confidence limits for gain and phase from time series analysis for simulated surface and soil temperatures.

Freq. (CPH)	Phaseupper Radians	Phaselower Radians	Gainupper	Gainlower
0.00000	0.	0.	2.9750E-01	2.9750E-01
.00417	-1.0354E+00	-1.0354E+00	1.3061E+00	1.3061E+00
.00833	-7.0156E-01	-7.0156E-01	7.9592E-01	7.9592E-01
.01250	-5.8001E-01	-5.8001E-01	7.8385E-01	7.8385E-01
.01667	-4.8766E-01	-4.8766E-01	6.3258E-01	6.3258E-01
.02083	-4.6400E-01	-4.6400E-01	6.3711E-01	6.3711E-01
.02500	-4.5317E-01	-4.5317E-01	6.3658E-01	6.3658E-01
.02917	-4.4033E-01	-4.5861E-01	6.4250E-01	6.3086E-01
.03333	-4.3937E-01	-4.5845E-01	6.4332E-01	6.3116E-01
.03750	-4.4242E-01	-4.5606E-01	6.4223E-01	6.3352E-01
.04167	-4.4438E-01	-4.5419E-01	6.4149E-01	6.3522E-01
.04583	-4.4186E-01	-4.5549E-01	6.4298E-01	6.3427E-01
.05000	-4.3818E-01	-4.5721E-01	6.4494E-01	6.3278E-01
.05417	-4.3826E-01	-4.5646E-01	6.4530E-01	6.3367E-01
.05833	-4.4952E-01	-4.4952E-01	6.4139E-01	6.4139E-01
.06250	-4.5673E-01	-4.5673E-01	6.4652E-01	6.4652E-01
.06667	-4.6476E-01	-4.6476E-01	6.6130E-01	6.6130E-01
.07083	-7.1542E-01	-7.1542E-01	6.5491E-01	6.5491E-01
.07500	-7.5855E-01	-7.5855E-01	7.4679E-01	7.4679E-01
.07917	-1.1642E+00	-1.1642E+00	1.2230E+00	1.2230E+00
.08333	3.1245E-13	3.1245E-13	8.5250E-01	8.5250E-01

Lag = 6; Degrees of Freedom = 88; Number of data pts = 200; Bandwidth (CPH) = .03704

TABLE 5--Continued

Freq. (CPH)	Phaseupper Radians	Phaselower Radians	Gainupper	Gainlower
0.00000	1.1112E-01	-1.1112E-01	4.2078E-01	3.3678E-01
.00417	-8.6860E-01	-8.6860E-01	8.3787E-01	8.3787E-01
.00833	-6.2356E-01	-6.2356E-01	6.9584E-01	6.9584E-01
.01250	-5.1507E-01	-5.1507E-01	6.5510E-01	6.5510E-01
.01667	-4.6845E-01	-4.6845E-01	6.4113E-01	6.4113E-01
.02083	-4.4271E-01	-4.5695E-01	6.4087E-01	6.3181E-01
.02500	-4.2759E-01	-4.6096E-01	6.4591E-01	6.2471E-01
.02917	-4.2846E-01	-4.6049E-01	6.4603E-01	6.2567E-01
.03333	-4.3418E-01	-4.5897E-01	6.4476E-01	6.2897E-01
.03750	-4.4063E-01	-4.5628E-01	6.4277E-01	6.3279E-01
.04167	-4.4400E-01	-4.5413E-01	6.4151E-01	6.3505E-01
.04583	-4.4025E-01	-4.5588E-01	6.4328E-01	6.3330E-01
.05000	-4.3340E-01	-4.5815E-01	6.4582E-01	6.3004E-01
.05417	-4.2725E-01	-4.5919E-01	6.4772E-01	6.2735E-01
.05833	-4.2581E-01	-4.5906E-01	6.4837E-01	6.2717E-01
.06250	-4.4008E-01	-4.5424E-01	6.4441E-01	6.3534E-01
.06667	-4.6434E-01	-4.6434E-01	6.4638E-01	6.4638E-01
.07083	-5.0780E-01	-5.0780E-01	6.6364E-01	6.6364E-01
.07500	-6.0698E-01	-6.0698E-01	7.1236E-01	7.1236E-01
.07917	-8.1008E-01	-8.1008E-01	8.8307E-01	8.8307E-01
.08333	5.4489E-02	-5.4489E-02	8.1322E-01	7.2922E-01

Lag = 4; Degrees of Freedom = 133; Number of Data pts = 200; Bandwidth (CPH) = .05556

TABLE 5--Continued

Freq. (CPH)	Phaseupper Radians	Phaselower Radians	Gainupper	Gainlower
0.00000	7.2589E-02	-7.2589E-02	6.1521E-01	5.3201E-01
.00417	-3.6588E-03	-1.4665E-01	6.1635E-01	5.3416E-01
.00833	-7.9341E-02	-2.1595E-01	6.1958E-01	5.4040E-01
.01250	-1.5186E-01	-2.7833E-01	6.2441E-01	5.5018E-01
.01667	-2.1899E-01	-3.3222E-01	6.3013E-01	5.6264E-01
.02083	-2.7908E-01	-3.7663E-01	6.3588E-01	5.7675E-01
.02500	-3.3095E-01	-4.1109E-01	6.4079E-01	5.9142E-01
.02917	-3.7388E-01	-4.3549E-01	6.4409E-01	6.0559E-01
.03333	-4.0740E-01	-4.4998E-01	6.4518E-01	6.1829E-01
.03750	-4.3092E-01	-4.5510E-01	6.4389E-01	6.2850E-01
.04167	-4.4116E-01	-4.5419E-01	6.4201E-01	6.3370E-01
.04583	-4.3063E-01	-4.5480E-01	6.4428E-01	6.2890E-01
.05000	-4.0686E-01	-4.4939E-01	6.4597E-01	6.1907E-01
.05417	-3.7314E-01	-4.3464E-01	6.4525E-01	6.0675E-01
.05833	-3.3009E-01	-4.1004E-01	6.4231E-01	5.9294E-01
.06250	-2.7819E-01	-3.7544E-01	6.3774E-01	5.7861E-01
.06667	-2.1818E-01	-3.3099E-01	6.3229E-01	5.6480E-01
.07083	-1.5122E-01	-2.7718E-01	6.2683E-01	5.5260E-01
.07500	-7.8982E-02	-2.1498E-01	6.2219E-01	5.4302E-01
.07917	-3.6414E-03	-1.4596E-01	6.1908E-01	5.3689E-01
.08333	7.2239E-02	-7.2239E-02	6.1799E-01	5.3479E-01

Lag = 2; Degrees of Freedom = 266; Number of data pts = 200; Bandwidth (CPH) = .11111

APPENDIX B

RESULTS OF TIME SERIES ANALYSIS OF 10- AND 15-CM TEMPERATURES, LOCATION I, DAVIS, CALIFORNIA, FROM WIERENGA (1968).

TABLE 6

Autocovariances and cross covariances for 10-cm (X) and 15-cm (Y) soil temperatures, Location I, from Wierenga (1968).

Lag	Autocovariances Input-X	Autocovariances Output-Y	Cross Covariances XY	Cross Covariances YX
0	2.13606E+01	1.28248E+01	1.55039E+01	1.55039E+01
1	2.10934E+01	1.26771E+01	1.58317E+01	1.48250E+01
2	2.04801E+01	1.23965E+01	1.59107E+01	1.40070E+01
3	1.96425E+01	1.20216E+01	1.58026E+01	1.31056E+01
4	1.86331E+01	1.15702E+01	1.55425E+01	1.21447E+01
5	1.74791E+01	1.10548E+01	1.51469E+01	1.11426E+01
6	1.62046E+01	1.04874E+01	1.46294E+01	1.01163E+01
7	1.48336E+01	9.87927E+00	1.40034E+01	9.08160E+00
8	1.33930E+01	9.24168E+00	1.32837E+01	8.05515E+00
9	1.19095E+01	8.58547E+00	1.24853E+01	7.05249E+00
10	1.04087E+01	7.92155E+00	1.16242E+01	6.08742E+00
11	8.91561E+00	7.26017E+00	1.07169E+01	5.17238E+00
12	7.45513E+00	6.61095E+00	9.78001E+00	4.31917E+00
13	6.04855E+00	5.98281E+00	8.82984E+00	3.53647E+00
14	4.71449E+00	5.38364E+00	7.88203E+00	2.83108E+00
15	3.46907E+00	4.82000E+00	6.95061E+00	2.20780E+00
16	2.32535E+00	4.29764E+00	6.04889E+00	1.66881E+00
17	1.29371E+00	3.82051E+00	5.18874E+00	1.21406E+00
18	3.80677E-01	3.39135E+00	4.38117E+00	8.40315E-01
19	-4.11553E-01	3.01056E+00	3.63353E+00	5.43177E-01
20	-1.08411E+00	2.67793E+00	2.95111E+00	3.17843E-01
21	-1.64102E+00	2.39191E+00	2.33662E+00	1.59010E-01
22	-2.08967E+00	2.15044E+00	1.79015E+00	6.05822E-02
23	-2.43678E+00	1.95119E+00	1.31014E+00	1.80810E-02
24	-2.68641E+00	1.79195E+00	8.95035E-01	2.95347E-02
25	-2.83962E+00	1.67153E+00	5.43481E-01	9.49054E-02
26	-2.89322E+00	1.58942E+00	2.55701E-01	2.15790E-01
27	-2.84509E+00	1.54532E+00	3.22419E-02	3.91487E-01
28	-2.69329E+00	1.53914E+00	-1.25545E-01	6.20064E-01
29	-2.43343E+00	1.57047E+00	-2.15406E-01	9.01427E-01
30	-2.06513E+00	1.63856E+00	-2.35586E-01	1.23193E+00
31	-1.59135E+00	1.74215E+00	-1.85022E-01	1.60589E+00
32	-1.01786E+00	1.87908E+00	-6.41182E-02	2.01641E+00
33	-3.53505E-01	2.04634E+00	1.25408E-01	2.45441E+00
34	3.91576E-01	2.24023E+00	3.80532E-01	2.91087E+00

TABLE 6--Continued

Autocovariances and cross covariances for 10-cm (X) and 15-cm (Y) soil temperatures, Location I, from Wierenga (1968).

Lag	Autocovariances Input-X	Autocovariances Output-Y	Cross Covariances XY	Cross Covariances YX
35	1.20491E+00	2.45622E+00	6.97603E-01	3.37530E+00
36	2.07160E+00	2.68915E+00	1.07202E+00	3.83680E+00
37	2.97445E+00	2.93320E+00	1.49723E+00	4.28413E+00
38	3.89615E+00	3.18207E+00	1.96543E+00	4.70640E+00
39	4.81771E+00	3.42886E+00	2.46691E+00	5.09184E+00
40	5.71954E+00	3.66642E+00	2.99131E+00	5.42878E+00
41	6.58066E+00	3.88709E+00	3.52724E+00	5.70544E+00
42	7.37883E+00	4.08312E+00	4.06228E+00	5.91077E+00
43	8.09016E+00	4.24678E+00	4.58258E+00	6.03407E+00
44	8.69272E+00	4.37063E+00	5.07379E+00	6.06660E+00
45	9.16399E+00	4.44767E+00	5.52127E+00	6.00030E+00
46	9.48302E+00	4.47136E+00	5.90975E+00	5.83036E+00
47	9.63365E+00	4.43664E+00	6.22451E+00	5.55533E+00
48	9.60670E+00	4.33991E+00	6.45280E+00	5.17800E+00
49	9.39777E+00	4.17943E+00	6.58396E+00	4.70417E+00
50	9.00944E+00	3.95598E+00	6.61073E+00	4.14395E+00
51	8.45016E+00	3.67235E+00	6.52883E+00	3.50963E+00
52	7.73505E+00	3.33338E+00	6.33810E+00	2.81604E+00
53	6.88293E+00	2.94544E+00	6.04215E+00	2.07808E+00
54	5.91542E+00	2.51596E+00	5.64780E+00	1.31098E+00
55	4.85471E+00	2.05271E+00	5.16361E+00	5.29416E-01
56	3.72314E+00	1.56406E+00	4.59977E+00	-2.52284E-01
57	2.54415E+00	1.05893E+00	3.96715E+00	-1.01927E+00
58	1.34177E+00	5.46451E-01	3.27872E+00	-1.75828E+00
59	1.39181E-01	3.58413E-02	2.54857E+00	-2.45734E+00
60	-1.04070E+00	-4.64420E-01	1.79131E+00	-3.10607E+00
61	-2.17639E+00	-9.46593E-01	1.02270E+00	-3.69578E+00
62	-3.25175E+00	-1.40362E+00	2.55972E-01	-4.21961E+00
63	-4.25149E+00	-1.82944E+00	-4.96697E-01	-4.67262E+00
64	-5.16065E+00	-2.21888E+00	-1.22213E+00	-5.05170E+00
65	-5.96878E+00	-2.56822E+00	-1.90824E+00	-5.35717E+00
66	-6.67009E+00	-2.87566E+00	-2.54570E+00	-5.59169E+00
67	-7.26474E+00	-3.14123E+00	-3.12877E+00	-5.76015E+00
68	-7.75691E+00	-3.36560E+00	-3.65545E+00	-5.86828E+00
69	-8.15046E+00	-3.55025E+00	-4.12444E+00	-5.92131E+00

TABLE 6--Continued

Autocovariances and cross covariances for 10-cm (X) and 15-cm (Y) soil temperatures, Location I, from Wierenga (1968).

Lag	Autocovariances Input-X	Autocovariances Output-Y	Cross Covariances XY	Cross Covariances YX
70	-8.45088E+00	-3.69687E+00	-4.53462E+00	-5.92492E+00
71	-8.66378E+00	-3.80792E+00	-4.88648E+00	-5.88269E+00
72	-8.79288E+00	-3.88526E+00	-5.18102E+00	-5.79590E+00
73	-8.83957E+00	-3.93018E+00	-5.41961E+00	-5.66460E+00
74	-8.80301E+00	-3.94372E+00	-5.60353E+00	-5.48828E+00
75	-8.68077E+00	-3.92632E+00	-5.73279E+00	-5.26663E+00
76	-8.47122E+00	-3.87824E+00	-5.80773E+00	-5.00007E+00
77	-8.17243E+00	-3.79913E+00	-5.82727E+00	-4.68966E+00
78	-7.78204E+00	-3.68953E+00	-5.78884E+00	-4.33752E+00
79	-7.30141E+00	-3.55025E+00	-5.69128E+00	-3.94769E+00
80	-6.73274E+00	-3.38252E+00	-5.53422E+00	-3.52465E+00
81	-6.08055E+00	-3.18835E+00	-5.31741E+00	-3.07525E+00
82	-5.35302E+00	-2.97060E+00	-5.04187E+00	-2.60758E+00
83	-4.56236E+00	-2.73328E+00	-4.71109E+00	-2.13135E+00
84	-3.72106E+00	-2.48077E+00	-4.32943E+00	-1.65636E+00
85	-2.84414E+00	-2.21836E+00	-3.90233E+00	-1.19437E+00
86	-1.94078E+00	-1.95214E+00	-3.43654E+00	-7.47831E-01
87	-9.67255E-01	-1.67255E+00	-2.92636E+00	-2.58734E-01
88	1.09658E-01	-1.31111E+00	-2.31253E+00	3.17616E-01
89	1.17972E+00	-9.19698E-01	-1.64462E+00	8.67924E-01
90	2.19706E+00	-5.32796E-01	-9.58063E-01	1.35358E+00
91	3.13556E+00	-1.64674E-01	-2.71735E-01	1.76013E+00
92	3.97279E+00	1.73714E-01	3.97577E-01	2.07800E+00
93	4.69018E+00	4.73381E-01	1.03418E+00	2.30147E+00
94	5.27325E+00	7.26975E-01	1.62346E+00	2.42808E+00
95	5.71011E+00	9.28957E-01	2.15250E+00	2.45706E+00
96	5.99289E+00	1.07560E+00	2.61014E+00	2.39074E+00
97	6.11862E+00	1.16469E+00	2.98682E+00	2.23442E+00
98	6.08861E+00	1.19575E+00	3.27554E+00	1.99521E+00
99	5.90824E+00	1.17010E+00	3.47199E+00	1.68195E+00

TABLE 6--Continued

Autocovariances and cross covariances for 10-cm (X) and 15-cm (Y) soil temperatures, Location I, from Wierenga (1968).

Lag	Autocovariances Input-X	Autocovariances Output-Y	Cross Covariances XY	Cross Covariances YX
100	5.58715E+00	1.09015E+00	3.57384E+00	1.30547E+00
101	5.13844E+00	9.59843E-01	3.58180E+00	8.77531E-01
102	4.57709E+00	7.84356E-01	3.49894E+00	4.10044E-01
103	3.92038E+00	5.69499E-01	3.33016E+00	-8.44024E-02
104	3.18648E+00	3.22074E-01	3.08264E+00	-5.93791E-01
105	2.39473E+00	4.87046E-02	2.76445E+00	-1.10613E+00
106	1.56414E+00	-2.43196E-01	2.38520E+00	-1.61043E+00
107	7.13360E-01	-5.46406E-01	1.95557E+00	-2.09660E+00
108	-1.40132E-01	-8.53914E-01	1.48663E+00	-2.55583E+00
109	-9.79978E-01	-1.15896E+00	9.89628E-01	-2.98019E+00
110	-1.79136E+00	-1.45528E+00	4.75707E-01	-3.36320E+00
111	-2.56175E+00	-1.73735E+00	-4.45719E-02	-3.70030E+00
112	-3.28124E+00	-2.00035E+00	-5.61225E-01	-3.98910E+00
113	-3.94262E+00	-2.24097E+00	-1.06594E+00	-4.22930E+00
114	-4.54058E+00	-2.45639E+00	-1.55090E+00	-4.42154E+00
115	-5.07193E+00	-2.64498E+00	-2.00987E+00	-4.56751E+00
116	-5.53499E+00	-2.80575E+00	-2.43791E+00	-4.66906E+00
117	-5.92923E+00	-2.93830E+00	-2.83069E+00	-4.72841E+00
118	-6.25435E+00	-3.04284E+00	-3.18537E+00	-4.74682E+00
119	-6.51042E+00	-3.11967E+00	-3.49973E+00	-4.72512E+00
120	-6.69760E+00	-3.16884E+00	-3.77213E+00	-4.66386E+00

TABLE 7

Time series analysis of 10- and 15-cm soil temperatures for Davis, California, Location I, from Wierenga (1968).

Freq. (CPH)	Autospec X $(Deg.\ C)^2$	Autospec Y $(Deg.\ C)^2$	Residual $(Deg.\ C)^2$	Coherency Sq	Gain	Phase Radians
0.00000	4.7413E+02	4.1494E+02	9.7983E+00	9.7639E-01	9.2439E-01	-0.
.04167	4.3015E+02	1.7120E+02	2.5377E+00	9.8518E-01	6.2617E-01	-1.2520E-01
.08333	4.3295E+01	1.7741E+01	7.1980E-01	9.5943E-01	6.2701E-01	1.5402E-02
.12500	4.6043E+00	2.3025E+00	2.5266E-01	8.9027E-01	6.6724E-01	4.7541E-01
.16667	3.3767E+00	1.4524E+00	1.7591E-01	8.7888E-01	6.1483E-01	5.9457E-01
.20833	1.4408E+00	7.2659E-01	8.5089E-02	8.8289E-01	6.6727E-01	9.2642E-01
.25000	9.9630E-01	4.7681E-01	6.3364E-02	8.6711E-01	6.4419E-01	1.1831E+00
.29167	6.3414E-01	3.2565E-01	4.3319E-02	8.6698E-01	6.6725E-01	1.4545E+00
.33333	4.2626E-01	2.3488E-01	3.7428E-02	8.4065E-01	6.8059E-01	-1.4343E+00
.37500	3.0854E-01	1.7316E-01	2.6534E-02	8.4676E-01	6.8937E-01	-1.1293E+00
.41667	2.2139E-01	1.3733E-01	2.2534E-02	8.3591E-01	7.2009E-01	-8.9183E-01
.45833	1.6793E-01	1.1014E-01	2.0050E-02	8.1795E-01	7.3243E-01	-6.0207E-01
.50000	1.2390E-01	9.1437E-02	1.7993E-02	8.0322E-01	7.6991E-01	-3.4609E-01
.54167	9.7881E-02	7.7947E-02	1.4287E-02	8.1671E-01	8.0647E-01	-5.8954E-02
.58333	7.9043E-02	6.6284E-02	1.1853E-02	8.2118E-01	8.2983E-01	2.2835E-01
.62500	6.3136E-02	5.7548E-02	9.8798E-03	8.2832E-01	8.6891E-01	5.4040E-01
.66667	5.4237E-02	5.1097E-02	6.8047E-03	8.6683E-01	9.0369E-01	8.2807E-01
.70833	4.1697E-02	4.6301E-02	5.0166E-03	8.9165E-01	9.9504E-01	1.1260E+00
.75000	3.9190E-02	4.2661E-02	3.6687E-03	9.1400E-01	9.9748E-01	1.4094E+00
.79167	3.2508E-02	3.9525E-02	2.4775E-03	9.3732E-01	1.0675E+00	-1.4530E+00
.83333	3.0804E-02	3.6892E-02	1.5214E-03	9.5876E-01	1.0716E+00	-1.1213E+00
.87500	2.7950E-02	3.5787E-02	1.0895E-03	9.6956E-01	1.1142E+00	-8.4582E-01
.91667	2.6939E-02	3.4383E-02	6.4502E-04	9.8124E-01	1.1191E+00	-5.7580E-01
.95833	2.7213E-02	3.4002E-02	4.5698E-04	9.8656E-01	1.1103E+00	-2.7471E-01
1.00000	2.7227E-02	3.4589E-02	1.3448E-04	9.9611E-01	1.1249E+00	-2.0361E-14

Lag = 91; Degrees of freedom = 11; Number of data pts = 384; Bandwidth (CPH) = .02930.

TABLE 7--Continued

Freq. (CPH)	Autospec X $(Deg.\ C)^2$	Autospec Y $(Deg.\ C)^2$	Residual $(Deg.\ C)^2$	Coherency Sq	Gain	Phase Radians
0.00000	4.6707E+02	4.1695E+02	1.0240E+01	9.7544E-01	9.3316E-01	-0.
.04167	5.1049E+02	2.0155E+02	2.6941E+00	9.8663E-01	6.2413E-01	-1.2732E-01
.08333	4.7964E+01	1.9562E+01	7.5447E-01	9.6143E-01	6.2619E-01	2.4045E-02
.12500	4.3906E+00	2.3812E+00	2.2990E-01	9.0345E-01	6.9999E-01	5.1035E-01
.16667	3.4489E+00	1.4921E+00	1.7790E-01	8.8077E-01	6.1731E-01	5.7559E-01
.20833	1.2923E+00	6.4863E-01	6.8541E-02	8.9433E-01	6.6999E-01	9.3722E-01
.25000	9.6430E-01	4.3602E-01	6.2948E-02	8.5563E-01	6.2200E-01	1.1905E+00
.29167	6.7903E-01	3.3536E-01	4.5716E-02	8.6368E-01	6.5311E-01	1.4682E+00
.33333	4.6212E-01	2.5825E-01	3.7765E-02	8.5377E-01	6.9073E-01	-1.4363E+00
.37500	3.0831E-01	1.8202E-01	2.7841E-02	8.4705E-01	7.0717E-01	-1.1440E+00
.41667	2.0470E-01	1.3068E-01	2.7245E-02	7.9151E-01	7.1084E-01	-9.1535E-01
.45833	1.5586E-01	9.9871E-02	1.9925E-02	8.0050E-01	7.1619E-01	-5.9146E-01
.50000	1.2681E-01	8.9292E-02	1.4592E-02	8.3658E-01	7.6752E-01	-3.2220E-01
.54167	1.0708E-01	8.4228E-02	1.3037E-02	8.4522E-01	8.1538E-01	-5.8424E-02
.58333	8.1346E-02	7.1114E-02	1.1201E-02	8.4249E-01	8.5821E-01	2.1078E-01
.62500	5.7541E-02	5.6160E-02	9.4342E-03	8.3201E-01	9.0114E-01	5.3589E-01
.66667	4.9982E-02	4.6906E-02	7.2591E-03	8.4524E-01	8.9063E-01	8.4993E-01
.70833	4.2706E-02	4.4557E-02	5.6636E-03	8.7289E-01	9.5432E-01	1.1409E+00
.75000	4.2991E-02	4.4621E-02	3.6791E-03	9.1755E-01	9.7589E-01	1.3958E+00
.79167	3.4370E-02	4.2340E-02	2.4580E-03	9.4195E-01	1.0772E+00	-1.4643E+00
.83333	2.9778E-02	3.7199E-02	1.3975E-03	9.6243E-01	1.0965E+00	-1.1116E+00
.87500	2.5842E-02	3.3637E-02	9.4373E-04	9.7194E-01	1.1248E+00	-8.2882E-01
.91667	2.5939E-02	3.2636E-02	5.9387E-04	9.8180E-01	1.1114E+00	-5.7830E-01
.95833	2.8177E-02	3.4791E-02	4.2704E-04	9.8773E-01	1.1043E+00	-2.8409E-01
1.00000	2.9034E-02	3.6794E-02	1.0736E-04	9.9708E-01	1.1241E+00	-1.3361E-14

Lag = 111; Degrees of Freedom = 9; Number of Data pts = 384; Bandwidth (CPH) = .02402

TABLE 7--Continued

Freq. (CPH)	Autospec X $(Deg.\ C)^2$	Autospec Y $(Deg.\ C)^2$	Residual $(Deg.\ C)^2$	Coherency Sq	Gain	Phase Radians
0.00000	4.1801E+02	3.6333E+02	6.6441E+00	9.8171E-01	9.2374E-01	-0.
.04167	3.2384E+02	1.3448E+02	2.7685E+00	9.7941E-01	6.3774E-01	-1.1324E-01
.08333	2.8906E+01	1.2874E+01	6.3294E-01	9.5083E-01	6.5075E-01	6.2601E-02
.12500	4.4932E+00	2.3617E+00	2.5248E-01	8.9309E-01	6.8514E-01	4.6228E-01
.16667	3.1716E+00	1.4394E+00	1.8481E-01	8.7161E-01	6.2895E-01	5.9478E-01
.20833	1.3581E+00	6.9458E-01	4.8505E-02	9.3017E-01	6.8973E-01	9.7594E-01
.25000	9.8040E-01	4.6923E-01	6.2690E-02	8.6640E-01	6.4394E-01	1.1950E+00
.29167	6.5444E-01	3.3079E-01	6.3951E-02	8.0667E-01	6.3854E-01	1.4187E+00
.33333	4.2829E-01	2.3154E-01	3.0840E-02	8.6680E-01	6.8455E-01	-1.4251E+00
.37500	3.1091E-01	1.7320E-01	2.3975E-02	8.6158E-01	6.9279E-01	-1.1352E+00
.41667	2.2971E-01	1.4104E-01	3.3538E-02	7.6222E-01	6.8410E-01	-9.1468E-01
.45833	1.6843E-01	1.1081E-01	1.9528E-02	8.2376E-01	7.3616E-01	-6.1001E-01
.50000	1.2121E-01	9.0272E-02	1.1675E-02	8.7067E-01	8.0526E-01	-3.3901E-01
.54167	9.8749E-02	7.8090E-02	1.6868E-02	7.8399E-01	7.8738E-01	-5.6749E-02
.58333	7.9051E-02	6.6392E-02	1.3003E-02	8.0415E-01	8.2181E-01	2.2224E-01
.62500	6.2004E-02	5.6959E-02	6.4804E-03	8.8623E-01	9.0228E-01	5.2389E-01
.66667	5.4737E-02	5.1349E-02	7.5817E-03	8.5235E-01	8.9420E-01	8.3430E-01
.70833	4.2856E-02	4.6531E-02	6.8015E-03	8.5383E-01	9.6283E-01	1.1374E+00
.75000	3.8055E-02	4.2262E-02	3.1780E-03	9.2480E-01	1.0134E+00	1.4051E+00
.79167	3.2875E-02	3.9441E-02	2.6171E-03	9.3364E-01	1.0584E+00	-1.4472E+00
.83333	3.1250E-02	3.7133E-02	2.1560E-03	9.4194E-01	1.0580E+00	-1.1202E+00
.87500	2.7602E-02	3.5749E-02	1.0422E-03	9.7085E-01	1.1213E+00	-8.5372E-01
.91667	2.6782E-02	3.4466E-02	6.1454E-04	9.8217E-01	1.1243E+00	-5.7651E-01
.95833	2.6919E-02	3.4025E-02	6.0770E-04	9.8214E-01	1.1142E+00	-2.7444E-01
1.00000	2.6584E-02	3.4308E-02	2.5863E-04	9.9246E-01	1.1317E+00	-2.2360E-14

Lag = 63; Degrees of Freedom = 16; Number of data pts = 384; Bandwidth (CPH) = .04233

TABLE 8

Upper and lower confidence limits for gain and and phase from time series analysis of 10- and 15-cm soil temperatures.

Freq. (CPH)	Phaseupper Radians	Phaselower Radians	Gainupper	Gainlower
0.00000	1.4863E-01	-1.4863E-01	1.0613E+00	7.8751E-01
.04167	-8.1334E-03	-2.4226E-01	6.9931E-01	5.5304E-01
.08333	2.1248E-01	-1.8168E-01	7.4979E-01	5.0424E-01
.12500	8.1627E-01	1.3456E-01	8.9029E-01	4.4419E-01
.16667	9.5585E-01	2.3328E-01	8.3216E-01	3.9750E-01
.20833	1.2806E+00	5.7228E-01	8.9867E-01	4.3587E-01
.25000	1.5651E+00	8.0109E-01	8.8432E-01	4.0406E-01
.29167	1.8368E+00	1.0723E+00	9.1612E-01	4.1839E-01
.33333	-1.0068E+00	-1.8617E+00	9.6274E-01	3.9844E-01
.37500	-7.1223E-01	-1.5463E+00	9.6860E-01	4.1013E-01
.41667	-4.5633E-01	-1.3273E+00	1.0239E+00	4.1631E-01
.45833	-1.3619E-01	-1.0680E+00	1.0614E+00	4.0342E-01
.50000	1.4467E-01	-8.3686E-01	1.1328E+00	4.0705E-01
.54167	4.0902E-01	-5.2693E-01	1.1702E+00	4.4268E-01
.58333	6.8878E-01	-2.3208E-01	1.1986E+00	4.6111E-01
.62500	9.8876E-01	9.2036E-02	1.2456E+00	4.9225E-01
.66667	1.2105E+00	4.4560E-01	1.2410E+00	5.6642E-01
.70833	1.4644E+00	7.8771E-01	1.3253E+00	6.6477E-01
.75000	1.7058E+00	1.1130E+00	1.2888E+00	7.0615E-01
.79167	-1.2042E+00	-1.7018E+00	1.3304E+00	8.0467E-01
.83333	-9.2256E-01	-1.3201E+00	1.2832E+00	8.5995E-01
.87500	-6.7629E-01	-1.0154E+00	1.3022E+00	9.2620E-01
.91667	-4.4375E-01	-7.0784E-01	1.2664E+00	9.7176E-01
.95833	-1.6334E-01	-3.8607E-01	1.2337E+00	9.8687E-01
1.00000	5.9522E-02	-5.9522E-02	1.1918E+00	1.0580E+00

Lag = 91; Degrees of Freedom = 11; Number of data pts = 384; Bandwidth (CPH) = .02930

Table 8--Continued

Freq. (CPH)	Phaseupper Radians	Phaselower Radians	Gainupper	Gainlower
0.00000	1.7901E-01	-1.7901E-01	1.0993E+00	7.6700E-01
.04167	3.6722E-03	-2.5831E-01	7.0566E-01	5.4261E-01
.08333	2.5074E-01	-2.0265E-01	7.6693E-01	4.8545E-01
.12500	8.8596E-01	1.3473E-01	9.5678E-01	4.4320E-01
.16667	1.0012E+00	1.4998E-01	8.7217E-01	3.6244E-01
.20833	1.3332E+00	5.4122E-01	9.2843E-01	4.1155E-01
.25000	1.6695E+00	7.1139E-01	9.0872E-01	3.3529E-01
.29167	1.9303E+00	1.0061E+00	9.4429E-01	3.6194E-01
.33333	-9.5336E-01	-1.9193E+00	1.0115E+00	3.6994E-01
.37500	-6.4696E-01	-1.6411E+00	1.0444E+00	3.6995E-01
.41667	-3.0160E-01	-1.5291E+00	1.1202E+00	3.0144E-01
.45833	3.1891E-03	-1.1861E+00	1.1174E+00	3.1497E-01
.50000	1.9675E-01	-8.4115E-01	1.1482E+00	3.8685E-01
.54167	4.4248E-01	-5.5933E-01	1.2069E+00	4.2382E-01
.58333	7.1740E-01	-2.9583E-01	1.2746E+00	4.4179E-01
.62500	1.0643E+00	7.2981E-03	1.3555E+00	4.4675E-01
.66667	1.3508E+00	3.4907E-01	1.3183E+00	4.6297E-01
.70833	1.5834E+00	6.9835E-01	1.3630E+00	5.4566E-01
.75000	1.7389E+00	1.0528E+00	1.3042E+00	6.4760E-01
.79167	-1.1819E+00	-1.7466E+00	1.3773E+00	7.7710E-01
.83333	-8.8799E-01	-1.3351E+00	1.3396E+00	8.5340E-01
.87500	-6.3698E-01	-1.0207E+00	1.3392E+00	9.1033E-01
.91667	-4.2492E-01	-7.3167E-01	1.2812E+00	9.4164E-01
.95833	-1.5866E-01	-4.0951E-01	1.2425E+00	9.6619E-01
1.00000	6.0743E-02	-6.0743E-02	1.1923E+00	1.0559E+00

Lag = 111; Degrees of Freedom = 9; Number of data pts = 384; Bandwidth (CPH) = .02402

TABLE 8--Continued

Freq. (CPH)	Phaseupper Radians	Phaselower Radians	Gainupper	Gainlower
0.00000	9.9174E-02	-9.9174E-02	1.0152E+00	8.3228E-01
.04167	-7.8712E-03	-2.1862E-01	7.0482E-01	5.7066E-01
.08333	2.2832E-01	-1.0312E-01	7.5809E-01	5.4340E-01
.12500	7.1599E-01	2.0857E-01	8.5710E-01	5.1317E-01
.16667	8.7694E-01	3.1262E-01	8.0407E-01	4.5383E-01
.20833	1.1760E+00	7.7583E-01	8.2683E-01	5.5263E-01
.25000	1.4839E+00	9.0616E-01	8.2739E-01	4.6050E-01
.29167	1.7818E+00	1.0556E+00	8.6531E-01	4.1176E-01
.33333	-1.1367E+00	-1.7135E+00	8.7922E-01	4.8988E-01
.37500	-8.4013E-01	-1.4302E+00	8.9424E-01	4.9134E-01
.41667	-4.9749E-01	-1.3319E+00	9.6130E-01	4.0691E-01
.45833	-2.6783E-01	-9.5220E-01	9.8318E-01	4.8915E-01
.50000	-5.5640E-02	-6.2238E-01	1.0304E+00	5.8012E-01
.54167	3.3391E-01	-4.4741E-01	1.0872E+00	4.8755E-01
.58333	5.8838E-01	-1.4390E-01	1.1160E+00	5.2759E-01
.62500	7.8684E-01	2.6094E-01	1.1368E+00	6.6775E-01
.66667	1.1410E+00	5.2757E-01	1.1642E+00	6.2421E-01
.70833	1.4422E+00	8.3251E-01	1.2518E+00	6.7383E-01
.75000	1.6135E+00	1.1967E+00	1.2231E+00	8.0378E-01
.79167	-1.2526E+00	-1.6418E+00	1.2630E+00	8.5367E-01
.83333	-9.3908E-01	-1.3013E+00	1.2485E+00	8.6741E-01
.87500	-7.2767E-01	-9.7976E-01	1.2623E+00	9.8037E-01
.91667	-4.7861E-01	-6.7441E-01	1.2342E+00	1.0144E+00
.95833	-1.7646E-01	-3.7243E-01	1.2232E+00	1.0052E+00
1.00000	6.3268E-02	-6.3268E-02	1.2033E+00	1.0602E+00

Lag = 63; Degrees of Freedom = 16; Number of data pts = 384; Bandwidth (CPH) = .04233.

LIST OF SYMBOLS

A, B	- constants
$\hat{A}_{xy}$	- smoothed cross amplitude spectrum estimate
C	- arbitrary constants, subscripted
CPH	- cycles per hour
$\hat{C}$	- smoothed spectral estimate of the power spectrum
D	- operation notation, $\frac{d}{dx}$
G	- gain function
$\hat{G}$	- smoothed gain function estimate
H	- the operator on input to produce a response or the sytem transfer function
I_o	- modified Bessel function of zero order and first kind
K_A	- air heat diffusivity
K_θ	- soil water diffusivity
K_E	- vapor diffusivity in air for evaporation
K_o	- modified Bessel function of zero order and second kind
K_S or K	- soil heat diffusivity
K_T	- vapor diffusivity in air for transpiration
$\hat{K}^2_{xy}$	- smoothed squared coherency function

K^2_{xy} - theoretical squared coherency function

K_1 - derivative of hydraulic conductivity with respect to moisture content

L - number of lags

$\hat{L}_{xy}$ - smoothed cospectrum estimate

M - truncation point for lag window

N - number of discrete data points

P - period of sinusoidal temperature

$\hat{Q}_{xy}$ - smoothed quadrature spectrum estimate

R_N - net radiation

$\hat{R}$ - smoothed spectral density function estimate

SD - standard deviation of convolution computed temperature from measured

SS - sum of the squares of the differences between analytical and convolution computed temperature

T_a - average temperature

T_{air} - air temperature

TD - convolution computed temperature

TDM - measured temperature

TM - analytically computed temperature

T_o - initial temperature

T(o, t) - temperature at x = 0 as a function of time

T_S - surface temperature

$\overline{T}_S(p)$ - surface temperature as a function of frequency

T_{soil} or T - soil temperature

$T(x,p)$ - temperature as a function of space and frequency

X - input to a system

$\overline{X}$ - population mean estimate

X_S - variable relating surface variables that define evapotranspiration

$W(u)$ - lag window for smoothing

Y - response to an input

$\hat{c}$ - autocovariance function estimate, subscripted

d - denotes total derivative

e_E - specific humidity of air for evaporation

e_o - initial specific humidity

e_{ES} - specific humidity for evaporation at the soil surface

e_{TS} - specific humidity for transpiration at the plant surface

e_T - specific humidity of air for transpiration

f,F - frequency, $1/P$

f_o - fundamental frequency

h - system impulse response

i - the imaginary number, $\sqrt{-1}$

$i\omega$ - imaginary part of Laplace transform or complex frequency, $\omega = 2\pi/P$

j,k,u,v - discrete time

$\hat{l}_{xy}$ - even cross covariance estimate

p - Laplace transform parameter for time and equals $\sigma + i\omega$

$\hat{q}_{xy}$ - odd covariance estimates

q_r - volumetric flow per unit length of root, the transpiration rate per unit length of root

r - radial distance from root

$\hat{r}$ - autocorrelation function estimate

r_o - outer radius of root

t, τ - time

x - vertical distance

x, y - used as subscripts and refer to properties of the time series of input, X, and time series of output, Y

Ψ - quadrature spectrum

ψ_{xy} - odd part of covariance function

ϕ - phase spectrum

$\hat{\phi}$ - smoothed phase function estimate

ϕ_A - phase angle for alignment

Λ_{xy} - theoretical cospectrum

λ_{xy} - even part of covariance function

∂ - denotes partial derivative

μ - mean of discrete values of population

ρ - correlation function, subscripted xx or yy designates autocorrelation and xy or yx designates cross correlation

Γ - theoretical power spectrum when subscripted xx or yy and cross power spectrum when subscripted xy

γ - autocovariance function, subscripted xx or yy designates autocovariance and xy or yx designated cross covariance

θ_{root} - soil moisture content for radial flow

θ_{soil} - soil moisture content for vertical flow

θ_o - initial soil moisture content

θ_S - surface soil moisture content

θ^* - transformed moisture content

θ^*_S - transformed surface soil moisture content

α_{xy} - cross amplitude spectrum

σ - real part of the Laplace transform, p

Δ - sampling interval

ΔT - amplitude of a sinusoidal temperature

ΔT_S - amplitude of the surface temperature

π - constant equal to 3.1416

$\bar{}$ - bar over a variable indicates Laplace transform

$\int$ - integral sign and the symbol for integration

$\mathcal{L}$ - indicates Laplace transform

REFERENCES

Cannon, R. H. 1967. Dynamics of Physical Systems. McGraw-Hill Book Company, New York.

Carslaw, H. S. and Jaeger, J. C. 1959. Conduction of Heat in Solids. Clarendon Press, Oxford, 2nd Ed.

Cowan, I. R. 1965. Transport of Water in the Soil-Plant-Atmosphere System. J. Appl. Ecology. 2:221-239.

Criddle, W. D. 1966. Empirical Methods of Predicting Evapotranspiration Using Air Temperature as the Primary Variable. in Evapotranspiration and its Role in Water Resources, Amer. Soc. of Agri. Engrs., St. Joseph, Mich., 54-56.

Eagleson, P. S., Mejia, R., and March, F. 1965. The Computation of Optimum Realizable Unit Hydrographs from Rainfall and Runoff Data. Hydrodynamics Lab Rept. No. 84, M.I.T., Cambridge, Mass.

Gardner, W. R. 1959. Solutions of the Flow Equations for the Drying of Soils and Other Porous Media. Soil Sci. Soc. Amer. Proc. 23:83-187.

Gardner, W. R. and Ehlig, G. F. 1963. The influence of Soil Water on Transpiration by Plants. J. Geophys. Res. 68:5719-5724.

Halstead, M. H., Richman, R. L., Covey, W. and Merryman, J.D. 1957. A Preliminary Report on the Design of a Computer for Micrometeorology. Jour. of Met., 14(8):308-325.

Hantush, M. S. 1964. Hydraulics of Wells. in Advances in Hydroscience, Academic Press, New York, 1:281-432.

Jenkins, G. M. and Watts, G. W. 1968. Spectral Analysis and its Applications. Holden-Day, San Francisco.

Jensen, M. E. 1966. Empirical Methods of Estimating or Predicting Evapotranspiration Using Radiation. In Evapotranspiration and its Role in Water Resources, Amer. Soc. of Agri. Engrs., St. Joseph, Mich., 49-53.

Lemon, E. R. 1966. Plant Factors and Transpiration — The Plant Community. In Evapotranspiration and its Role in Water Resources, Amer. Soc. of Agri. Engrs., St. Joseph, Mich., 17-21.

Melsa, J. L. and Schultz, D. G. 1969. Linear Control Systems. McGraw-Hill Book Company, New York.

Milsum, J. H. 1966. Biological Control Systems Analysis. McGraw-Hill Book Company, New York.

Ohmsteade, W. D. 1966. Numerical Solution of the Transport and Energy Equations in the Planetary Boundary Layer. Tech. Rept. ECOM-6020, U. S. Army Electronics Command, Fort Huachuca, Ariz.

Phillip, J. R. 1966. Plant Water Relations: Some Physical Aspects. Ann. Rev. Plant Physiol. 17:245-268.

Phillip, J. R. 1969. Theory of Infiltration. In Advances in Hydroscience, Academic Press, New York, 6:215-296.

Pruitt, W. O. 1966. Empirical Methods Using Primarily Evaporation Pans. In Evapotranspiration and its Role in Water Resources. Amer. Soc. of Agri. Engrs. St. Joseph, Mich., 57-61.

Schwarz, R. J. and Friedland, B. 1965. Linear Systems. McGraw-Hill Book Company, New York.

Sellers, W. D. 1965. Physical Climatology. The University of Chicago Press, Chicago.

Stapleton, H. N. and Meyers, R. P. 1969. Modeling Subsystems for Cotton -- The Cotton Plant Simulation. ASAE Paper No. 69-940 for Presentation at the Winter Meeting, Amer. Soc. of Agri. Engrs., Chicago, Ill.

Van Bavel, C. H. M. 1966. Potential Evaporation: The Combination Concept and its Experimental Verification. Water Resources Res. 2(3):455-467.

Wierenga, P. J. 1968. An analysis of Temperature Behavior in Irrigation Soil Profiles. Water Science and Engineering Paper 7002, Dept. of Water Sci. and Engr., Univ. of Calif., Davis, Sept., 152 pp.

Wierenga, P. J., Nielson, R. M. and Hagan, R. M. 1969. Thermal Properties of a Soil Based Upon Field and Laboratory Measurements. Soil Sci. Soc. Amer. Proc., 33:354-360.

Wierenga, P. J., Hagan, R. M., and Nielson, D. R. 1970. Soil Temperature Profiles During Infiltration and Redistribution of Cool and Warm Irrigation Water, Water Resources Res., 6(1):230-238.

Woo, K. B., Boersma, L., and Stone, L. N. 1966. Dynamic Simulation Model of the Transpiration Process. Water Resources Res., 2(1):85-97.